

University of Alberta

**A composite earth flow – spread in glaciomarine sediments near Terrace, British
Columbia**

by

Marten Geertsema



**A thesis submitted to the Faculty of Graduate Studies and Research in partial
fulfillment of the requirements for the degree of Master of Science**

Department of Earth and Atmospheric Sciences

Edmonton, Alberta

Fall 2004



Library and
Archives Canada

Bibliothèque et
Archives Canada

Published Heritage
Branch

Direction du
Patrimoine de l'édition

395 Wellington Street
Ottawa ON K1A 0N4
Canada

395, rue Wellington
Ottawa ON K1A 0N4
Canada

Your file *Votre référence*

ISBN: 0-612-95750-0

Our file *Notre référence*

ISBN: 0-612-95750-0

The author has granted a non-exclusive license allowing the Library and Archives Canada to reproduce, loan, distribute or sell copies of this thesis in microform, paper or electronic formats.

L'auteur a accordé une licence non exclusive permettant à la Bibliothèque et Archives Canada de reproduire, prêter, distribuer ou vendre des copies de cette thèse sous la forme de microfiche/film, de reproduction sur papier ou sur format électronique.

The author retains ownership of the copyright in this thesis. Neither the thesis nor substantial extracts from it may be printed or otherwise reproduced without the author's permission.

L'auteur conserve la propriété du droit d'auteur qui protège cette thèse. Ni la thèse ni des extraits substantiels de celle-ci ne doivent être imprimés ou autrement reproduits sans son autorisation.

In compliance with the Canadian Privacy Act some supporting forms may have been removed from this thesis.

Conformément à la loi canadienne sur la protection de la vie privée, quelques formulaires secondaires ont été enlevés de cette thèse.

While these forms may be included in the document page count, their removal does not represent any loss of content from the thesis.

Bien que ces formulaires aient inclus dans la pagination, il n'y aura aucun contenu manquant.

Canada

DEDICATION

"The earth is the Lord's and the fullness thereof" Psalm 24:1

I dedicate this thesis to my parents, Jakob and Anny Geertsema, for their care and nurturing all these years.

ACKNOWLEDGEMENTS

I began work on what was to become my thesis topic in 1994 with the research section of the Prince Rupert Forest Region in Smithers, BC. I am grateful to the Ministry of Forests for allowing me to venture from operations to research, and for giving me a free rein in conducting my research, and later, supporting my graduate studies. Here, Dr. Jim Pojar taught me to think as a field ecologist, and Jim Schwab mentored me in the art and science of field-based slope stability analysis.

Early work on the Mink Creek landslide benefited greatly from advice and analyses of two specialists in sensitive clays, Drs. Michael Carson and Ken Torrance. Frank Maximchuk, then Geotechnical Engineer with the BC Ministry of Transportation and Highways in Terrace, generously opened up his laboratory and provided a drill truck for the extraction of a core. He and his co-workers are thanked. Many individuals provided assistance in the field. These include Doug Boersema, Jennifer Cooney, Pauline Favero, Solvej Patschke, Jim Schwab, Dirk and Judith Septer, and Irene Weiland. Bliksem, Barley, Reno, Sheila, and Frodo, are canine friends who hauled in the heavy vane shear borer by sled.

Once this project evolved into my Masters thesis, Dr. Dave Cruden mentored me throughout the process. I thank him for his patience and advice. Students and staff who assisted me include Vanessa Egginton, Mike Kirk, Denise Michaud, David Stuart, and Mike Wolowicz.

Finally, I thank Karen, my wife, for her patience during the long winter when I attended classes in Edmonton.

TABLE OF CONTENTS

CHAPTER 1: INTRODUCTION	1
1.1. Setting	1
1.2. Climate	2
1.3. Quaternary history	7
1.4. Conditions for sensitive clay development.....	8
1.5. Earlier landslides in the study area.....	8
1.6. Topographic Mapping.....	9
1.7. Assumptions	9
CHAPTER 2: STRATIGRAPHY AT THE MINK CREEK LANDSLIDE.....	11
2.1. Introduction	11
2.2. Stratigraphy	11
2.3. Thickness of Displaced Material in the Zone of Depletion	12
2.4. Conclusions.....	21
CHAPTER 3: MORPHOLOGY OF THE ZONE OF DEPLETION	22
3.1. Introduction	22
3.2. Detailed Morphology of the Zone of Depletion	22
3.2.1. Overview.....	22
3.3. Zone 1.....	29
3.3.1.1. Horizontally Exposed Rupture Surface.....	29
3.3.1.2. Horizontally Stratified Ridges.....	30
3.3.1.3. Thin, Remoulded Linear Ridges	30
3.4. Zone 2.....	37
3.4.1.1. Zone 2a	37
3.4.1.2. Zone 2b.....	37
3.2.3.2.1 The Broad Bands.....	38
3.2.3.2.1 Lobate Forms and Mottled Topography	38
3.2.3.2.1 Shear Zones	38
3.2.3.2.1 Elevation of the Rupture Surface	39
3.4.2. Zone 3	43
3.4.3. Zone 4	46
3.4.3.1. Ridges.....	46
3.4.3.2. Excavations.....	52
3.4.4. Zone 5	56
3.4.5. Zone 6	57

3.4.6.	Zone 7	61
3.5.	Discussion/Conclusions	65
CHAPTER 4: MORPHOLOGY OF THE ZONE OF ACCUMULATION		66
4.1.	Introduction	66
4.2.	Dimensions of Displaced Material in the Zone of Accumulation	66
4.3.	Morphology of the Zone of Accumulation	66
4.3.1.	Material Characteristics	66
4.3.2.	Landform Features	77
4.3.2.1.	Ridges	77
4.3.2.2.	Shear Zones	77
4.3.2.3.	Dewatering Structures	78
4.4.	Trees Controlling Movement	78
4.5.	The Western Landslide	79
4.6.	Conclusions	86
CHAPTER 5: GEOTECHNICAL PROPERTIES, MINERALOGY, AND SALINITY OF SEDIMENT ASSOCIATED WITH THE MINK CREEK LANDSLIDE		87
5.1.	Introduction	87
5.2.	Geotechnical Properties	87
5.2.1.	Particle Size Analysis	87
5.2.2.	Atterberg Limits	88
5.2.3.	Shear Strength	92
5.2.4.	Density and Stability Numbers	94
5.3.	Mineralogy	98
5.4.	Salinity and pH	98
5.5.	Conclusions	102
CHAPTER 6: MOVEMENT HISTORY OF THE MINK CREEK LANDSLIDE		103
6.1.	Introduction	103
6.2.	Triggers	103
6.3.	Inferred Movement History and Supporting Evidence	104
6.3.1.	Initial landslide	104
6.3.2.	The First Flow	107
6.3.3.	Spreading into a Central Zone of Depletion	107

6.3.3.	Spreading into a Central Zone of Depletion	107
6.3.4.	Further Spreading in Response to Lateral Movement	107
6.3.5.	Subsidence Associated with Spreading	111
6.3.6.	Spreading and Flow in the Western Widening	113
6.3.7.	Late Stage Movements	113
6.3.8.	Movement Classification	113
6.4.	Comparison to Other Landslides in Marine Sediments	114
6.4.1.	Other Landslides	114
6.4.2.	Rissa Landslide, Norway	115
6.5.	Conclusions	118
CHAPTER 7: POTENTIAL FOR FUTURE LARGE RETROGRESSIVE LANDSLIDES		120
7.1.	Introduction	120
7.2.	Prehistoric Landslides in the Terrace-Kitimat Area	120
7.2.1.	Prehistoric Landslide Depressions	120
7.2.2.	Landslide Distribution	121
7.2.3.	Landslide Ages	127
7.3.	Influence of Valley Formation	132
7.4.	Climatic Conditions Leading up to the Landslide	133
7.5.	Climate Change Scenarios	134
7.6.	Conclusions	139
CHAPTER 8: CONCLUSIONS		140
REFERENCES		142

LIST OF TABLES

Table 3.1 Characteristics of horizontally stratified ridges	28
Table 5.1 Material properties of the samples from borehole	94
Table 5.2 Vane shear data.....	99
Table 5.3 Salinity and pH from a borehole at the Mink Creek landslide.....	103

LIST OF FIGURES

Figure 1.1 Digitally stitched image of 35 mm aerial photographs (spring 1994) of the Mink Creek landslide that occurred sometime between 1 December 1993 and 9 January 1994. The creek flows west, via Lakelse River into Skeena River.....	3
Figure 1.2 Oblique view of the Mink Creek landslide – spring 1994. Note CN railway track (red) and the approximate location of pre-slide Mink Creek (blue). Displacement was down the creek toward viewer.....	4
Figure 1.3 Map of the study area. Note the location of the Mink Creek landslide, as well as the 1962 Lakelse landslides and the 2003 Khyex River landslide. The dashed lines represent areas of glaciomarine sediment. I produced the hillshade image from a TRIM digital elevation model, with a false sun set at an azimuth of 315°, at an altitude of 45° degrees using ArcView.....	5
Figure 1.4 Pre-slide aerial photographs of the Mink Creek area in 1985 and 1988 showing the outline of the landslide and mature and logged forest of different ages. BC Government airphotos, 30BCC374: 158 (left) and 30BC88019: 245 (right).....	6
Figure 2.1 Digital elevation model (DEM) of the Mink Creek landslide showing excavated trenches, point excavation locations, and a borehole. The DEM is based on aerial photographs taken in 1994.....	14
Figure 2.2 This excavation in the main scarp shows 4 m of brown weathered crust overlying grey depth material.....	15
Figure 2.3 Colour banded grey sediment (depth material) is exposed in a near vertical wall of the Butte in the zone of depletion. See section 2.5.7 for a detailed description of the Butte. Shovel (centre) is 1.5 m in length.....	16
Figure 2.4 Digital elevation model of pre-slide topography at Mink Creek. Black stippled line outlines the 1993/1994 main scarp. Yellow dashed lines represent the scarp of a 5000 year old landslide. The 73 m contour marks the elevation of the surface of rupture where it daylight in the valley, thus the landslide is perched above the valley bottom. The DEM is based on aerial photographs taken in 1988.....	17
Figure 2.5 Excavation at the intersection of the main scarps of the prehistoric landslide and the 1993/1994 landslide (site 2 in Figure 2.2). Note the concave surface of rupture separating	

horizontal from rotated bedding. The horizontal bedding is undisturbed material outside of the prehistoric landslide. Shovel is 1.5 m long.....	18
Figure 2.6 A fissure in prehistoric displaced material exposed in the main scarp has been infilled with sediment. Note the bedding on either side of the fissure and the brecciated structure of the infilled material. A Canadian dime (1.8 cm diameter) provides scale.....	19
Figure 2.7 An excavation in the main scarp shows vertically oriented <i>Equisetum arvense</i> roots (arrow). These horsetail roots are ubiquitous in the weathered crust and extend to depths of 4.6 m. The coin is 2.8 cm in diameter. The inset photo provides a closer view of these roots.	20
Figure 3.1 Aerial photo (35 mm) of the zone of depletion, April 1994. Note the locations of the eastern and western widenings, and numbered zones.	24
Figure 3.2 Aerial photo (35 mm) of the zone of depletion, April 1994. Note the locations of the numbered sites, most of which are transverse, horizontally stratified ridges. The yellow line is the boundary between the zone of depletion and the zone of accumulation.....	25
Figure 3.3 1994 aerial photograph of the Mink Creek landslide and schematic diagrams of parabolic and arcuate ridges with interpreted direction of movement.	26
Figure 3.4 Possible evolution of lobate parabolic ridges to longitudinal ridges. Movement to South.	27
Figure 3.5 The Dance Floor, a remarkable 15 x 40 m expanse of exposed rupture surface dipping 2-3° to the south. Note the prominent fissures. The two ridges at the far end of the surface cleared it by late stage sliding.	31
Figure 3.6 A transverse scarp in an exposed rupture surface in zone 1. Continuous bedding indicates the scarp is not a fault. It probably formed along a fissure.	32
Figure 3.7 A lateral scarp in an exposed grey rupture surface in zone 1. Continuous bedding reveals that the scarp is not a fault. Brown material is a lag of surficial soil.....	33
Figure 3.8 A convex rupture surface at site 36 (same as vane shear site E), at the toe of the rupture surface, separating the zone of depletion from the zone of accumulation. Note the pronounced striated slickensides. Bedding is at 3° and the surface of rupture here has cut across the bedding.....	34
Figure 3.9 Split ridges at sites 8 (<i>Top</i>) and 10 (<i>Bottom</i>). Only the leading side of these ridges tends to be covered with a thin veneer of brown surficial material. The ridges are 2.5 m high.....	35

Figure 3.10 Linear ridges of primarily surficial material on an exposed grey rupture surface in zone 1. The dashed circle outlines the same conifer on both images. Movement was to the south.....	36
Figure 3.11 A horizontally stratified ridge at site 11 in zone 2a, has had its upper strata removed during the landslide process.	40
Figure 3.12 Secondary movement of a 10 cm thick stratum in a tilted block in zone 2a.....	40
Figure 3.13 1994 aerial photograph of Zone 2b. Note the locations of broad bands of grey and brown material (BB), linear ridges (LR), lobate forms (LF), mottled topography (MT), and a prominent shear zone (SZ). The Dance Floor (DF) is in zone 1. The movement was to the south.	41
Figure 3.14 Oblique aerial view of zones 1 and 2b. Note the conspicuous exposed rupture surface referred to as the Dance Floor (DF), the thin disturbed linear ridges (LR) and the alternating grey and brown broad bands (BB). Movement is towards the South, parallel to the ridges.	42
Figure 3.15 Ridge 5, horizontally stratified, is found in zone 2, the East Marginal Zone. Note the irregular wavy shear zone (within the dotted lines) that separates the ridge from the displaced wedge on its leading face. The remoulded displaced material is dense, while the only partly disturbed material in the ridge is soft enough to penetrate with a finger. The shear zone shows evidence of fluidization.....	45
Figure 3.16 1994 aerial photograph showing zone 6, the Butte. The upper surface (4a) is flanked by an intermediate surface (4b) and a lower surface (4c). Trenches (blue lines) bisect ridges 17 and 18, and the south wall of 4a and the surface of 4c.	48
Figure 3.17 Topple and block fall of desiccated glaciomarine sediment exposed in the 6 m tall east wall of the Butte.....	49
Figure 3.18 The east wall of the Butte showing the surfaces zones 4a and b (Figure 12). The dotted white lines represent perched rupture surfaces. Note that the horizontal bands below the rupture surfaces continue from zone 4b into 4a (inset).	50
Figure 3.19 The south wall of the Butte showing an exposed rupture surface (dashed line). Note how central portions of the ridges have collapsed.	51
Figure 3.20 Rotational movement of grabens (wedges) along ridge 17 on the middle surface of the Butte.	53

Figure 3.21 The crest of ridge 18 contains horsetail roots, but is 1.5 m lower than surrounding surface material indicating local subsidence.....	53
Figure 3.22 <i>Top</i> : West side of trench in zone 6c (Figure 3.16). Note the horizontal bedding in the undisturbed strata, and the smooth gradation of the rupture surface from inclined to horizontal. <i>Movement to South. Bottom</i> : East side of trench in zone 4c (Figure 3.16). Note the sharp transition from inclined to horizontal orientation. Movement to the South.	54
Figure 3.23 Exposure of a horizontal rupture surface in a 10 cm thick blue stratum between ridge 17 and 18. The ridge in the inset photo is 17. Note the rotational wedge.	55
Figure 3.24 Zones 5 and 6 of the western widening. Note the number of trees in these zones, and especially in zone 6, in comparison to zones 2 and 4. Also note the prominent shear zone in zone 5	58
Figure 3.25 Plastic deformation below thorough remoulding with mottles of surficial material in zone 5, south of the Butte.	59
Figure 3.26 Site 31 – a horizontally stratified ridge in zone 5.	59
Figure 3.27 Upright trees, are common on grabens in zone 6.	60
Figure 3.28 A split graben in zone 6, similar to site 18 on the Butte.....	60
Figure 3.29 Back tilted blocks separate horizontally stratified ridge 6 from the East lateral scarp in the Main Scarp Marginal Zone.	62
Figure 3.30 Complex movement of blocks in the Main Scarp Marginal Zone. Cartoon depicts a cross-section along the blue dotted line. Note brown surface material overlying grey weathered material in the cartoon.....	63
Figure 3.31 A horizontally bedded wedge separates Ridge 33 from the scarp on the western edge of the landslide.	64
Figure 4.1 This digital elevation model show the difference in elevation between the pre and post landslide surfaces. Up to 14 m of material was deposited in the valley of Mink Creek.	68
Figure 4.2 Infilled valley of Mink Creek. Note the braided channel patterns and numerous vertically transported trees. Most trees are oriented prone in the direction of flow. The depth of fill is as high as 14 m above the thalweg of the pre-slide creek. The deposit is 90 to 100 m wide.	69

Figure 4.3 The landslide impounded Mink Creek resulting in the damming of two lakes..... 70

Figure 4.4 Horizontal strata occur at the tip of the landslide in the zone of accumulation. 71

Figure 4.5 Horizontally bedded strata exposed in the bank of the newly incised creek, in the zone of accumulation south of Zone 1..... 72

Figure 4.6 Plastic deformation of horizontal strata is combined here with injection of brown surficial sediment. Pencil is 15 cm long. 73

Figure 4.7 Horizontal, leaning, and vertical trees occur in the zone of accumulation below the forest remnant. Some vertical trees are transported (VT), others are in place (IP). Note that prone trees are oriented in the direction of movement. 74

Figure 4.8 Trees rafted in the vertical position. This is a common phenomenon in the zone of accumulation as well as in Zones 5 and 6 in the western widening of the zone of depletion..... 75

Figure 4.9 Muddy clasts of weathered surficial material range from coarse sand to cobble size in the post-landslide creek. 76

Figure 4.10 A transported ridge in the zone of accumulation. 80

Figure 4.11 Trees and mud are jumbled together in a 4 m tall ridge at site 35 in the zone of accumulation (Figure 3.2). 80

Figure 4.12 Mud has built up against a resisting network of trees to form ridge 37 (Figure 3.2), east of the forest remnant. The resultant wall is 11 m high. Note the dense interlocking network of trees and stripping of bark (inset). 81

Figure 4.13 Shear zones (arrows) in the zone of accumulation are prominent and continuations of shear zones in the zone of depletion. Note the distinction between transport zones of (A) forested and (B) clearcut materials. View to the west..... 81

Figure 4.14 A linear shear zone in the zone of accumulation. The absence of a lateral shear ridge attests to the fluid nature of the displaced material. Location is southeast of the forest remnant. 82

Figure 4.15 A mud volcano in the zone of accumulation indicating liquefaction. The field book is 20 cm long. Location is south of Zone 1. 83

Figure 4.16 Mud lines on trees with the highest mark in the up flow direction. <i>Bottom</i> : Note the steep gradient from the leading to the down flow side of the tree. Directly south of Zones 1 and 5, respectively.	84
Figure 4.17 The western landslide was a separate event. Arrows indicate movement direction and narrow linear depressions.	85
Figure 5.1 Orthophoto of the Mink Creek landslide showing vane shear and soil sample sites (including a borehole at site B).....	89
Figure 5.2 A rupture surface is exposed in a blue layer (10 cm thick) in a trench in Zone 4b (Figure 3.16). Perhaps this was a layer of high rapidity. The displaced material is dense and remoulded while the lower material is soft and undisturbed. The inset photo shows the colour banded nature of the sediment at depth. Photos courtesy of Nichole Boulton.	96
Figure 5.3 Profiles of the stability number (Ns) –see Figure 3.1 for locations). Depths are relative to site A.	97
Figure 5.4 Scanning electron micrograph of flocculated glaciomarine sediment from the Mink Creek landslide. Image provided by J.K. Torrance.	101
Figure 6.1 1994 orthophoto of the Mink Creek flowslide. Note the numbered zones distinguished on the basis of morphology and style and direction of movement (Chapter 3). The landslide to the southwest is separate from the main landslide. Red and blue arrows indicate direction of primary and secondary movements, respectively.	105
Figure 6.2 Hillshade image of pre and post landslide topography. Note the locations of the cross-sections, the gully to the east of the landslide, and the scarp of a 5000 year old landslide.	106
Figure 6.3 Cross-section 1 trends E_W through the zone of depletion (see Figure 6.2 for location). The red lines represent various surfaces of rupture. The dashed line extends the perched rupture surface of the Butte (zone 4a) to illustrate how H and Ns would become too small at that elevation for westward retrogression to continue (see Figure 6.1 for movement directions). Note the preslide gully to the east of the landslide.	109
Figure 6.4 Cross-section 3 (see figure 6.2 for location). Spreading occurred in zones 4 a to c (Figure 6.1). In zone 4c the initial spread occurred on the upper rupture surface, followed by subsidence to the lower surface. The grey blocks represent translational ridges from the initial spread (Figure 6.5). The preslide slope between zones 4c and 5 illustrates why the spread was constrained to the south. Flow occurred in zone 5 and rotational sliding in zone 7.	110

Figure 6.5 Top. The upper and lower surfaces of the Butte (zone 4). Dashed blue line represents the perched rupture surface. The white lines represent the pattern of arcuate ridges shown below. The blue arrows indicate the direction of first movement (spreading). The red arrows indicate subsequent collapse. Bottom. Vertical airphoto (1994) showing the zones on the Butte and the arcuate planform of the ridges. Note the similarity of the collapsed ridges in zone 4c and the broad bands (BB) to the east in zone 2a. Note the transverse faulting of the grey ridge at A. 117

Figure 6.6 Plot of Undisturbed shear strength vs. depth for various types of flowslides. While most of the Mink Creek data plot under flows, the vane shear data were obtained from near the area in the slide that flowed rather than spread..... 117

Figure 7.1 Distribution of landslide scarps in glaciomarine sediment in the Terrace-Kitimat area. 123

Figure 7.2 A prehistoric earth flow with a "bottleneck" shape, south of Nalbeelah Creek. Stipple pattern outlines its scarp. Outlet is about 70 m wide. Note the presence of the major gully immediately to the left of the landslide. Deep gullies often control the dimensions of landslides. 124

Figure 7.3 The foreslope of the Onion Lake delta with prehistoric earth flows..... 125

Figure 7.4 An earth flow filled with peat at Nalbeelah Creek..... 126

Figure 7.5 A Hiller peat corer showing the marine clay – peat interface. I sampled peat at these contacts to obtain minimum ages for the landslides. 129

Figure 7.6 Scatter graph showing distribution of minimum landslide ages (from peat) plotted against peat thickness..... 131

Figure 7.7 Percent cumulative deviation from mean precipitation at Terrace Airport for the period 1953 to 2002. The graph shows a period of increasing precipitation from 1986 to 1994. Environment Canada data. 135

Figure 7.8 Percent cumulative deviation from mean temperature at Terrace Airport for the period 1953 to 2002. The graph shows a period of increasing temperature from 1985 to 1995. Environment Canada data. 136

Figure 7.9 Terrace airport daily precipitation and temperature data for the period September 1993 to January 1994. Note that this period experienced warmer than average temperatures. Most of the precipitation was rain. Environment Canada data. 137

Figure 7.10 Annual climate change scenarios for 2020, 2050, and 2080 for Terrace, British Columbia, with respect to a 1961-1990 global climate model baseline. The points represent the

results of 58 different global circulation models, generally predicting a progressively warmer and wetter climate for Terrace. The data was obtained from the Canadian Institute for Climate Studies website (<http://www.cics.uvic.ca>) 138

Chapter 1

Introduction

Sometime between 1 December 1993 and 9 January 1994, 43 ha of forest land was involved in a landslide in sensitive glaciomarine sediments at Mink Creek, near Terrace, British Columbia (Figures 1.1 and 1.2). Such landslides are common and well documented on plains and extremely gentle slopes in sensitive glaciomarine sediments in Eastern Canada and Scandinavia. They are also common, but not widely reported, in uplifted fjordal valleys of British Columbia. Although the geotechnical, mineralogical, and chemical properties of associated sediments are relatively well understood, the kinematics of these landslides remain incompletely described.

The objectives of the thesis research are as follows:

1. To describe the stratigraphy of landslide at Mink Creek (Chapter 2);
2. To describe the morphology of the zone of depletion (Chapter 3)
3. To describe the morphology of the zone of accumulation (Chapter 4)
4. To describe the physical properties of the sediment (Chapter 5);
5. To infer style and sequence of movement of the landslide from the morphology and physical properties of the displaced material and compare the Mink Creek landslide to similar landslides (Chapter 6);
6. To consider the potential for future landslides in the area (Chapter 7).

In this thesis I follow the landslide terminology of Cruden and Varnes (1996). The landslide I describe moved by both flowing and spreading. I will use the term *landslide* to refer to these movements together, and *flow*, *spread* and *slide* as appropriate when I refer to movements within the landslide.

1.1. Setting

The study area is situated in the Kitimat Ranges of the Coast Mountains in the Western System of the Canadian Cordillera (Holland 1976) at the head of Kitimat Arm in Douglas Channel. It occupies a broad north-south trending depression known as the Kitimat-Kitsumkalum trough ranging from 1 to 15 km in width (Clague 1984). Although the trough extends north of Terrace, the study area is restricted to a zone between Terrace

and Kitimat (Figure 1.2), and in this zone, is an uplifted fjordal valley. The trough is drained by Skeena River near Terrace, and by Kitimat River near Kitimat -- rivers too small to have carved the wide valley, suggesting different paleodrainage systems and some faulting (Duffell and Souther 1964; Clague 1984).

The predominantly forested Kitimat-Kitsumkalum trough is filled with rolling to flat, gullied glacial and postglacial sediments with occasional bedrock hillocks. The bulk of the valley fill is comprised of glaciomarine mud and glaciofluvial gravels. Based on drilling results, the depth of glaciomarine sediment ranges from extremely shallow to in excess of 30 m. Till is also common, and bedrock is exposed in cut banks and on some hillocks. Postglacial materials include alluvial floodplains and fans, bogs and fens, and colluvium. The largest waterbody in the study area is Lakelse Lake. The surficial geology of the area has been mapped by Clague (1984) and is dealt with in more detail in section 1.4.

Mountains rise abruptly on either side of the Kitimat-Kitsumkalum trough with peaks ranging from about 1000 to 1500 m in elevation. Bedrock geology is dominated by granodioritic Cretaceous (or younger) Coast Intrusions, with a lesser amount of Mesozoic volcanics, and also inclusions of still older sedimentary rock including limestone (Duffell and Souther 1964).

Portions of the forests around the Mink Creek landslide were harvested in 1981 and 1985, respectively (Figure 1.3).

1.2. Climate

The climate of the study area is classified as wet subarctic. Mean annual precipitation ranges from about 2300 mm at Kitimat to about 1300 mm near Terrace, of which about 1800 and 1000 mm, respectively, occurs between October and April. Mean annual temperature ranges from 5.9°C near Terrace to 6.4°C at Kitimat. Respective extremes are about -27 and 36°C near Terrace, and -25 and 36°C at Kitimat (British Columbia Ministry of Forests 1997).

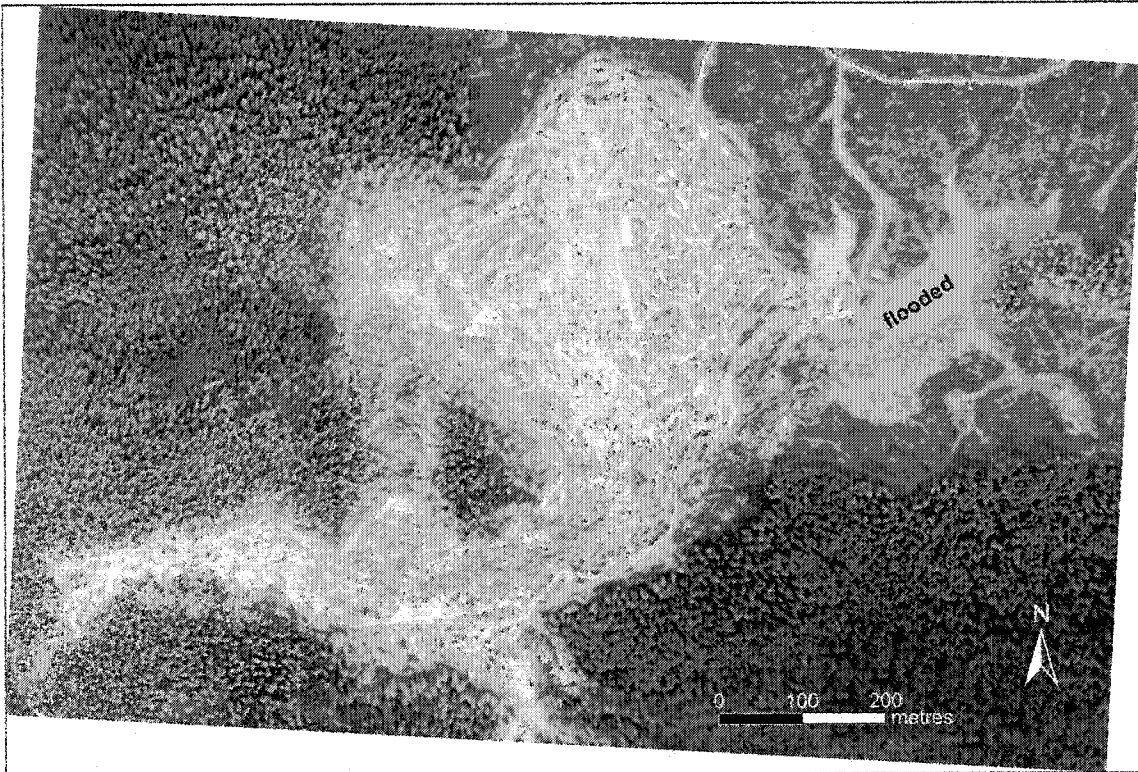


Figure 1.1 Digitally stitched image of 35 mm aerial photographs (spring 1994) of the Mink Creek landslide that occurred sometime between 1 December 1993 and 9 January 1994. The creek flows west, via Lakelse River into Skeena River.

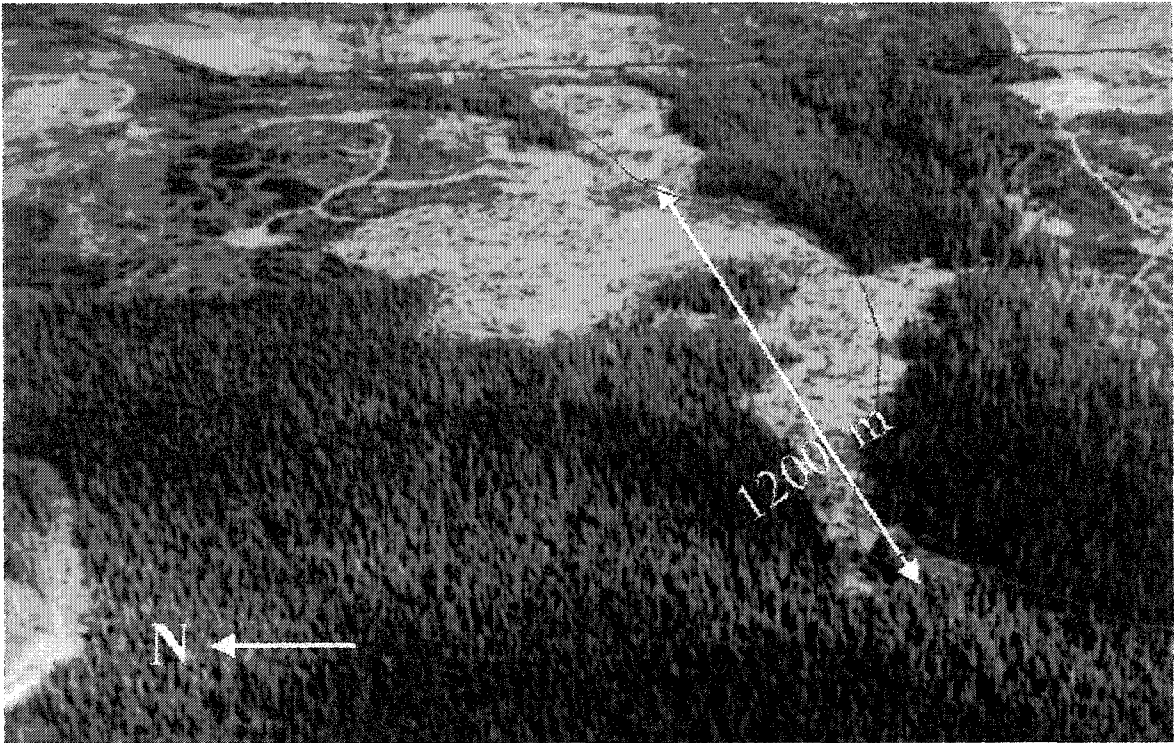


Figure 1.2 Oblique view of the Mink Creek landslide – spring 1994. Note CN railway track (red) and the approximate location of pre-slide Mink Creek (blue). Displacement was down the creek toward viewer.

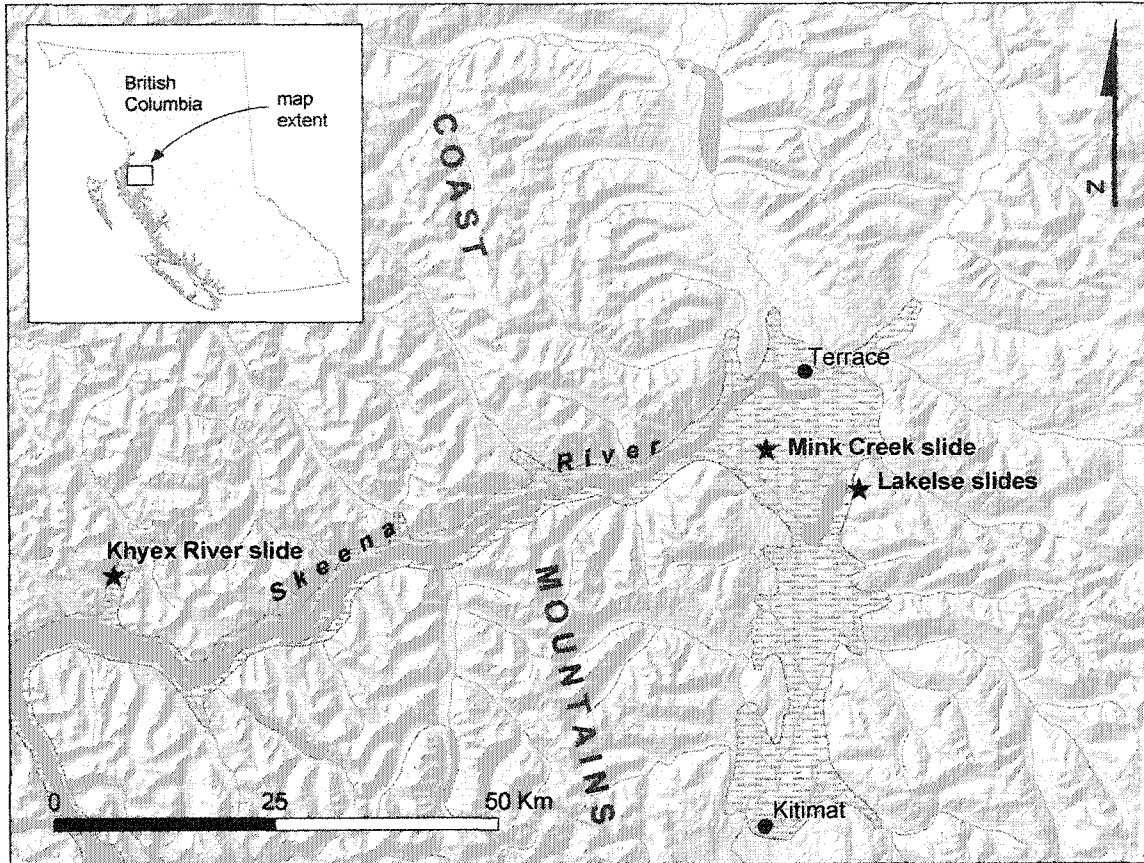


Figure 1.3 Map of the study area. Note the location of the Mink Creek landslide, as well as the 1962 Lakelse landslides and the 2003 Khyex River landslide. The dashed lines represent areas of glaciomarine sediment. I produced the hillshade image from a TRIM digital elevation model, with a false sun set at an azimuth of 315°, at an altitude of 45° degrees using ArcView.

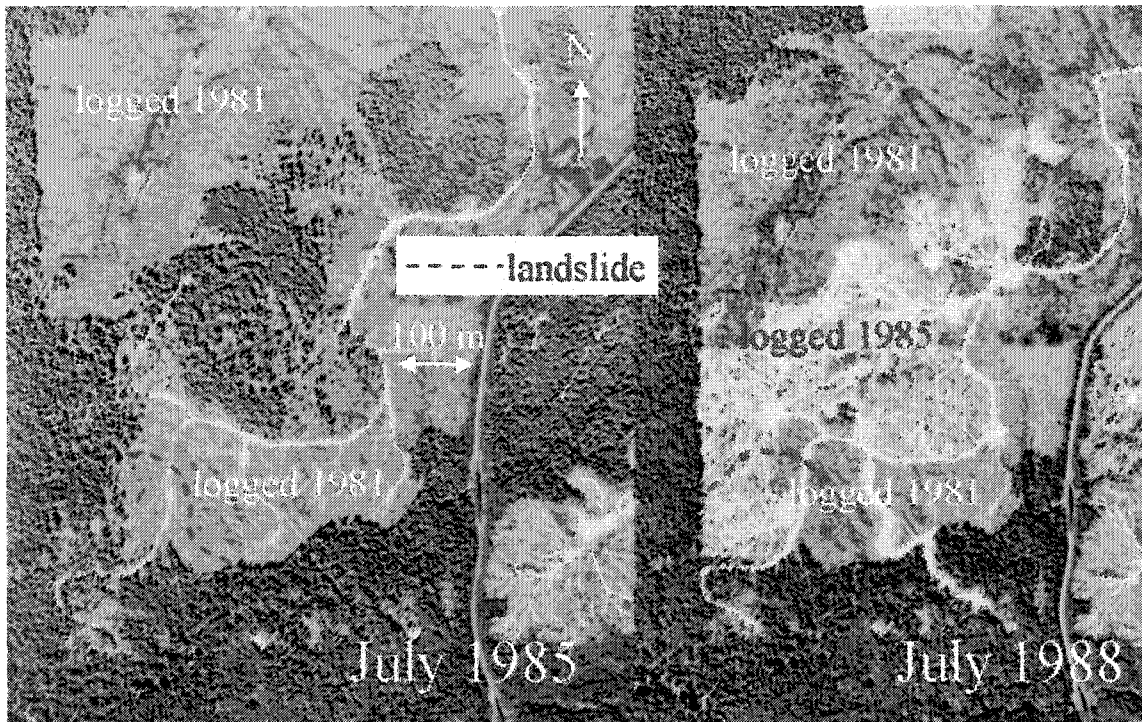


Figure 1.4 Pre-slide aerial photographs of the Mink Creek area in 1985 and 1988 showing the outline of the landslide and mature and logged forest of different ages. BC Government airphotos, 30BCC374: 158 (left) and 30BC88019: 245 (right).

1.3. Quaternary History

The Quaternary geology and deglacial chronology of the study area has been described and mapped regionally by Clague (1984). The remainder of this section is a brief summary of Clague's report. Dates are given as uncalibrated ^{14}C years before present (BP) (A.D. 1950).

The terminus of the glacier occupying the Kitsumkalum-Kitimat trough was in contact with the sea as the ice retreated inland and to the north. The glacier snout retreated from the present location of Kitimat towards Terrace about 11000 years before present. Terrace was ice-free by about 10100 BP. Although this recession was rapid it was halted by three significant stillstands. The first, occurring at about 11000 BP, is marked by a large arcuate end moraine at the present location of Kitimat. The second stillstand occurred 20 km to the north of Kitimat. An ice-contact delta constructed during this stillstand blocked the northward transgression of the sea. The third stillstand occurred near Terrace. A delta was built into a sea that transgressed eastward with a retreating ice front up Skeena Valley. It was in this sea that the sediments associated with the Mink Creek landslide were deposited.

Deglaciation was complete by about 10100 BP, but isostatic rebound continued until about 8000 years ago when local sea level had subsided to near its present level. Shorelines 11000 years old are now at 200m above sea level (asl), 10100 year shorelines at 120m asl, and 9300 year old shorelines at 35 m asl.

Shortly after deglaciation, high rates of erosion and mass wasting of sparsely vegetated and oversteepened slopes choked streams with sediment. The sediment was deposited on floodplains, fans, and deltas. The deposits were subsequently incised, partly in response to falling base levels, and many fans and tributary deltas, for instance, are now relict features. The bulk of post-glacial alluvium was deposited within 1000 years after deglaciation.

1.4. Conditions for Sensitive Clay Development

In most freshwater environments clay particles settle even more slowly than silts and tend to accumulate with a parallel orientation. In salt water, however, as in the fjord that occupied the Kitsumkalum-Kitimat trough, silts and clays form aggregates (small floccules) and settle together in a random pattern (Torrance 1983). This random alignment of particles (house-of-cards structure) gives the flocculated material a higher-than-normal amount of pore space and water content.

When the porewater of such material has a high salt content, interparticle bonds are strong. Leaching by freshwater (whether from groundwater springs or rainfall), or diffusion of salts from saline porewater to fresh porewater, particularly in the vicinity of aquifers, gradually lowers the salinity. Certain types of marine clay become prone to structural collapse, on disturbance, once the salinity of the porewater falls below a certain threshold. This is because repulsive forces between the particles increase (Rosenqvist 1953; Bjerrum 1954; Quigley 1980; Torrance 1983), and prevent the disturbed particles from reflocculating. Clays that exhibit this type of behaviour are usually called sensitive clays. In extreme cases with sensitivity, S_t , greater than 30 and remoulded undrained shear strength, C_{ur} , less than 0.5 kPa, the deposits are called quick clays (Torrance 1983). The most notable characteristic of sensitive clays is the remarkable difference in strength between an undisturbed and a remoulded soil, with the remoulded soil behaving as a fluid.

1.5. Earlier Landslides in the Study Area

The landslide that occurred between mid-December, 1993, and 9 January 1994, was not the most recent landslide in sensitive glaciomarine sediments near Terrace, British Columbia. On 28 November 2003, another large glaciomarine flowslide impounded Khyex River (Figure 1.2) between Terrace and Prince Rupert. Nor was the landslide at Mink Creek the first. The landslide is located less than 10 km from the sites of two other large flowslides that occurred in May and June 1962 at Lakelse Lake. These two landslides generated a mineralogical and geotechnical investigation (Brawner 1962, unpublished report on file with the British Columbia Ministry of Transportation and Highways, Terrace, BC), but, with the exception of an undergraduate thesis (Fair 1978), the results were never published. Other workers have referred to the Lakelse landslides

in general discussions of surficial geology and terrain hazards (Clague 1978, 1984; Evans 1982). Five thousand radiocarbon years ago, a previous landslide occurred adjacent to the site of the 1994 Mink Creek landslide. I provide more information on this ancient landslide in Chapter 2. Since the Mink Creek landslide occurred, I have identified prehistoric flowslides in the area through air photo analysis. Regional prehistoric landslides are discussed in Chapter 7.

1.6. Topographic Mapping

Morphologic mapping is based on 35 mm aerial photographs taken from a helicopter in June 1994, on field observations, and on detailed pre and post landslide topographic mapping. Pre-slide maps were generated from 1988 aerial photographs (30BC88019:244-246) and presented with 1 m contours at a 1:2500 scale. Post-slide maps were generated with 0.25 m contours and presented at a 1:500 scale. The post slide maps were created from 1994 aerial photographs (IAS(94)5369:1-27 and IAS(94)5407:1-6) with surveyed ground targets providing control.

An arbitrary elevation of 100 metres was chosen at site 1 (Figure 2.2) for survey purposes. This elevation is within 5 metres of true mean elevation above sea level, based on measurements by pocket altimeter.

Derivative products of the topographic maps include digital elevation models and cross-sections, which I made using the program ArcView.

1.7. Assumptions

I make several assumptions about our observations of features in the landslide, and briefly discuss these below.

I interpret preserved stratification in blocks to be evidence of translational movement, without internal disturbance. This material is generally soft. Convoluted strata and mottles represent disturbed material that has undergone varying degrees of remoulding and plastic deformation. This material is dense. In the zone of depletion contacts between dense remoulded material and subjacent horizontal strata represent rupture surfaces.

I interpret horizontally stratified grey ridges and intervening wedges of surface material to be evidence of spreading. The ridges are thought to be oriented transverse to flow, products of translational movement along near-horizontal rupture surfaces (Odenstad 1951; Carson 1977). Brown veneers of weathered material that drape ridges are thought to occur on the leading, down-flow edges of ridges (Carson 1979; Geertsema and Schwab 1996).

Areal expanses of grey sediment with near horizontal strata represent exposed rupture surfaces (failure planes). In these situations the depth of the depleted mass remaining above the rupture surface is zero. Carson and Lajoie (1981) refer to such zones of depletion as clean craters.

The presence of horsetail roots in the main scarp is discussed under stratigraphy. Horsetail root tips occur in some ridge crests and represent pre-slide depths of about 4 – 4.5 m.

All depths given in this paper, unless indicated to the contrary, refer to the ground surface at Site A (elevation 100.0 m, an arbitrary elevation chosen for survey purposes, which corresponds within about 5 m of actual mean elevation above sea level). Site A is the highest point on the main scarp of the landslide.

Chapter 2

Stratigraphy at the Mink Creek Landslide

2.1. Introduction

In this chapter I describe the stratigraphy of material in the Mink Creek landslide (Figure 1.2). I also discuss the thickness of the displaced material remaining in the zone of depletion.

I observed stratigraphy from exposures and excavations in the zone of depletion and from a borehole above the main scarp (see Figure 2.1 for locations). Cohesive glaciomarine deposits in excess of 100 m thick have been encountered in drill holes in the area between Terrace and Kitimat (Clague 1984). The borehole (location in Figure 2.1, summarized in Table 5.1) shows the deposit is at least 30 m thick above the landslide.

2.2. Stratigraphy

The sediment is composed of bedded silty clay with silt partings, occasional sand lenses, and rare drop stones. In general a fissured upper brown oxidized crust, 3.5 to 4.5 m thick (Figure 2.2), overlaid fissured, colour-banded, grey sediment (Figure 2.3). The material at the soil surface, formed sand-size aggregates of silty clay composition. In Mink Creek the silty clay formed aggregates ranging from sand size to gravel size clasts. More detail on material properties is provided in Chapter 3.

Some near surface complexity is imparted by the presence of the zone of depletion of a prehistoric landslide (Figure 2.4). The main scarp and depleted mass of this ancient landslide were displaced by the 1994 slide and its rupture surface was exposed in the main and eastern lateral scarps of the new slide.

I located the main scarp of the prehistoric landslide by airphoto analysis and examined excavated sections in the 1994 scarp to determine the location of its rupture surface. I simply distinguished between undisturbed horizontal bedding and tilted bedding to differentiate undisturbed sediment from displaced landslide material. Using a tracked excavator to expose the prehistoric scarp, I found undisturbed bedding and the tilted bedding of a rotational block confirming an earlier landslide (Figure 2.5). Accelerator Mass Spectrometry (AMS) analysis of buried organic material

at the base of the rotated strata gave ^{14}C year dates of 5160 +/- 50 BP and 5190 +/- 90 BP (Beta-12749 and Beta-12750, respectively).

The rupture surface of the prehistoric landslide was located at scarp site 3 at a depth of 4.2 m below the surface which translates to an elevation of 88.3 m with respect to the elevations on the topographic map. A rotational rupture surface was located at scarp site 2 (Figures 2.1 and 2.5), but the translational surface was not found and here the rupture surface is below the 94 m contour. Elsewhere, a fissure in the 5,000 year old displaced material was infilled with brecciated mud (Figure 2.6). An excavation at scarp site 4 confirmed the placement of the boundary of the prehistoric landslide. No disturbed or tilted bedding was observed at these locations, thus I infer that these sites lay outside of the boundaries of the old slide.

The upper 10 m of sediment examined from the borehole at (Figure 2.1) show signs of disturbance, including open fissures, as might be expected from the location within an old landslide's zone of depletion. Thin silt seams occurred throughout the core, with sand lenses and laminae becoming increasingly frequent at local depths more than 15 m. These seams sometimes had dips of 10 to 20 degrees, and may have been tilted blocks from the 5000 ka landslide. Convolute bedding occurred even at a local depth of 20 m, though whether this is from the prior episode of landsliding is not known.

I made two other important observations during the excavations. 1. *Equisetum arvense* (horsetail) roots penetrate vertically through the soil (Figure 2.7) to depths ranging from 4.0 to 4.6 m. The roots also penetrate through tilted strata vertically, in line with findings of Cody and Wagner (1981). 2. The brown, oxidized crust is up to 0.5 m thinner outside of the prehistoric slide, than within it.

2.3. Thickness of Displaced Material in the Zone of Depletion

Visual assessment of the amount of remaining displaced material in the zone of depletion of any landslide is difficult, being largely influenced by the height of the scarps. Small main scarps do not always indicate thick displaced material: they can result from relatively shallow basal rupture surfaces (Geertsema and Schwab 1997).

At Mink Creek, however, the rupture surface itself is exposed over a fairly large part of the central area of the zone of depletion suggesting that the amount of residual displaced material in the zone of depletion is relatively small (Figure 2.11). It is thicker in the western part of the landslide. Figures 2.1 and 2.4 are digital elevation models of the landslide showing the pre and post landslide

topography. The slide surface slopes towards the creek (60 to 62 masl), dropping in elevation from 79.5 m to 76 m over a distance of 100 metres, corresponding to a slope of 2-3°. The mean elevation across the zone of depletion over the entire landslide is only about 78 m asl compared to 90-95 m asl for the original ground surface. The displaced material thickness along this section is therefore only about 10 to 15 percent of the original sediment thickness. The lowest exposed surface of rupture occurs at an elevation of 73 m. This observation confirms the minimal thickness of displaced material and also indicates that the Mink Creek landslide was a perched landslide, with the rupture surface being about 10 m above the pre-slide level of the creek.

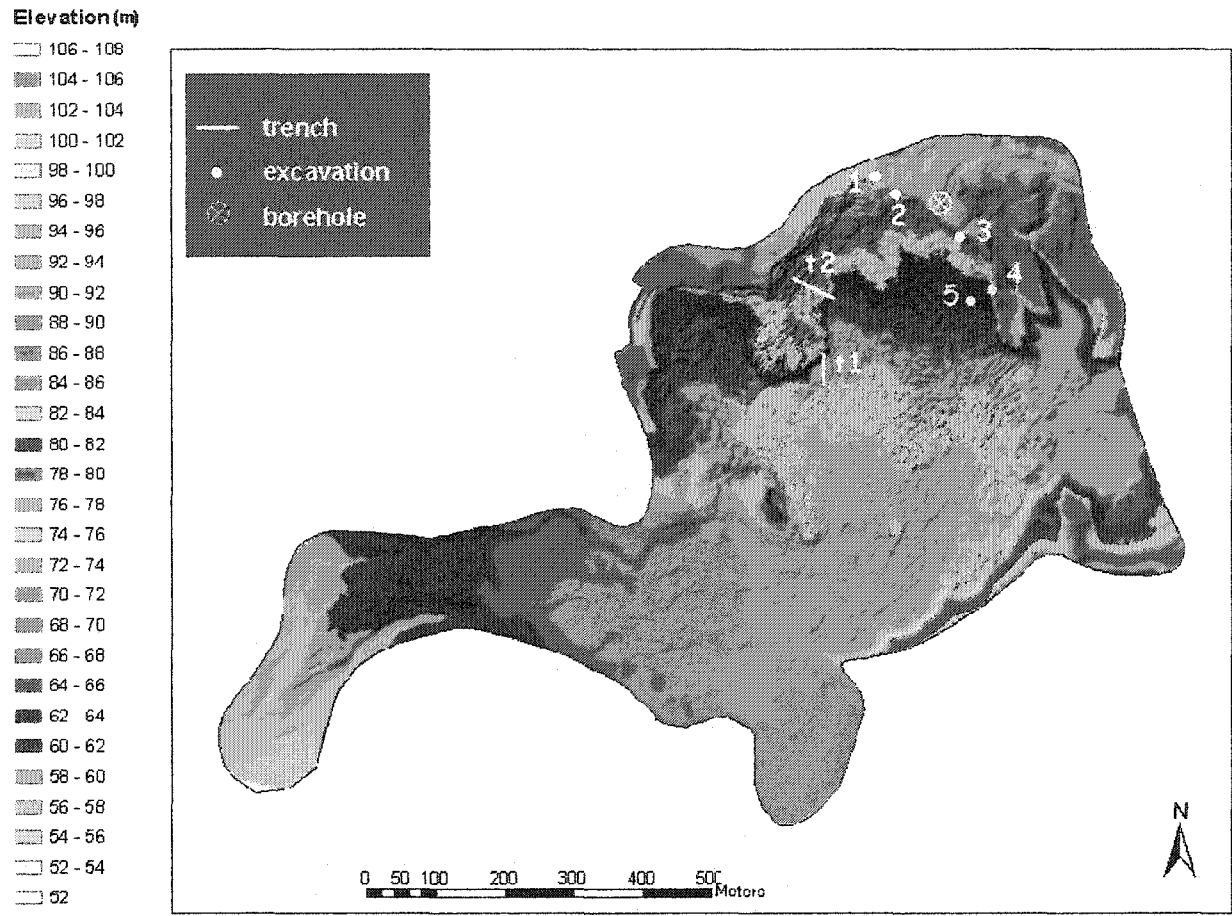


Figure 2.1 Digital elevation model (DEM) of the Mink Creek landslide showing excavated trenches, point excavation locations, and a borehole. The DEM is based on aerial photographs taken in 1994.

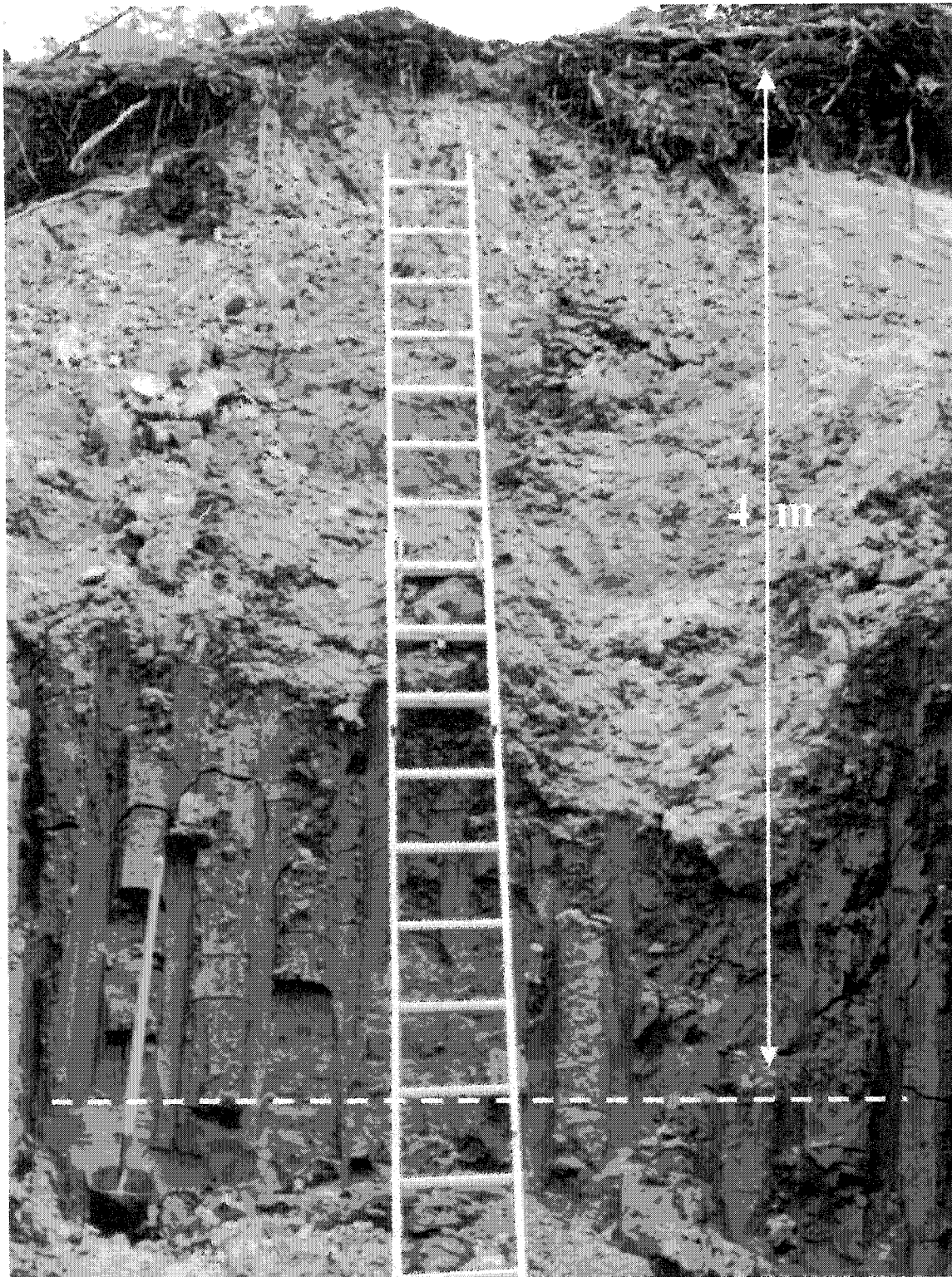


Figure 2.2 This excavation in the main scarp shows 4 m of brown weathered crust overlying grey depth material.

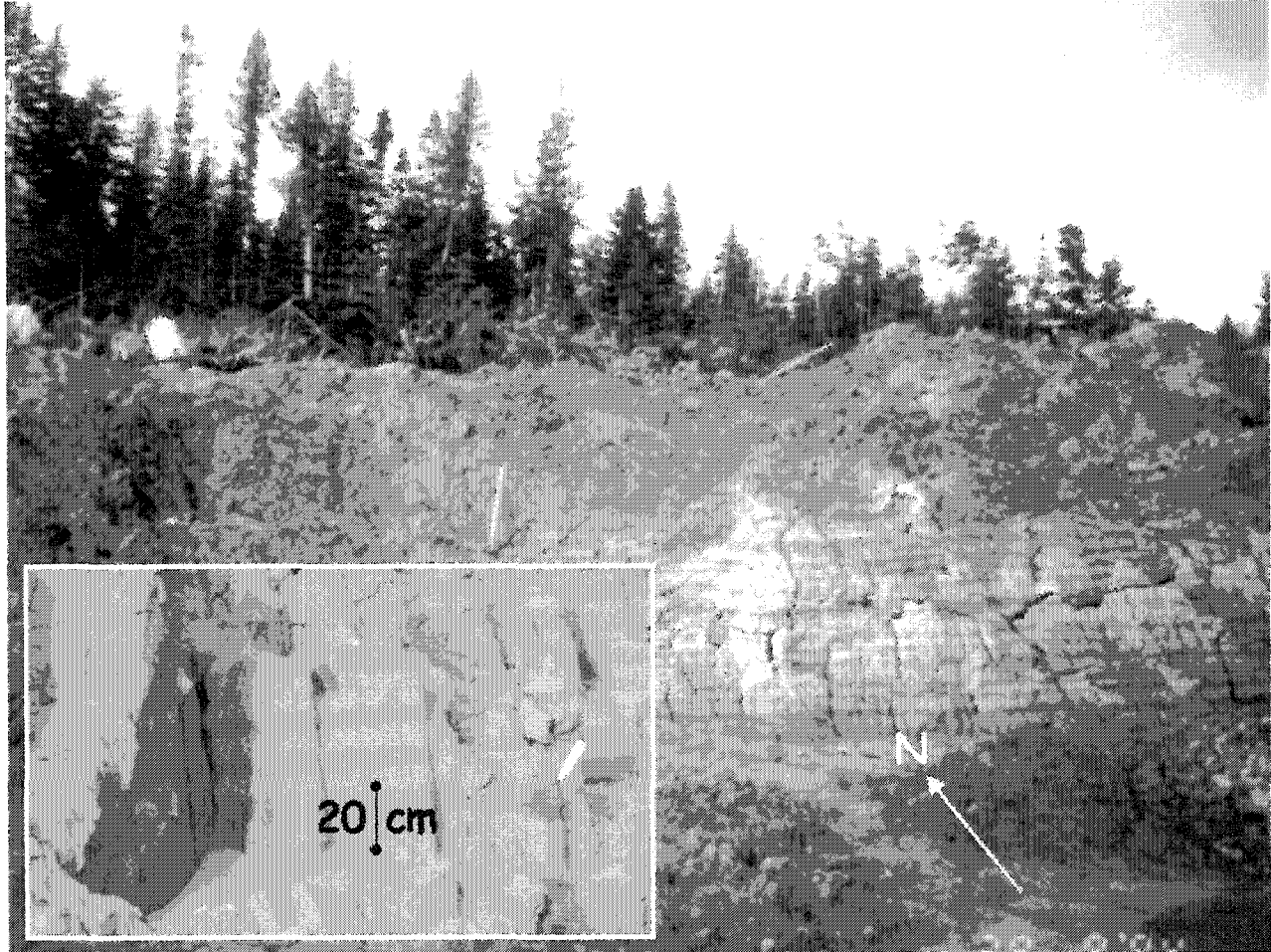


Figure 2.3 Colour banded grey sediment (depth material) is exposed in a near vertical wall of the Butte in the zone of depletion. See section 2.5.7 for a detailed description of the Butte. Shovel (centre) is 1.5 m in length.

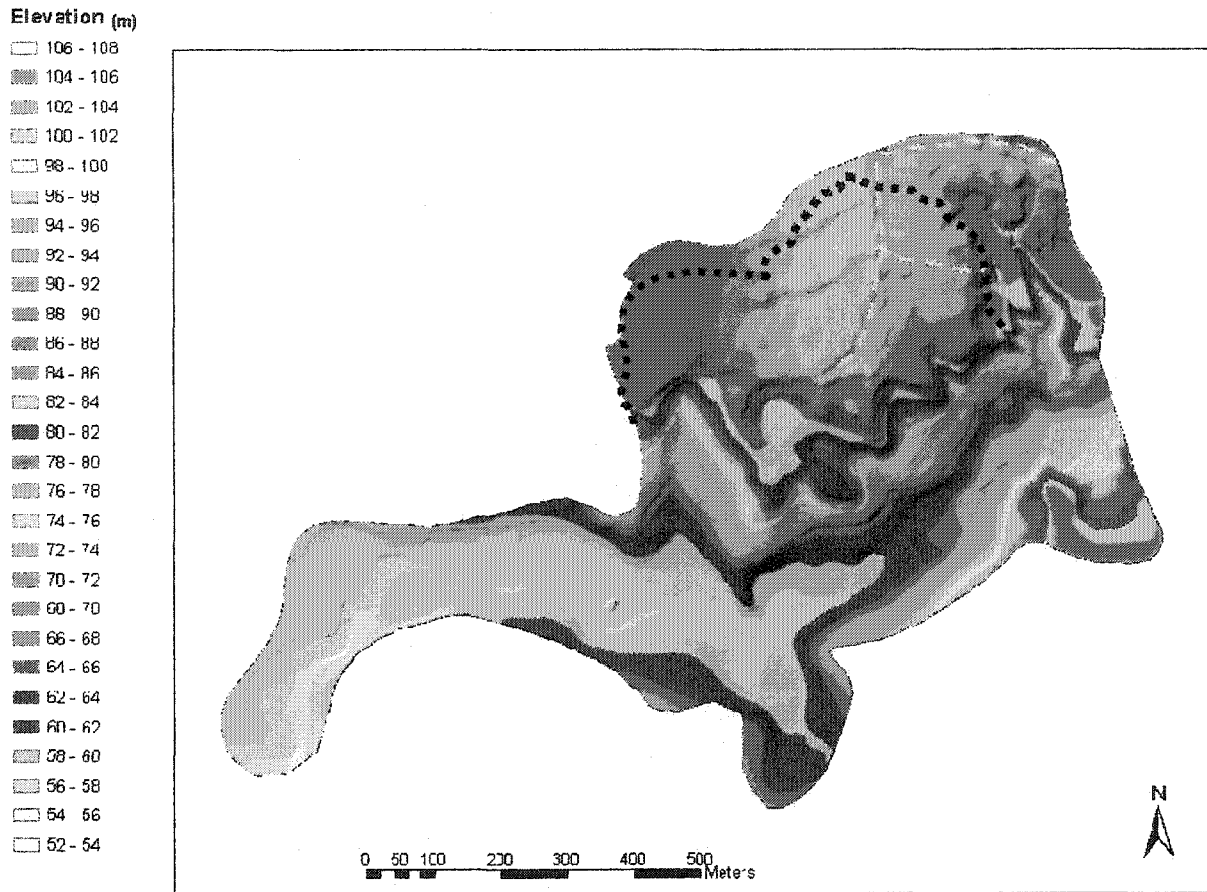


Figure 2.4 Digital elevation model of pre-slide topography at Mink Creek. Black stippled line outlines the 1993/1994 main scarp. Yellow dashed lines represent the scarp of a 5000 year old landslide. The 73 m contour marks the elevation of the surface of rupture where it daylight in the valley, thus the landslide is perched above the valley bottom. The DEM is based on aerial photographs taken in 1988.



Figure 2.5 Excavation at the intersection of the main scarps of the prehistoric landslide and the 1993/1994 landslide (site 2 in Figure 2.2). Note the concave surface of rupture separating horizontal from rotated bedding. The horizontal bedding is undisturbed material outside of the prehistoric landslide. Shovel is 1.5 m long.

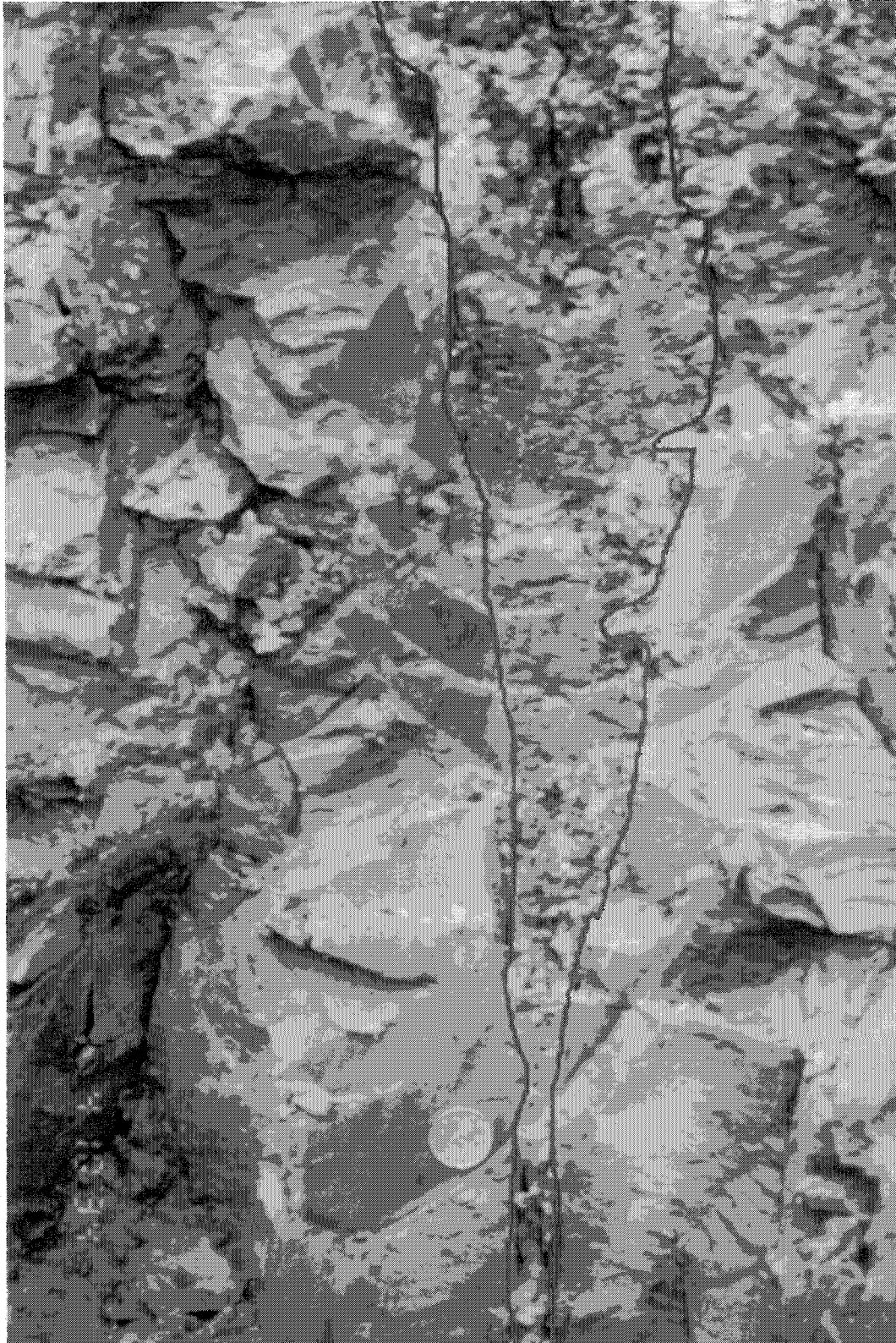


Figure 2.6 A fissure in prehistoric displaced material exposed in the main scarp has been infilled with sediment. Note the bedding on either side of the fissure and the brecciated structure of the infilled material. A Canadian dime (1.8 cm diameter) provides scale.

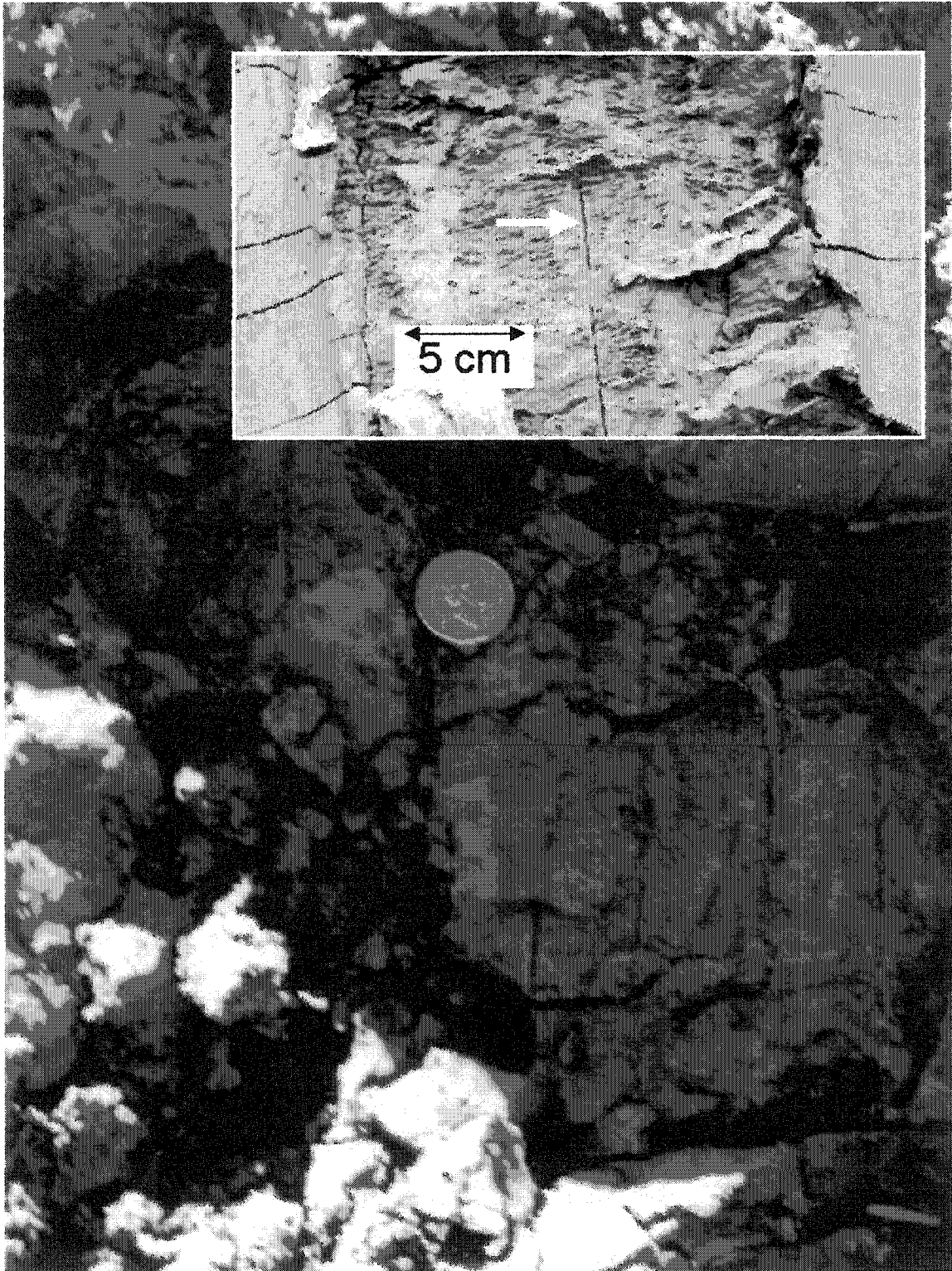


Figure 2.7 An excavation in the main scarp shows vertically oriented *Equisetum arvense* roots (arrow). These horsetail roots are ubiquitous in the weathered crust and extend to depths of 4.6 m. The coin is 2.8 cm in diameter. The inset photo provides a closer view of these roots.

2.4. Conclusions

Although the stratigraphy of the glaciomarine sediment at Mink Creek is relatively simple, there are a number of important points. The brown upper crust is weathered and much stronger than lower grey material. Evidence is provided in Chapter 5. Banding of various colours is evident in the lower sediment, and is further discussed in Chapters 5 and 6. Distinctions can be made between disturbed and undisturbed material exposed in the main scarp, indicating the presence of an old landslide deposit. The presence, vertical orientation, and maximum depth of horsetail roots exposed in the main scarp, are critical in Chapters 3 and 6, for documenting the degree of lowering of ridge crests, and therefore interpreting the mode of movement.

Although the thickness of displaced material is variable in the landslide, there is in general little remaining depleted mass in the zone of depletion. This becomes important in the interpretation of movement in Chapter 6.

Chapter 3

Morphology of the Zone of Depletion

3.1. Introduction

In this chapter I describe the morphology of the displaced material in the Mink Creek landslide. I describe zones (Figure 3.1) within the zone of depletion and the associated morphology of the surface materials in each zone. Here I also describe meso scale movements – local movements at the metre scale (1 to 10 m). Macro scale movements (at the 100 m scale), synthesizing meso scale movements, are dealt with in Chapter 5.

3.2. Detailed Morphology of the Zone of Depletion

3.2.1. Overview

The Mink Creek landslide deposits have a variety of patterns in plan form (Figure 3.1). Grey ridge crests range from wavy to, crescentic, to slightly curvilinear, to straight with slightly curved ends, to straight. Vegetated surfaces, often, follow the patterns of these ridges, but have, in other cases, irregularly shaped plan forms. Most of the surface of the zone of depletion is covered with weathered, brown surficial sediment, in forms that include linear and curvilinear ridges, and broad areas with hummocky surface expression. In the centre of the zone of depletion there are also grey, planar rupture surfaces up to 700 m², dipping 2 to 3° to the south. There is only one example where such a surface is convex rather than planar.

Ridges exhibit a variable internal disturbance. Grey ridges may be undisturbed, preserving horizontal preslide bedding, slightly disturbed, tilted, or severely remoulded. I have numbered prominent ridges and refer to these and other sites in Figure 3.2. Brown ridges of surface material are invariably highly disturbed.

As discussed in Section 1.7, I interpret ridges as indicators of slide movement. Undisturbed grey ridge crests are oriented transverse to interpreted movement directions. These ridges are similar to those reported in other landslides (e.g., Odenstad 1951, Carson 1977, Evans and Brooks 1994), where it is accepted that their alignment is at right angles to local movement. Ridges with crescentic, arcuate planforms indicate centripetal movement, while some tilted grey ridges have parabolic, lobate planforms, with centrifugal movement (Figure 3.3). Brown ridges exhibit lobate or

longitudinal planforms. The distribution and orientations of ridges in different zones in the zone of depletion, indicate complex movement patterns. In Figure 3.4 I show a possible evolution of lobate parabolic ridges to longitudinal ridges.

Attributes of horizontally stratified ridges are listed in Table 3.1. Brown surficial soil veneers drape the down flow sides of two thirds of the grey ridges. Carson (1979) also makes this observation. Only in two cases (6%) do they drape both sides of ridges. Thus a survey of veneer orientation may be useful in interpreting the direction of movement. Nearly one fourth of the ridges have horsetail roots in their crests. From the observations in Chapter 2 it is clear that these roots extend to maximum depths of 4.0 to 4.6 m, just to the base of the weathered crust. Observations of horsetail roots in these ridges are, to my knowledge, not reported elsewhere in the literature. Folded ridge crests, oriented down flow, occur in 21% of the ridges. In these cases only the upper 10-15 cm is folded, the lower sediment is all horizontally stratified. As with the soil veneers, these features can be used to interpret the direction of movement. This phenomenon, to my knowledge, has also not been previously reported. Five of the ridges underwent back toppling, a product of ridge degradation upon transport (Carson 1979). Other ridges have split in cross-section and longitudinally.

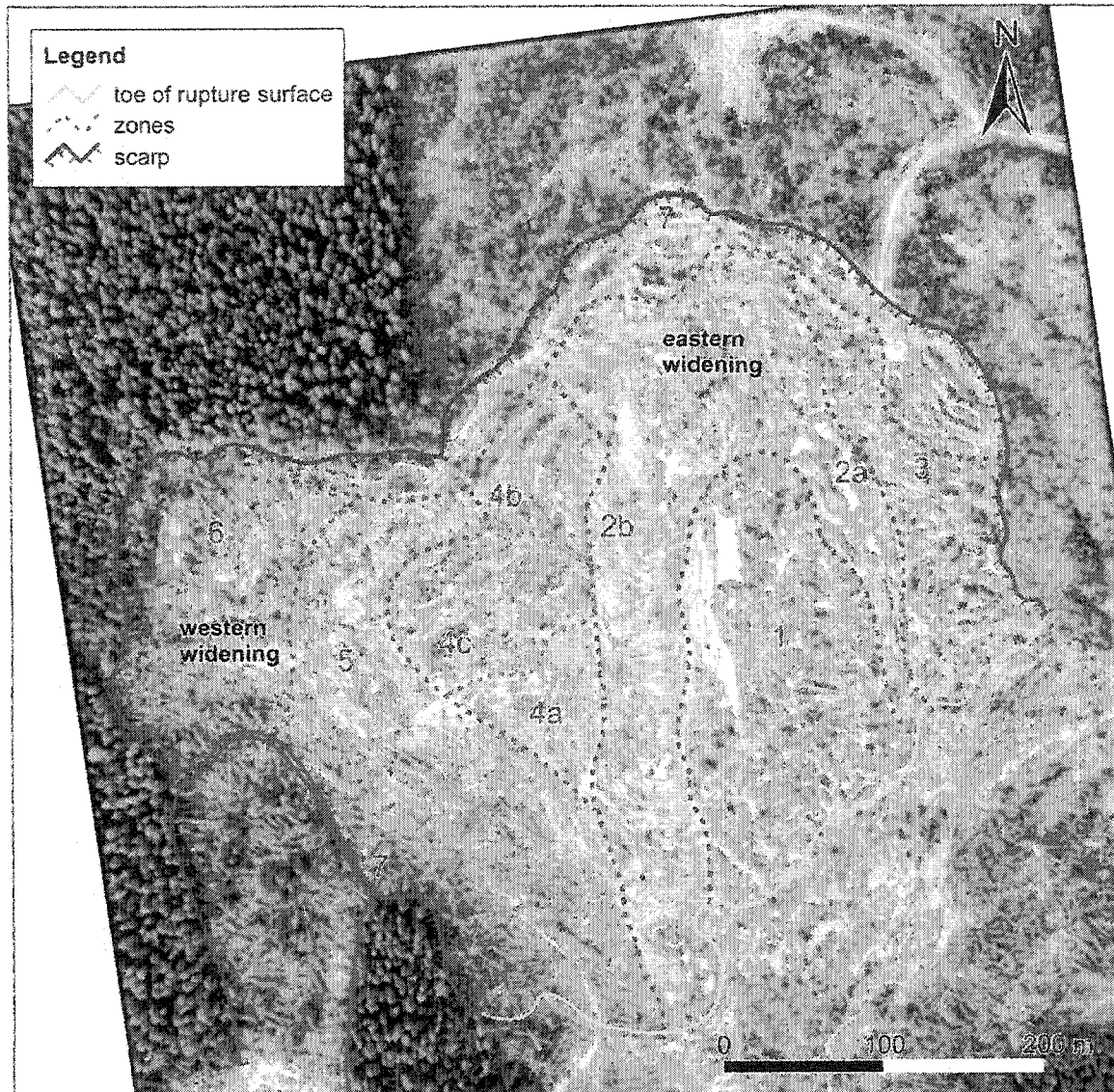


Figure 3.1 Aerial photo (35 mm) of the zone of depletion, April 1994. Note the locations of the eastern and western widenings, and numbered zones.

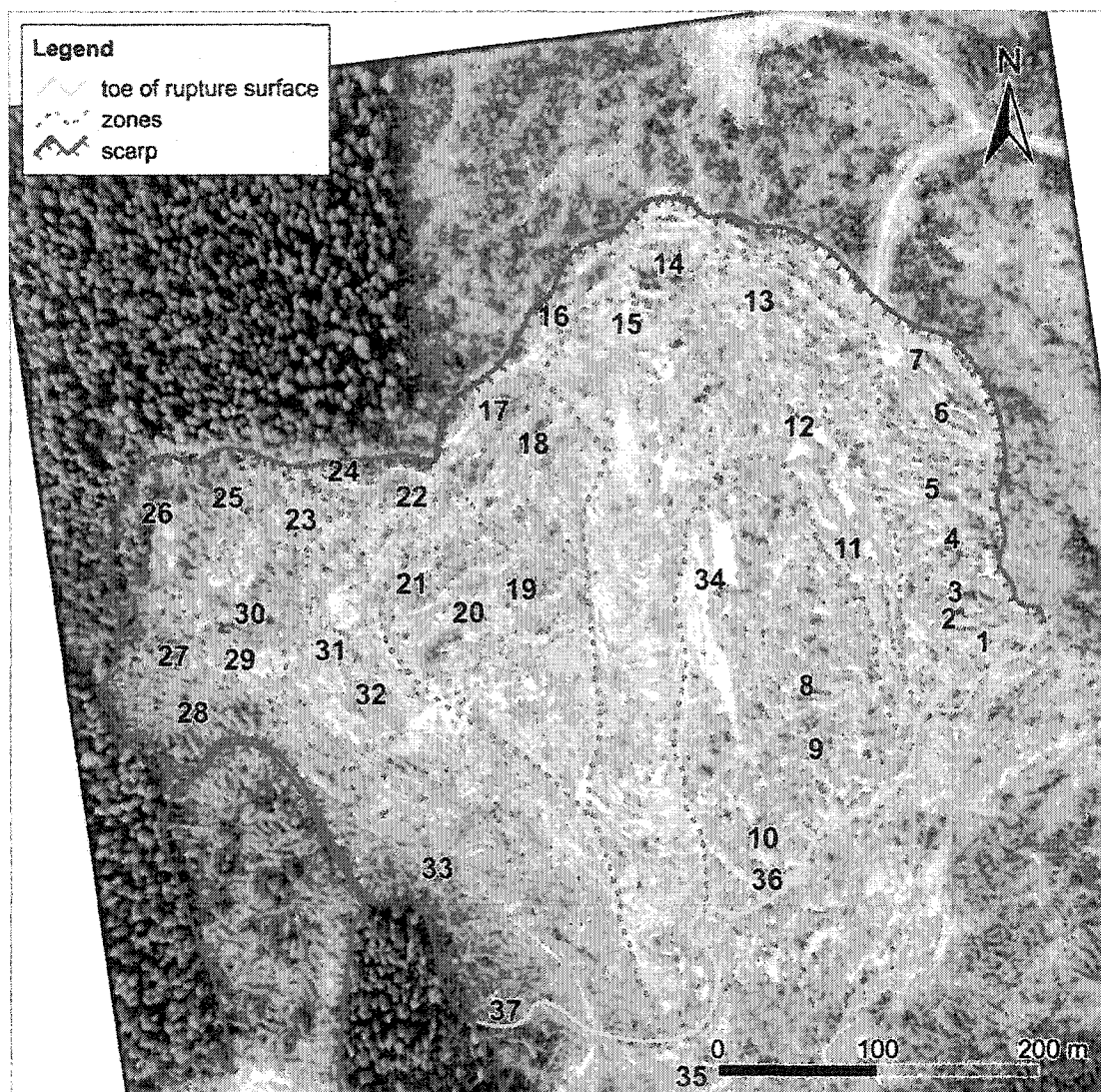
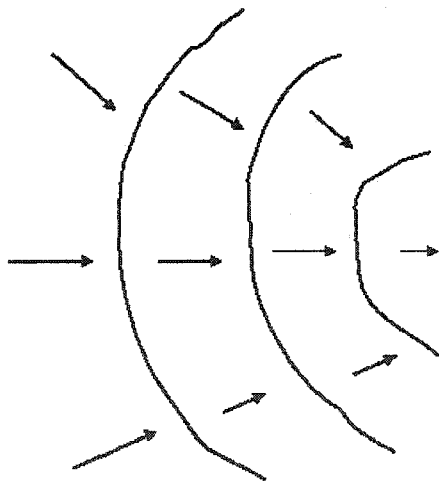
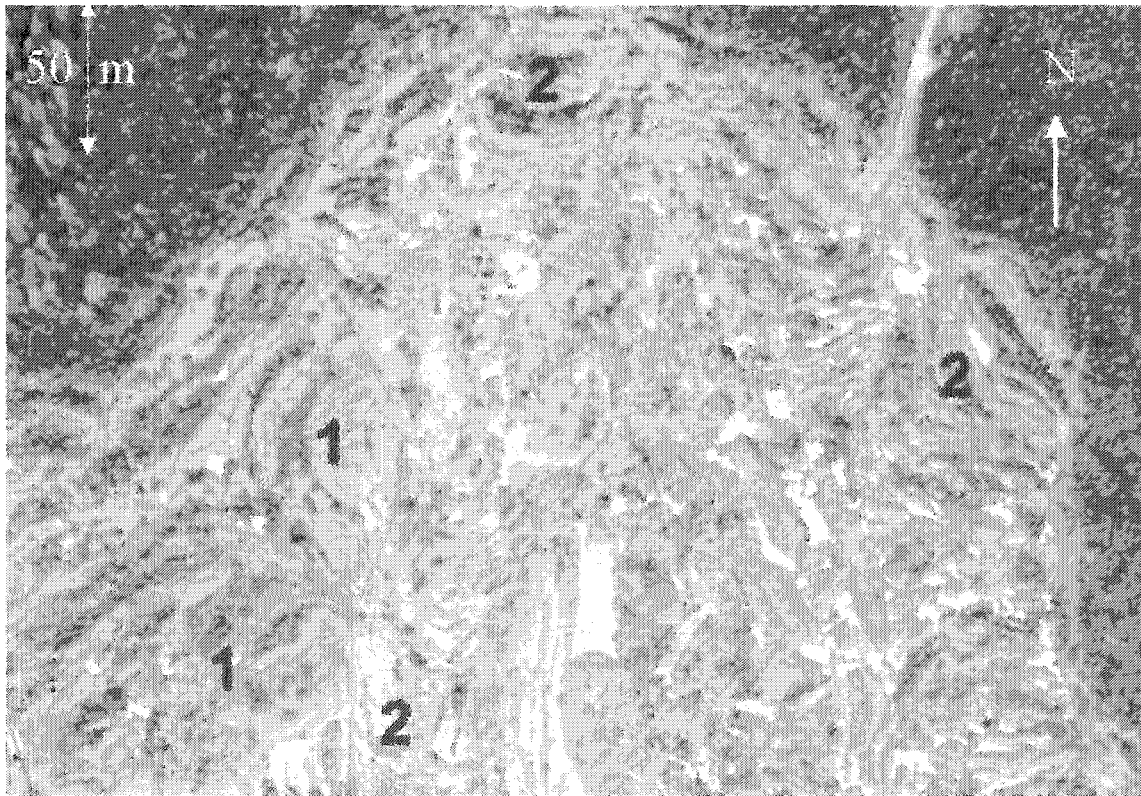
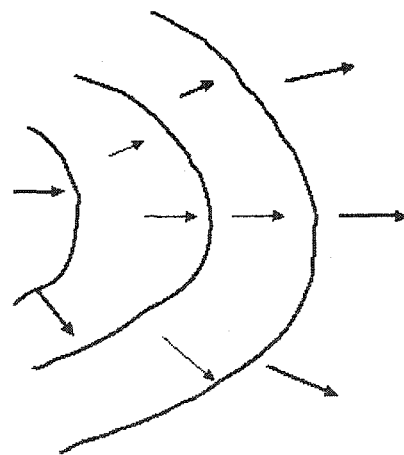


Figure 3.2 Aerial photo (35 mm) of the zone of depletion, April 1994. Note the locations of the numbered sites, most of which are transverse, horizontally stratified ridges. The yellow line is the boundary between the zone of depletion and the zone of accumulation.



1. Arcuate ridges with centripetal movement.



2. Parabolic ridges with centrifugal movement.

Figure 3.3 1994 aerial photograph of the Mink Creek landslide and schematic diagrams of parabolic and arcuate ridges with interpreted direction of movement.

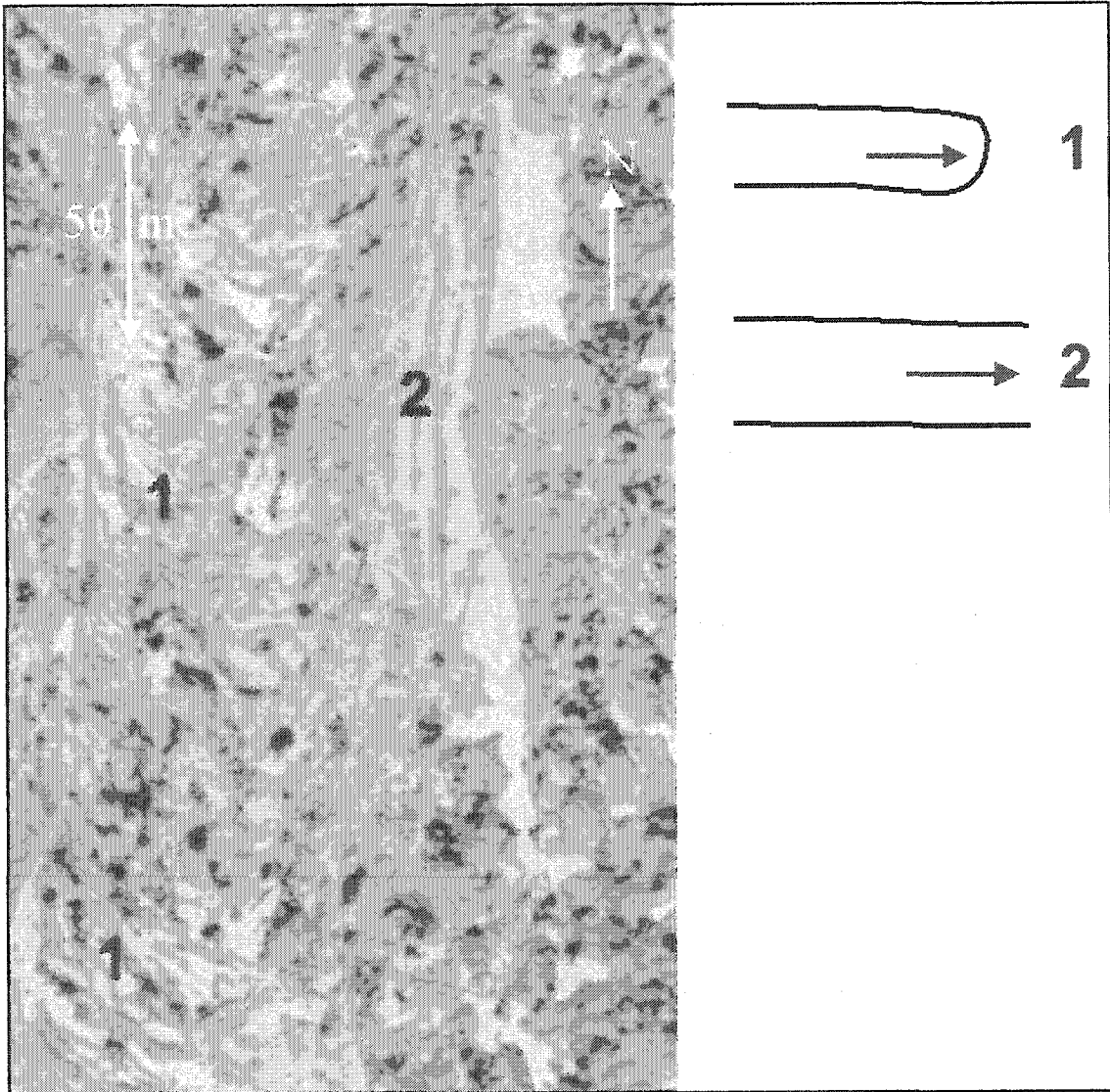


Figure 3.4 Possible evolution of lobate parabolic ridges to longitudinal ridges. Movement to South.

Table 3.1. Characteristics of horizontally stratified ridges.

Ridge	soil veneer (down flow)	soil veneer (up flow)	horsetail roots	folded crest	back topple
1	slight	yes	yes		
2			yes		yes
3					
4	yes			yes	yes
5	yes		yes	yes	
6	yes				
8	yes				yes
9	yes				
10	yes				
11	yes				
15	yes				
16	yes		yes		
17	yes				
18			yes		
19	yes		yes	yes	
20	yes		yes		
21	yes			yes	
22				yes	
23	yes				yes
24					
25					
26	yes		yes	yes	yes
27					
28				yes	
29					
30	yes				
31					
32	yes	yes			
33					

3.3. Zone 1

Zone 1 (Figure 3.1) is the zone in which I believe the first movements have occurred. The zone is 300 m long and up to 150 m wide at the toe of the rupture surface. It is something of an eclectic zone containing clusters of horizontally stratified ridges trending roughly E-W, wide expanses of hummocks of brown surficial material, as well as areas of exposed rupture surface which slope upward to the crown of the landslide along a stratigraphic dip of 2-3°.

3.3.1.1. Horizontally Exposed Rupture Surface

The Dance Floor is the most extensive area of exposed rupture surface. It measures about 15 m wide by 40 m long (Figures 3.5, 3.13, and 3.14). Two blocks of grey material with disturbed bedding are located at the downslope side of the exposed surface. A 0.5 m thick discontinuous ridge runs longitudinally down the exposed surface joining the two blocks at their contact. These blocks then appear to have cleared the Dance Floor, exposing the rupture surface. The rupture surface, exposed here, is 1 m higher in elevation than a covered rupture surface directly to the west. The Dance Floor has a dip of 2-3° to the South. Its surface is heavily fissured, with dominant fissure sets oriented near vertically and at nearly right angles in plan form (Figure 3.5).

On the exposed surface I found a small, decimetre high, up flow facing scarp (Figure 3.6), as well as a lateral scarp (Figure 3.7). In both cases bedding was continuous from the lower surface through the upper surface ruling out normal faulting due to differential subsidence.

A convexly curved rupture surface at site 36 (Figures 3.4 and 3.8) is exposed at the southern boundary of this zone at an elevation of 73 m. This is the location of the toe of the rupture surface, separating the zone of depletion from the zone of accumulation. This elevation is about 10 m above the bottom of the 1988, preslide valley. Interestingly, the main rupture surface cuts across bedding here, dipping to 25°. Elsewhere the rupture surface occurs along the bedding planes of the sediment.

Exposed rupture surfaces also occur to the west of the Dance Floor, and are here, covered with thin north-south trending lineaments of oxidized weathered material with irregular spacing.

3.3.1.2. Horizontally Stratified Ridges

Ridges at sites 8 and 10 (Figures 3.4 and 3.9) occur in spaced clusters, with only the downslide face of the leading ridge covered with a veneer of weathered material. It is clear from the airphoto (Figure 3.4) that these ridges have fractured with only the leading edges of the entire ridge cluster veneered with brown soil. The thickness of the beds is also noteworthy here. In intact ridges thick beds correspond to stratigraphically lower zones than thin beds. Variations in bed thickness show stratigraphic elevational differences of up to 2 m in these ridges. This indicates that portions of the ridge have subsided up to 2 m during movement.

In addition to ridge fracturing, it seems that there is also late stage fracturing of more disturbed units of the slide mass.

3.3.1.3. Thin, Remoulded Linear Ridges

Figure 3.10 shows continuous and discontinuous ridges of structureless brown and grey material. The ridges are seldom more than 1 m high and wide, but extend longitudinally for up to 100 m. These ridges, oriented parallel to the direction of movement, and separated from each other by exposed rupture surface, only occur in the vicinity of the Dance Floor. They appear to be remnant streaks on an eroded surface. In places these ridges have undergone late phase extension.



Figure 3.5 The Dance Floor, a remarkable 15 x 40 m expanse of exposed rupture surface dipping 2-3° to the south. Note the prominent fissures. The two ridges at the far end of the surface cleared it by late stage sliding.

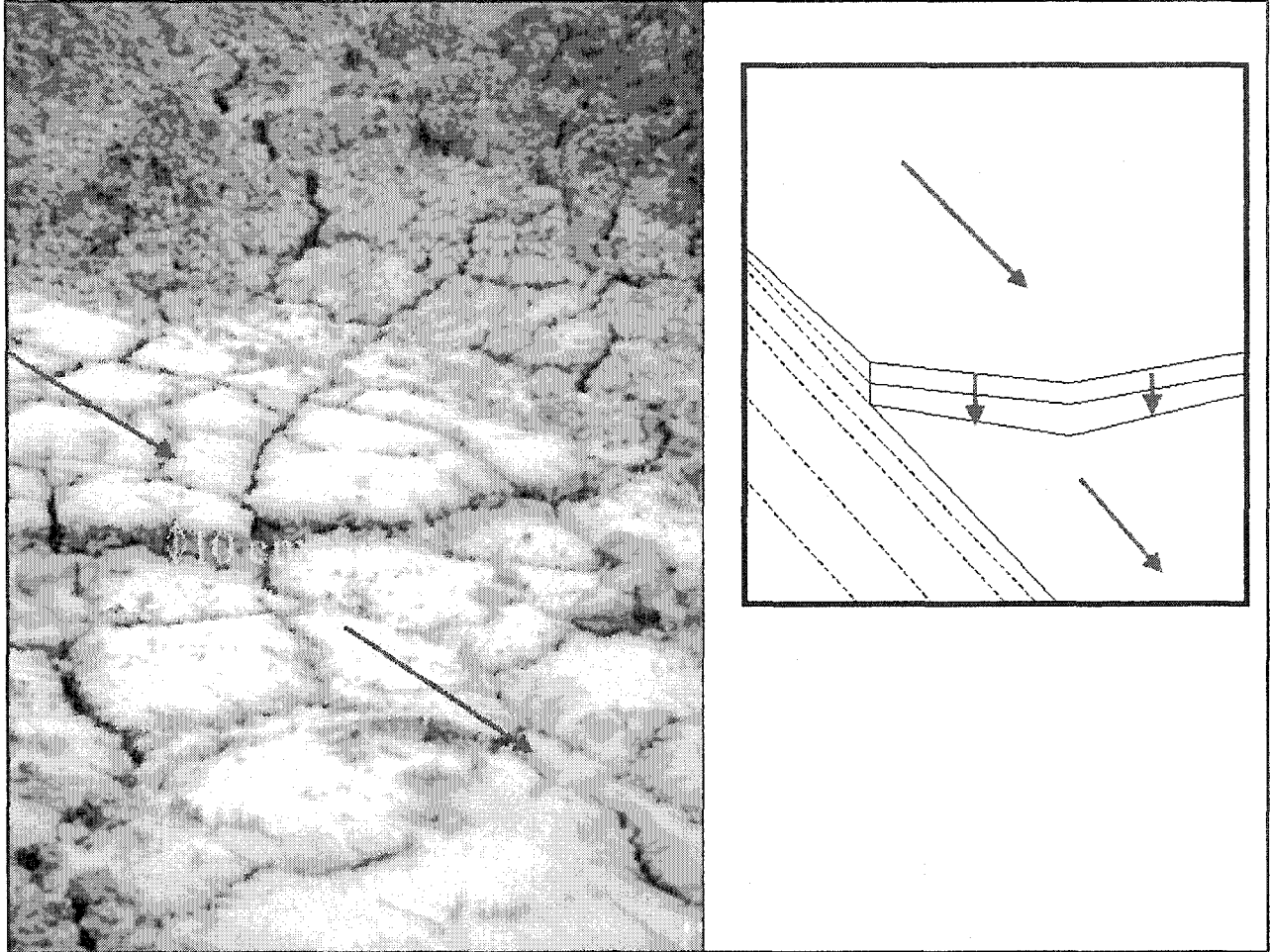


Figure 3.6 A transverse scarp in an exposed rupture surface in zone 1. Continuous bedding indicates the scarp is not a fault. It probably formed along a fissure.

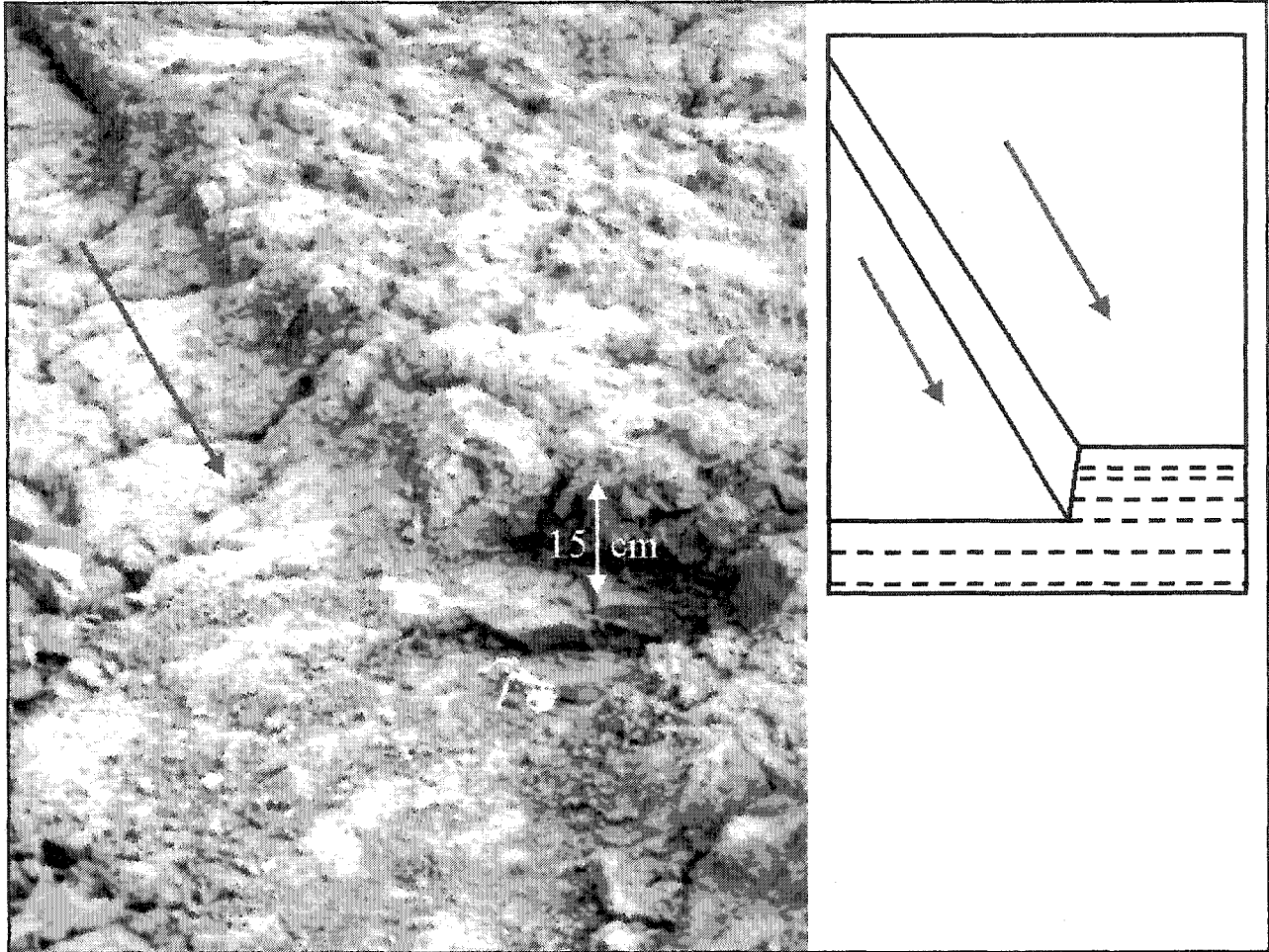


Figure 3.7 A lateral scarp in an exposed grey rupture surface in zone 1. Continuous bedding reveals that the scarp is not a fault. Brown material is a lag of surficial soil.



Figure 3.8 A convex rupture surface at site 36 (same as vane shear site E), at the toe of the rupture surface, separating the zone of depletion from the zone of accumulation. Note the pronounced striated slickensides. Bedding is at 3° and the surface of rupture here has cut across the bedding.

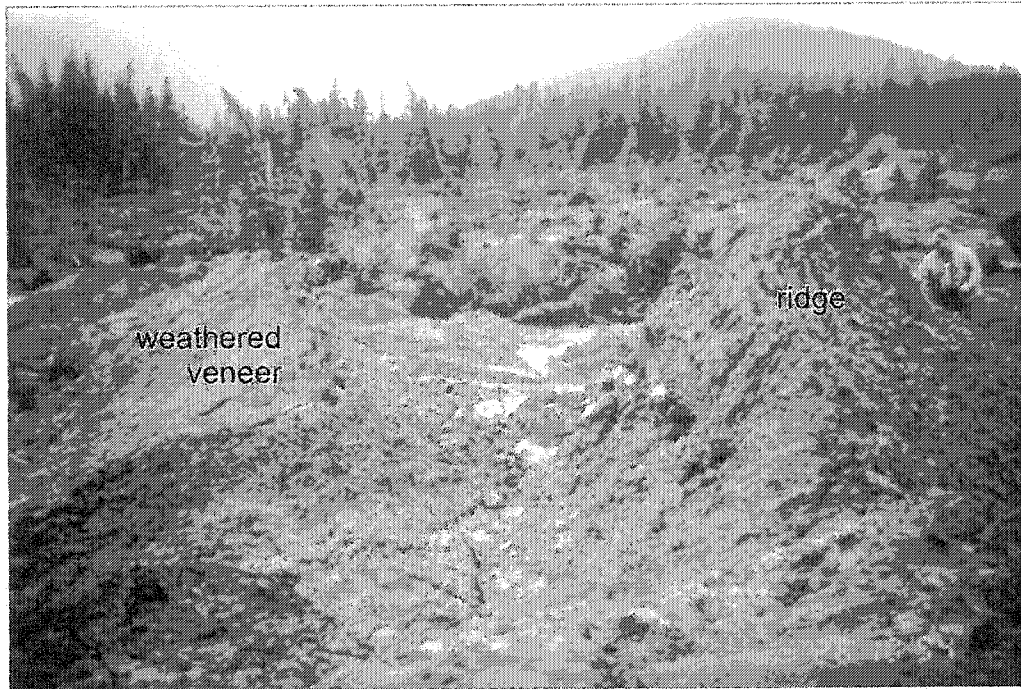


Figure 3.9 Split ridges at sites 8 (*Top*) and 10 (*Bottom*). Only the leading side of these ridges tends to be covered with a thin veneer of brown surficial material. The ridges are 2.5 m high.

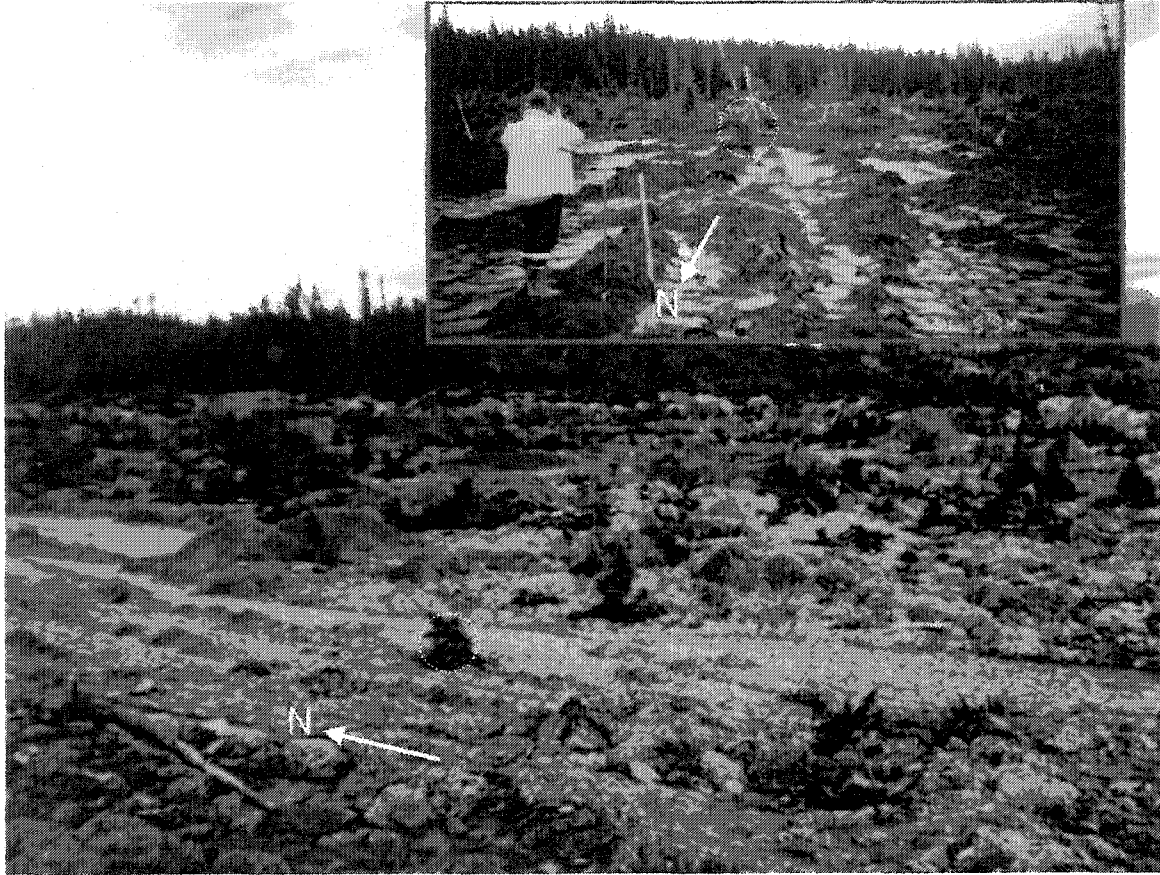


Figure 3.10 Linear ridges of primarily surficial material on an exposed grey rupture surface in zone 1. The dashed circle outlines the same conifer on both images. Movement was to the south.

3.4. Zone 2

Zone 2 is horseshoe – shaped with two limbs surrounding zone 1 (Figure 3.1). Ridges in this zone trend roughly north-south, arching together north of zone 1. Zone 2a forms the eastern limb of zone 2. It is characterized by ridges with preserved horizontal bedding that trend roughly north-south. Zone 2b, the western limb of zone 2 is flanked to the west by the escarpment of zone 4, and by merging flows of zone 5. This zone contains no undisturbed ridges, and has extensive areas of exposed rupture surface.

3.4.1.1. Zone 2a

Zone 2a separates zone 1 from zone 3. It is characterized by grey ridges trending roughly north-south (Figure 3.1). The zone is narrow, 25 m wide over its southern 75 m. Grey ridges with horizontal bedding in this zone have split during movement. Back-tilted ridges (40° dip E) are stratigraphically higher than the horizontally stratified central ridges. The leading edges of the back-tilted ridges are covered with a thin veneer of oxidized mud. Intact ridges with horizontal bedding had slightly back-tilted tops.

Ridge 11 is horizontally stratified with a tabular top, and its surface is coincident with the bedding in the ridge (Figure 3.11). Presumably the upper prism slid off.

In the northern, wider part of this zone, tilted blocks, up to 2.5 m high, trend 340° with bedding dipping 25° at approximately 70°. Slabs of grey mud, 10 cm thick, moved along bedding planes in tilted ridges (Figure 3.12).

3.4.1.2. Zone 2b

Disturbed grey and brown ridges up to 2 m wide are oriented north-south, or in south pointing lobes. Broad grey and brown bands up to 200 m long and 15 m wide (Figures 3.13 and 3.14), oriented north-south are located in the northern part of zone 2b and south of the Butte (zone 4). The orientations of these broad bands mirror the orientation of ridges in zone 2a, and have similar spacing as the ridges in zone 4 (Figure 3.1). Well-developed lateral and internal shear zones also occur within this zone.

3.2.3.2.1 The Broad Bands

Alternating brown and grey bands of disturbed material up to 15 m wide and 250 m long occur east (Figures 3.13 and 3.14) and south of the Butte in zone 4a (Figure 3.16). There is very little mixing between grey and brown materials within these bands. The bands east of the Butte, in particular, appear to have been longitudinally extended resulting in the formation of cavities between hummocks and ridges with up to 1 m vertical relief. The bands south of the Butte are continuous with ridges and wedges on the Butte, essentially mirroring their plan form orientation, so that together they join to form an arcuate widening. The bands east of the Butte trend north-south, bend about 20° east of north, following an orientation similar to the mirror of the planform pattern of the Far East Central Zone. These bands are relatively close to the contact zone with the Butte.

The longitudinal preservation of these bands and their sharp lateral boundaries suggest little post-development movement, but rather widespread instantaneous subsidence through liquefaction of subsurface material, with post-subsidence longitudinal extension on a gently dipping rupture surface, with little lateral displacement or mixing. What is further noteworthy is that the centres of these bands have similar spacing to ridges on the Butte.

3.2.3.2.1 Lobate Forms and Mottled Topography

Although lobate forms are not confined to zone 2b (they also occur in zone 5), they are the most conspicuous there (Figure 3.13). This may be in part due to the lack of tree cover on the displaced material in this zone. The lobes are composed of highly remoulded brown and grey ridges generally less than 1 m in height. They are constrained by well-developed lateral shear zones, but also occur through the broad bands described above.

Dispersed throughout the lobate patterns are mottled zones with disturbed grey and brown hummocks and extensional depressions (Figure 3.13). Both forms appear to be associated with thinning by flow and longitudinal extension.

3.2.3.2.1 Shear Zones

Shear zones are found in the form of long linear grooves (Figures 3.1 and 3.13), rather than ridges common in viscous earth flows (Bovis 1985). One lateral shear zone forms the boundary between

zone 2b and zone 4, and zone 2b and zone 5. Another lateral shear zone forms a partial boundary between zone 2b and zone 1. The shear zones extend beyond the zone of depletion into the zone of accumulation. A short arcuate shear zone forms a triple junction with the upper and northern middle Butte surfaces at their eastern margin (Figure 3.16).

3.2.3.2.1 Elevation of the Rupture Surface

Excavations reveal that the lobate ridges do not directly overlie the rupture surface adjacent to the Butte, but rather overly approximately 1 m of remoulded grey mud. South of the Butte, the rupture surface is 2.3 m below the ground surface. Thus, there the elevation of the rupture surface is about 74.75 m, while it is about 76.25 m due west on the areally exposed rupture surface. Perhaps the rupture surface was lowered during the liquefaction process.



Figure 3.11 A horizontally stratified ridge at site 11 in zone 2a, has had its upper strata removed during the landslide process.



Figure 3.12 Secondary movement of a 10 cm thick stratum in a tilted block in zone 2a.

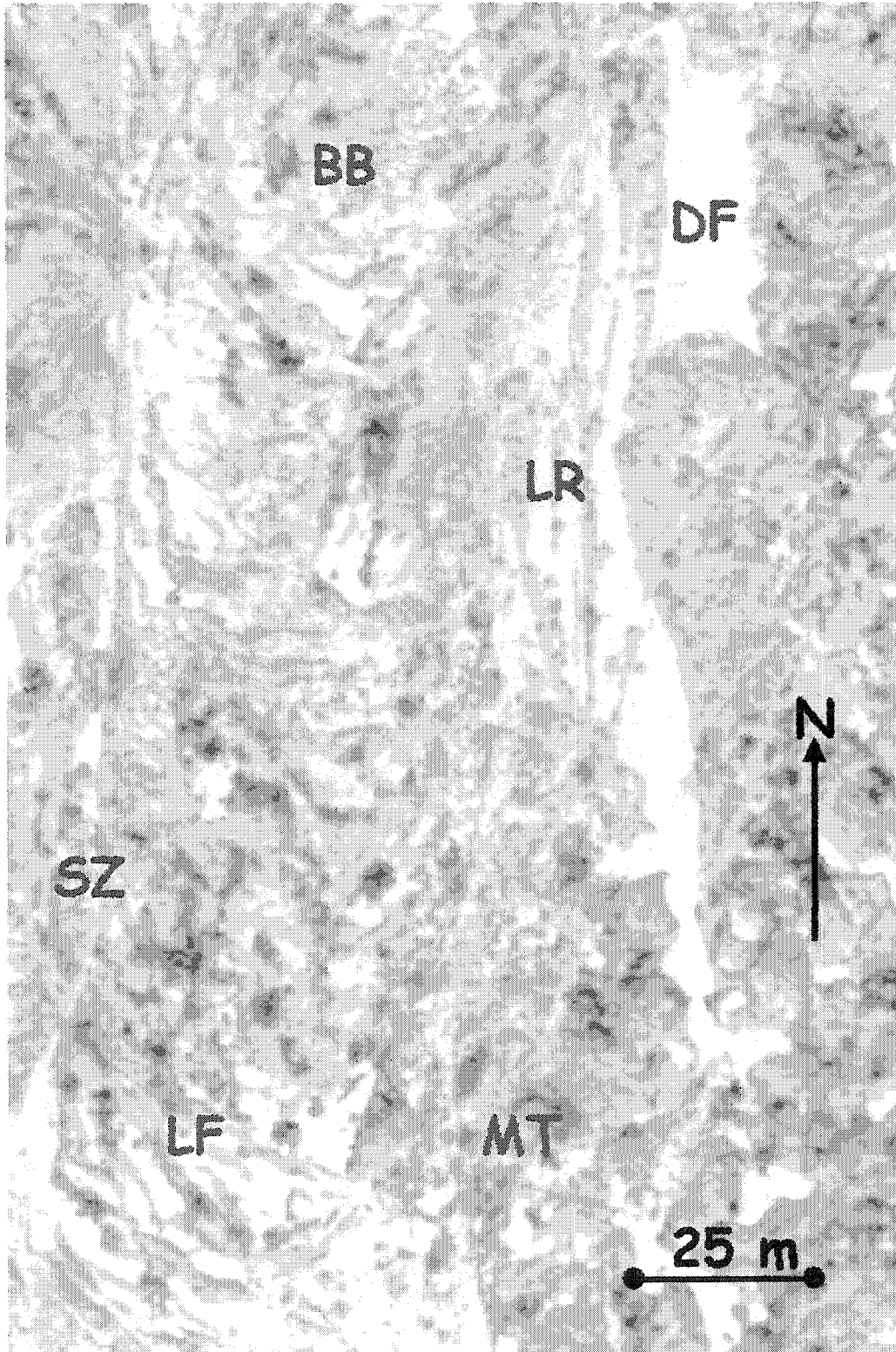


Figure 3.13 1994 aerial photograph of Zone 2b. Note the locations of broad bands of grey and brown material (BB), linear ridges (LR), lobate forms (LF), mottled topography (MT), and a prominent shear zone (SZ). The Dance Floor (DF) is in zone 1. The movement was to the south.

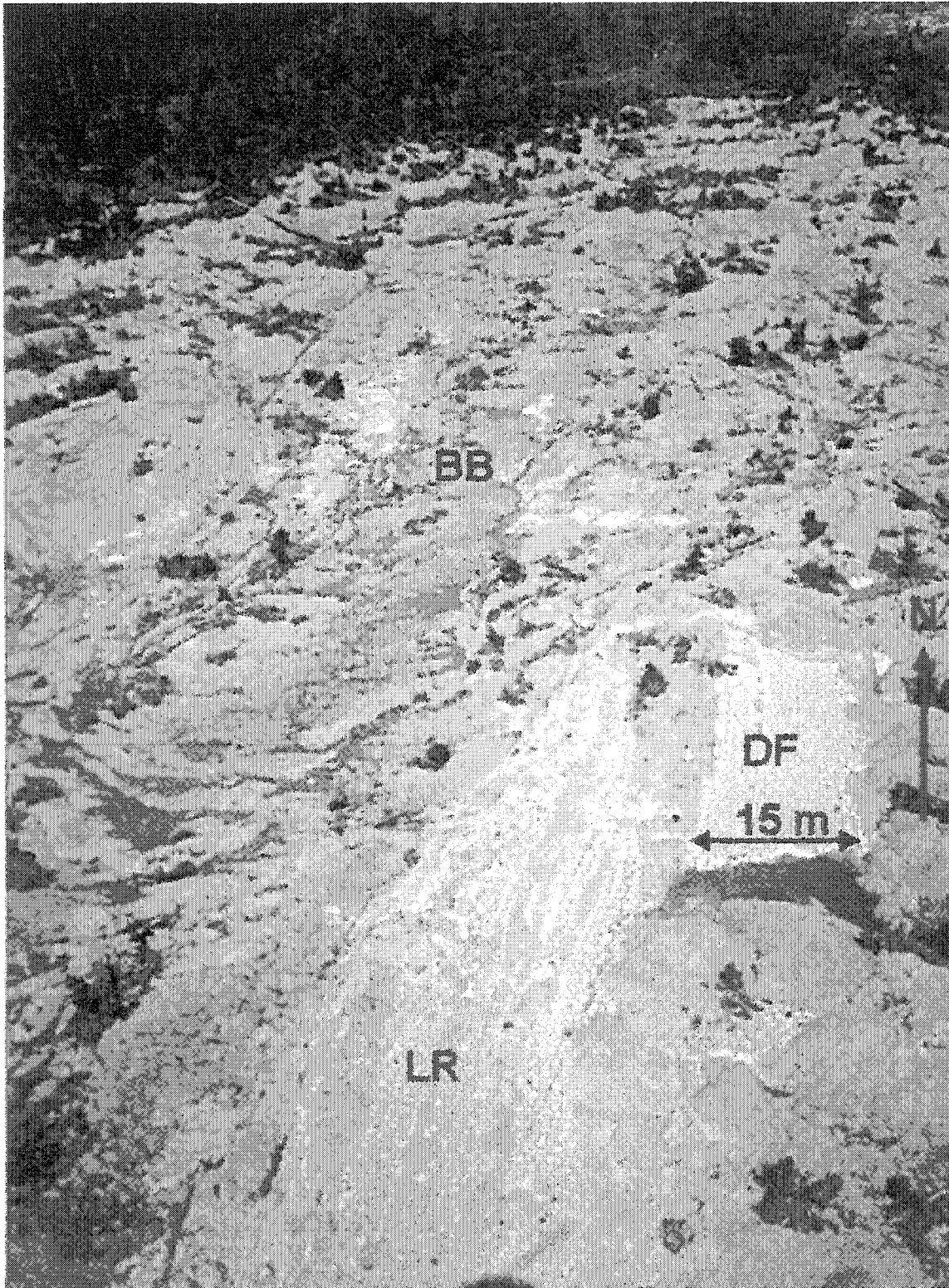


Figure 3.14 Oblique aerial view of zones 1 and 2b. Note the conspicuous exposed rupture surface referred to as the Dance Floor (DF), the thin disturbed linear ridges (LR) and the alternating grey and brown broad bands (BB). Movement is towards the South, parallel to the ridges.

3.4.2. Zone 3

Zone 3 is characterized by grey ridges aligned roughly E-W and thus essentially perpendicular to the main scarp which it abuts on the east side of the zone. Ridges occur in clusters and are separated by areas of brown weathered material. Ridge orientation is markedly different from that in the adjacent zone 2a where grey, horizontally-bedded ridges are aligned roughly N-S, indicating different directions of movement. There also appear to be longitudinal shears inside this zone forming offsets in the displaced slide mass. Many of the low ridges in this zone are composed of blocks with bedding dipping 40 to 60° to the north.

Ridge 1, 1.5 m above the slide surface, trends 250° along its crest (Figure 3.2). It has grey bedding dipping 6° to the NNW and has 50° side slopes. A brown weathered veneer drapes both side slopes, but is more prominent on the southern, down flow, side. Vertical *Equisetum arvense* root channels extend down to 1 m below the ridge crest. This suggests that the ridge crest was a mere 3.6 m from the original ground surface, as the maximum recorded extent of these roots was 4.6 m in the main scarp.

Ridge 2, 3.5 m above the slide surface has a weakly sinusoidal trend to its crest, however the overall trend is 250° (Figure 3.2). Its grey bedding is nearly horizontal. The southern slope of the ridge is 80°, while the, northern, back slope is 60°. No vertical root channels were observed. The ridge is slightly back tilted. Blue grey beds from the crest of ridge 2 match up with beds from the base of ridge 1, indicating a stratigraphic elevation difference of about 3 m. Perhaps this was part of the same ridge – at any rate there was substantial subsidence and collapse in ridge 2.

Ridge 5 forms a prominent horizontally stratified prism, rising 4.5 m above the surrounding landslide surface with a 60° slope (Figure 3.15). The south, lee side of the crest of this prism has folded beds dipping to the south. The lee slope also contained a veneer of weathered material. Oxidized weathered inclusions occurred to a depth of 1.7 m from the crest as do vertical and tilted *Equisetum arvense* root channels. Tilted channels probably indicate tilting during the landslide process since these roots grow vertically (Figure 2.7).

An excavation at the lee side of this ridge indicates that the ridge has been subjected to internal faulting (Figure 3.15). Further, the contact between the ridge and remoulded materials is not planar as the exposed part of the ridge is. Instead, the contact is slightly wavy and soft material in the ridge is separated from strong, dense remoulded material, by a, up to 1 cm thick, fluidized zone

with streaks paralleling the slope of the prism (Figure 3.15). This zone suggests shearing along the leading face of this ridge.

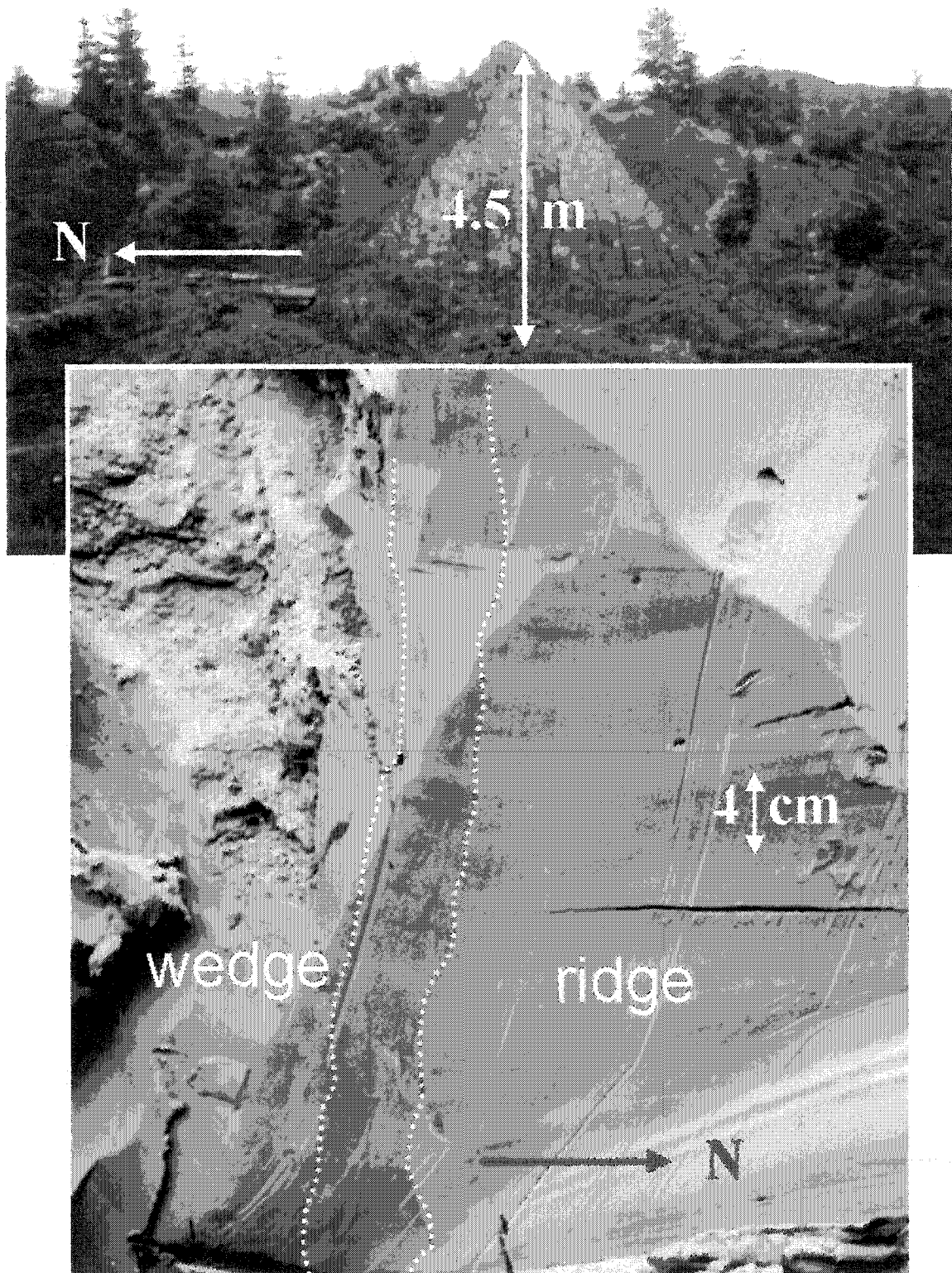


Figure 3.15 Ridge 5, horizontally stratified, is found in zone 2, the East Marginal Zone. Note the irregular wavy shear zone (within the dotted lines) that separates the ridge from the displaced wedge on its leading face. The remoulded displaced material is dense, while the only partly disturbed material in the ridge is soft enough to penetrate with a finger. The shear zone shows evidence of fluidization.

3.4.3. Zone 4

Zone 4, the Butte, is a remarkable feature with near vertical walls and horizontal rupture surfaces at three elevations - the areas labelled 4a to 4c, from highest to lowest (Figure 3.16). The walls are straight rather than arcuate and steep with slopes ranging from 45 to 80°. Upon drying, the walls are prone to toppling (Figure 3.17). Banding in the walls, in zones 4a and 4b, reveal horizontal strata below rupture surfaces (Figure 3.18). The upper rupture surface in zone 4a is 8 m higher than the lowest rupture surface in zone 4c, and about 6 m above the slide floor. The rupture surface in zone 4b is 3 m above the slide surface. Horizontal bands exposed in the wall of 4b continue into the wall of 4a (Figure 3.18), indicating that material below the rupture surface in zone 4b was not lowered by subsidence. The orientation of the southern and southwestern walls is strikingly similar to the orientation of the main scarp 75 m to the NNE (Figure 3.16). Zone 4c has no wall since the elevation of rupture surface is below the main slide floor.

Although the walls of the Butte are straight, horizontally bedded grey ridges and ridge fragments up to 4.5 m high on top of the Butte are arcuate in plan form (Figure 3.16). There is a convergence of material at the contact zone between zones 4a and 4b. This convergence suggests that either eastward movement out of the two embayments occurred simultaneously and at the same level, or alternatively that the upper embayment formed first and converged against an existing slope. It also suggests that the northern Butte surface was lowered by subsurface liquefaction after initial eastward movement.

3.4.3.1. Ridges

Transverse ridges on the southern edge of the upper butte surface have steep cross-sectional faces accordant with the butte wall (Figure 3.18). The grey ridges are separated by brown material representing collapsed wedges in zones 4a and b. There are no horizontally stratified ridges in zone 4c, yet the alternating pattern of grey and brown material is preserved and matches with the pattern of ridges and wedges in zone 4a, suggesting that these were once continuous ridges forming a single arcuate widening.

There are two ridges in zone 4b (Figure 3.16) that require some closer attention. The westernmost ridge (ridge 17) is 3m higher than the ridge to the east (ridge 18), but is stratigraphically lower as it contains no horsetail roots in its crest while the lower ridge does. The top of this eastern ridge is less than one metre above the rupture surface of zone 4b. Inter ridge spacing is about 30 m.

Ridge 17 is a 60 m long ridge with back-tilted blocks against its slopes (Figure 3.20). The leading face of ridge 17 is draped with weathered material. The block of material back-tilted against the leading face of ridge 17 is separated from a forward-tilted forest floor- surfaced block by a small horizontally stratified ridge with root channels in its crest. No root channels were found in the crest of ridge 17.

The crest of ridge 17 is about 3 m higher in elevation than ridge 18, even though it is stratigraphically lower than the crest of ridge 18 (Figure 3.21), as indicated by the presence of *Equisetum arvense* root channels in ridge 18. By implication, ridge 18 has subsided more than 3 m. The rupture surface of the zone 4b exposed at the boundary of zone 2b is approximately 80 m a.s.l., while the crest of ridge 18 is less than 1 m above this elevation.

A broad grey zone about 30 m east of ridge 18 (Figure 3.16), is similar to broad zones described for the Inner Zone, but is less disturbed. It is noteworthy that the difference in elevation between the upper surface of rupture and the middle surface of rupture here is about 2.5 m. This zone is about 30 m from the crest of ridge 18, similar to the ridge spacing on the upper surface.

These observations are consistent with the suggestion that initial movement was followed by subsidence, suggested in the previous section.

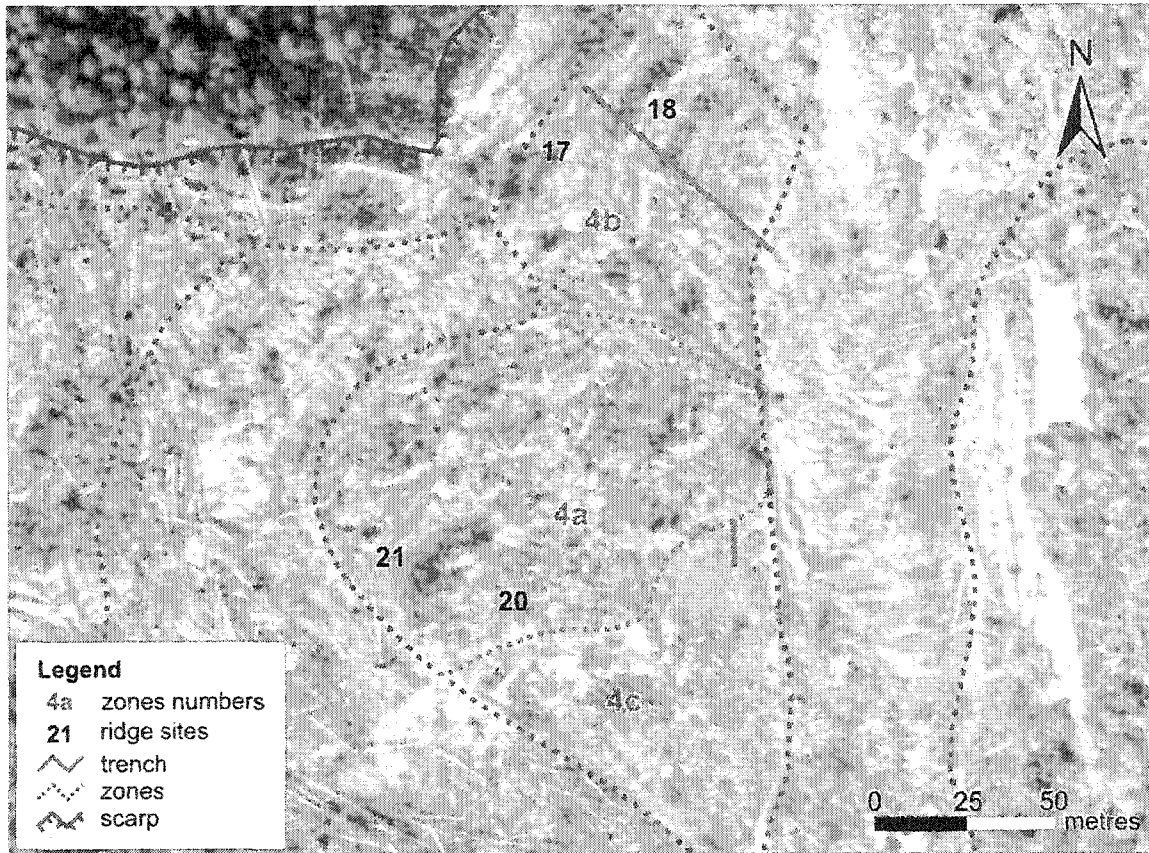


Figure 3.16 1994 aerial photograph showing zone 6, the Butte. The upper surface (4a) is flanked by an intermediate surface (4b) and a lower surface (4c). Trenches (blue lines) bisect ridges 17 and 18, and the south wall of 4a and the surface of 4c.



Figure 3.17 Topple and block fall of desiccated glaciomarine sediment exposed in the 6 m tall east wall of the Butte.

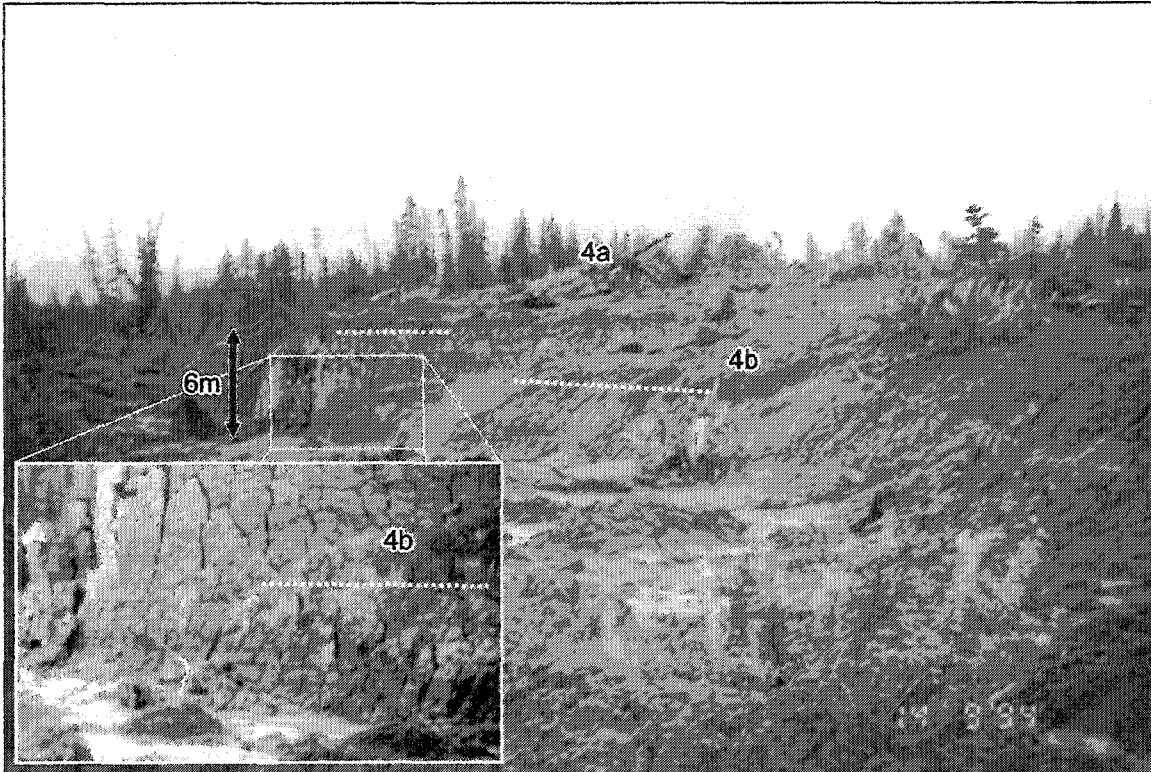


Figure 3.18 The east wall of the Butte showing the surfaces zones 4a and b (Figure 12). The dotted white lines represent perched rupture surfaces. Note that the horizontal bands below the rupture surfaces continue from zone 4b into 4a (inset).

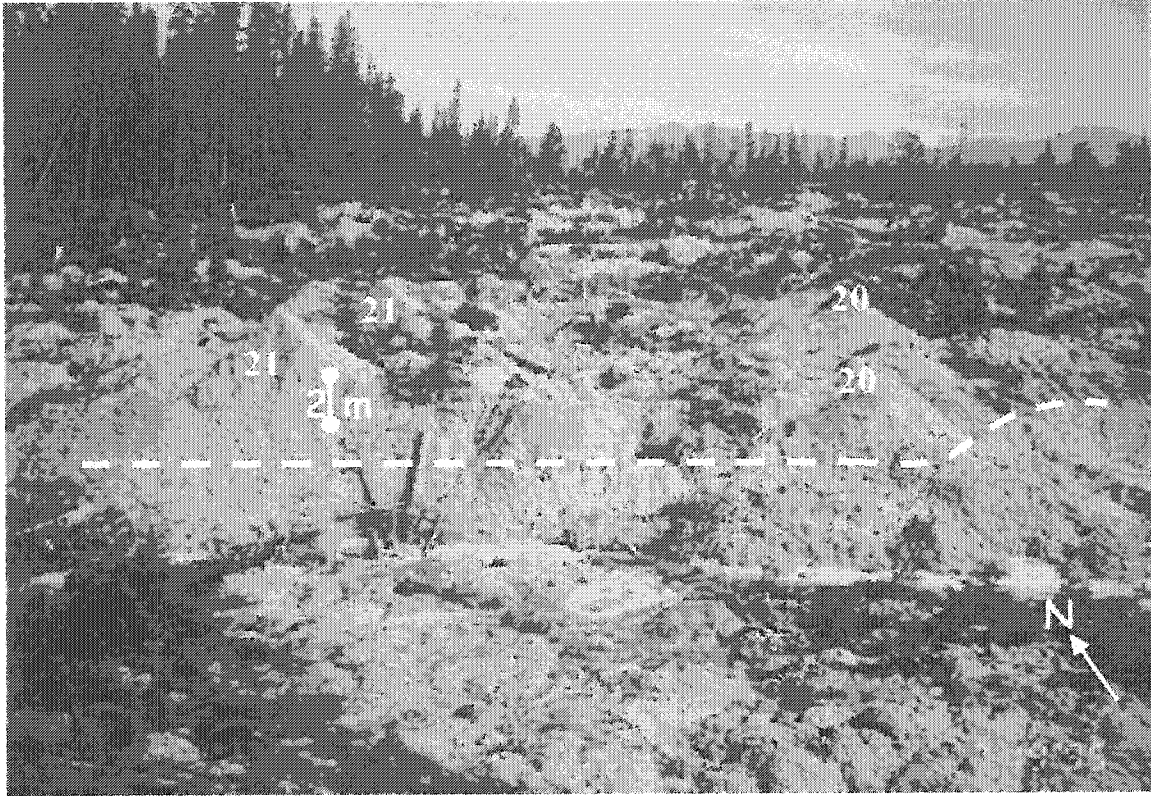


Figure 3.19 The south wall of the Butte showing an exposed rupture surface (dashed line). Note how central portions of the ridges have collapsed.

3.4.3.2. Excavations

I excavated the displaced material at the base of the Butte in zone 4c to examine the contact of the rupture surface (Figure 3.16). Using a tracked excavator I excavated a trench at the base of the Butte about 5 m wide, 4 m deep and 10 m long (Figure 3.22). The rupture surface was easily discerned due to striking contrasts between undisturbed and remoulded sediment. The undisturbed sediment had horizontal beds and was easily indented with a finger. The overlying remoulded sediment was much stronger, not bedded, but completely remoulded and mottled (Figures 3.22). In the eastern face of the excavation the knick point contact between the Butte wall and the horizontal rupture surface was angular, while in the western face it was slightly curved.

The thickness of displaced material at the base of the Butte was 2.3 m, giving the rupture surface an elevation of 74.75 m according to the topographic map. The upper Butte rupture surface is at approximately 82.75 m elevation here, thus there was approximately 8 m of subsidence on the lower surface.

I also excavated a trench through ridges 17 and 18 in zone 4b (Figures 3.16, and 3.23). In this case the rupture surface occurred in a blue stratum. Although I could find no strength differences between subjacent bands of differing colour, the blue layers always flowed out of excavations more readily. This may relate to the rapidity of the sediment (Söderblom 1974) and is further discussed in Chapters 5 and 6.



Figure 3.20 Rotational movement of grabens (wedges) along ridge 17 on the middle surface of the Butte.



Figure 3.21 The crest of ridge 18 contains horsetail roots, but is 1.5 m lower than surrounding surface material indicating local subsidence.

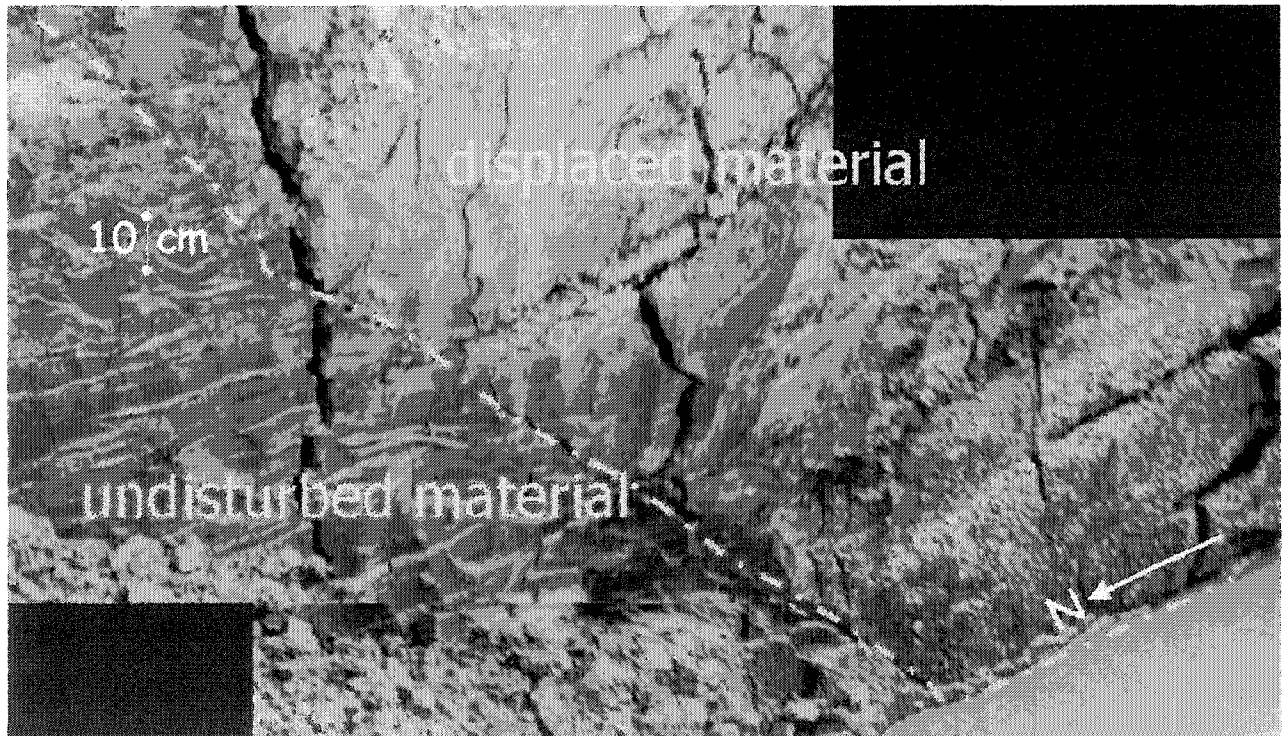
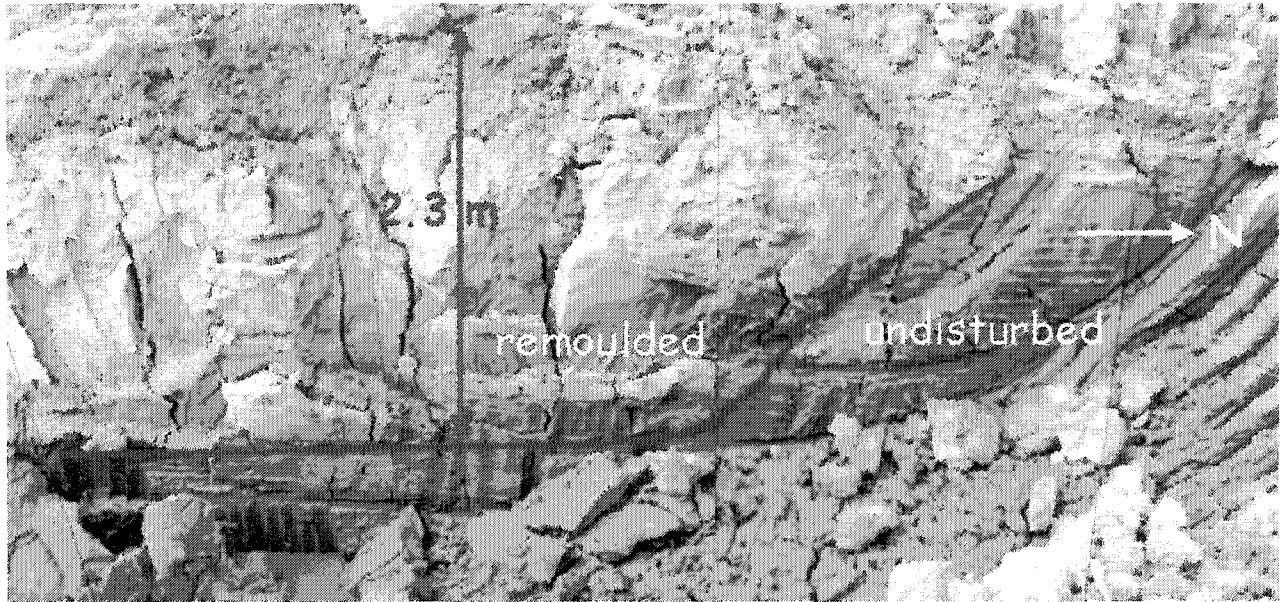


Figure 3.22 *Top*: West side of trench in zone 6c (Figure 3.16). Note the horizontal bedding in the undisturbed strata, and the smooth gradation of the rupture surface from inclined to horizontal. Movement to South. *Bottom*: East side of trench in zone 4c (Figure 3.16). Note the sharp transition from inclined to horizontal orientation. Movement to the South.

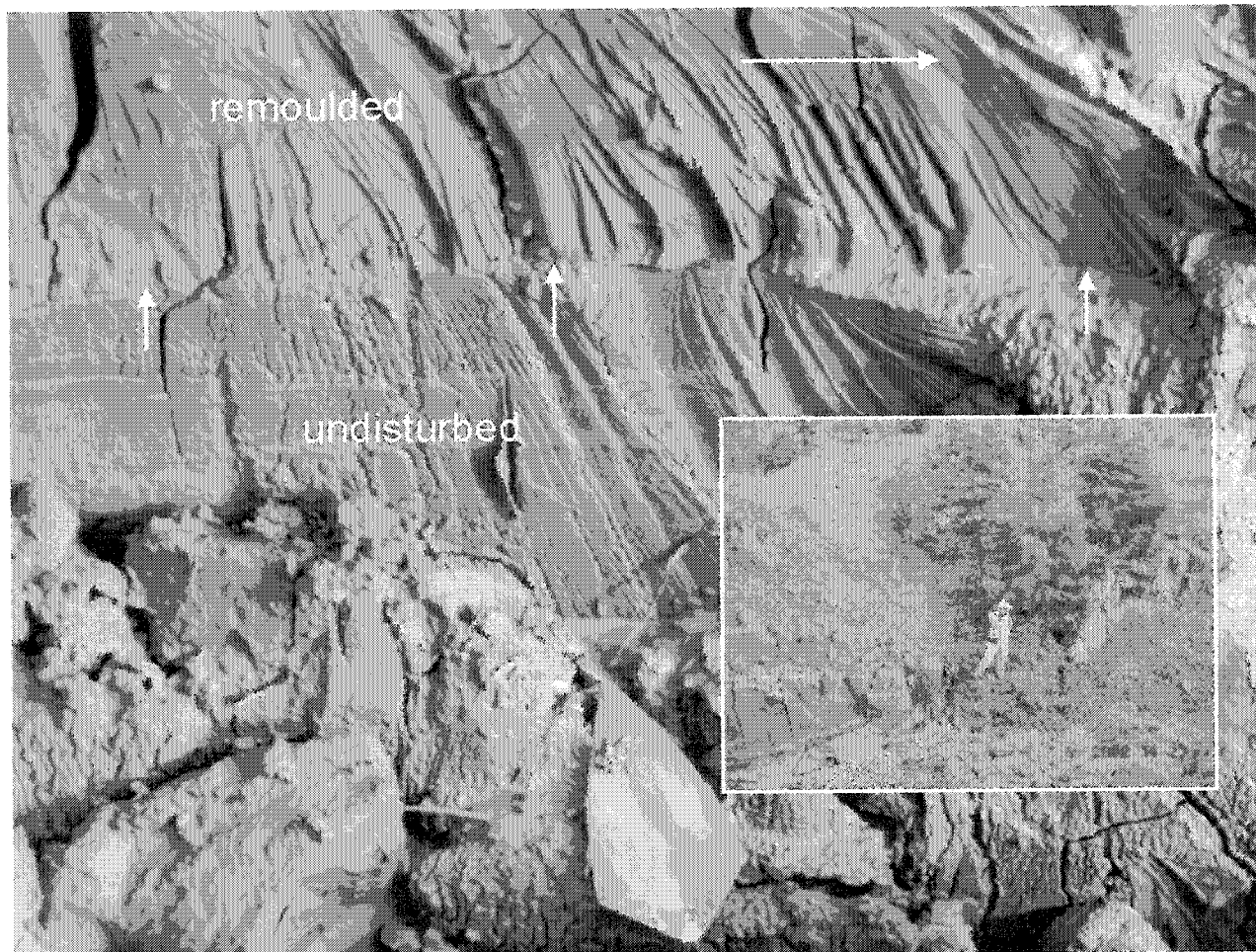


Figure 3.23 Exposure of a horizontal rupture surface in a, 10 cm thick, blue stratum, between ridge 17 and 18. The ridge in the inset photo is 17. Note the rotational wedge.

3.4.4. Zone 5

Zones 5 and 6 occur on the western side of The Butte. The elevation of rupture surfaces in zone 5 is variable, being at least 1.5 m higher adjacent to zone 4b, than in other portions of the zone. Zone 5 is characterized by pronounced lateral and internal shear zones. These extend the length of the zone and extend beyond it into the zone of accumulation (Figure 3.24). The zone, which contains few undisturbed ridges, incorporates two main flows: one, incorporating material from the clearcut, moving southwest from behind the Butte, turning southeast, and flowing over Zone 4c; the other, a channel for material from Zone 6, along the south margin (and at least 2 m below) the rupture surface of zone 4b. The more southerly flow path is characterized by large coniferous trees, most of them laying oriented parallel to the flow direction.

Zone 5, up to 150 m wide and 300 m long is characterized by pronounced lateral and internal shear zones (Figure 3.24) that indicate flow. These shear zones equal the length of this zone and extend beyond it into the zone of depletion. This zone contains no undisturbed ridges. The zone incorporates two main flows. A flow moving southwest from behind the Butte, turning southeast, and, flowing over the southwestern middle Butte surface, incorporates material from the clearcut. This flow terminates at a longitudinal shear produced by the west margin of the zone 2b. A second flow path acting as a channel for the western zone flows along the south margin (and at least 2 m below) the southwestern middle Butte. The flow merges with the western margin of zone 2b and is separated by a longitudinal shear that extends well into the zone of accumulation.

Further evidence for flow comes from thoroughly remoulded sediment (Figure 3.25) south of the Butte. This sediment is plastically deformed below the zone of thorough remoulding.

This, more southerly flow path is characterized by large coniferous trees, most of them laying oriented parallel to the flow direction. Some trees, however, managed to remain standing after considerable displacement, extending into the zone of accumulation (see Figure 4.8 later).

Ridges 31 (Figure 3.26) and 32 occur on an extension of the Butte, 3-4 m lower than the upper surface of the Butte, but more than 2.5 m above the downflow topography. There are two main points to be made about this surface. 1. The two ridges on this surface (31 and 32) trend perpendicular to the ridges on the upper Butte. They may be fragments of a single ridge separated by collapse and longitudinal extension towards the southeast. Ridge 32 is atypical in that both of its slopes are draped with weathered soil. 2. Subsequent to the formation of these

ridges, flow curving around the northeast side of the Butte, flowed southeastward, parallel to, and along the sides of ridge 32, and over the scarp of the middle surface.

3.4.5. Zone 6

Zone 6, the far western zone, can be initially distinguished from the other zones by the presence of a large number of standing conifers. The zone contains horst-graben topography with vertical subsidence and less translational movement than in other zones. As a result, many trees on grabens remain rooted in the vertical position (Figure 3.27). Some of the prominent grey ridges are separated from the main scarp by a single graben. This zone contains the boundary between flow from the clearcut (around the Butte), and southeasterly flow from the forested western zone via the midwest zone. There appears to be increased disturbance of the ridges towards the eastern margin of the zone.

Some arcuate ridges and depressions form above the head of the western landslide (Chapter 4). Other prominent grey ridges, separated from the main scarp by a single graben, are discussed under zone 7, in Section 3.2.8. There appears to be increased disturbance of the ridges towards the eastern margin of the zone. Split grabens, similar to those at site 18 on the lower Butte, occur here (Figure 3.28). Site 23 (Figure 3.2) is the boundary between first southwesterly and then southeasterly flow from the clearcut (around the Butte), and southeasterly flow from the forested western zone via zone 5.

The abundance of standing trees and relatively high amount of remaining depleted mass in zone 6 suggests little flow occurred.

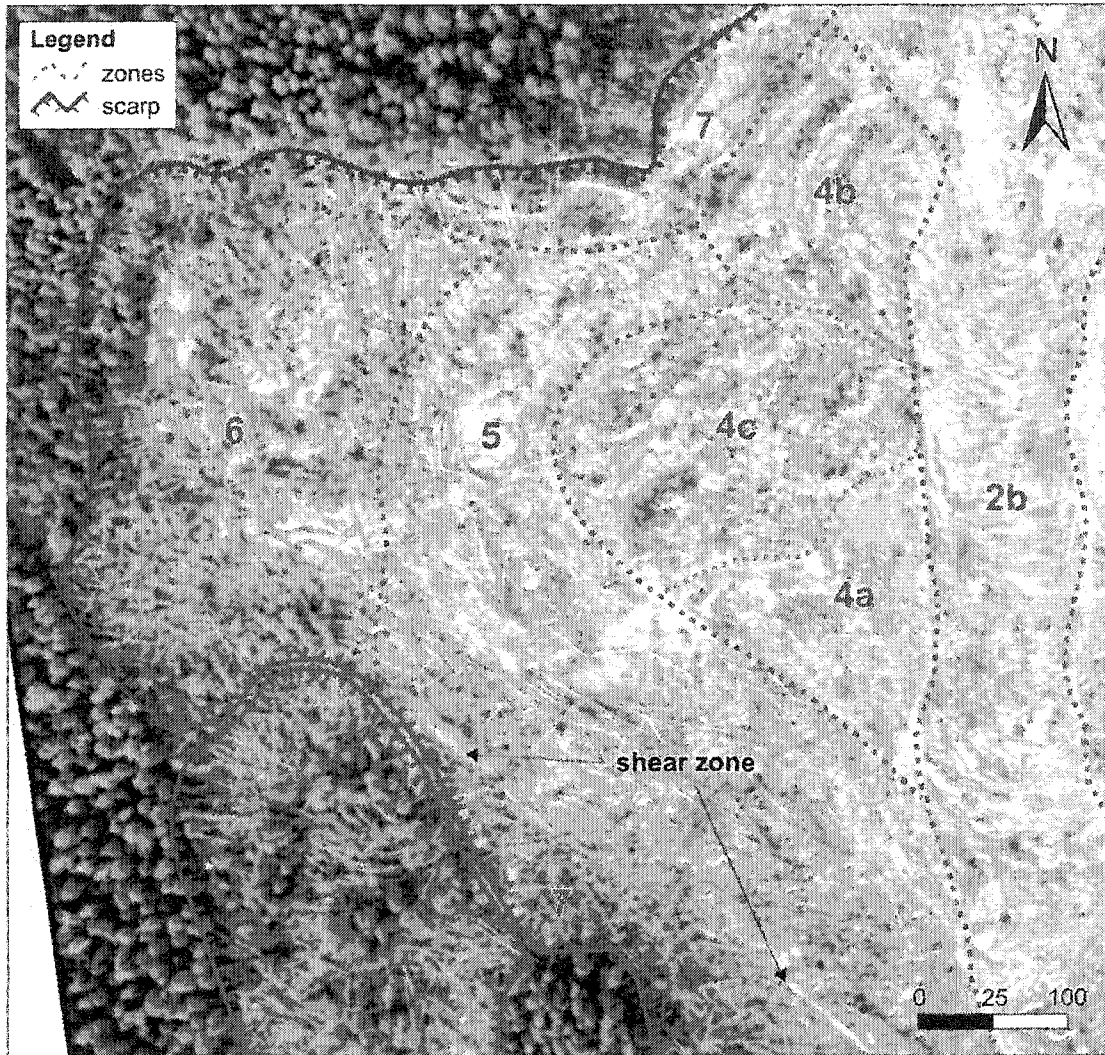


Figure 3.24 Zones 5 and 6 of the western widening. Note the number of trees in these zones, and especially in zone 6, in comparison to zones 2 and 4. Also note the prominent shear zone in zone 5.

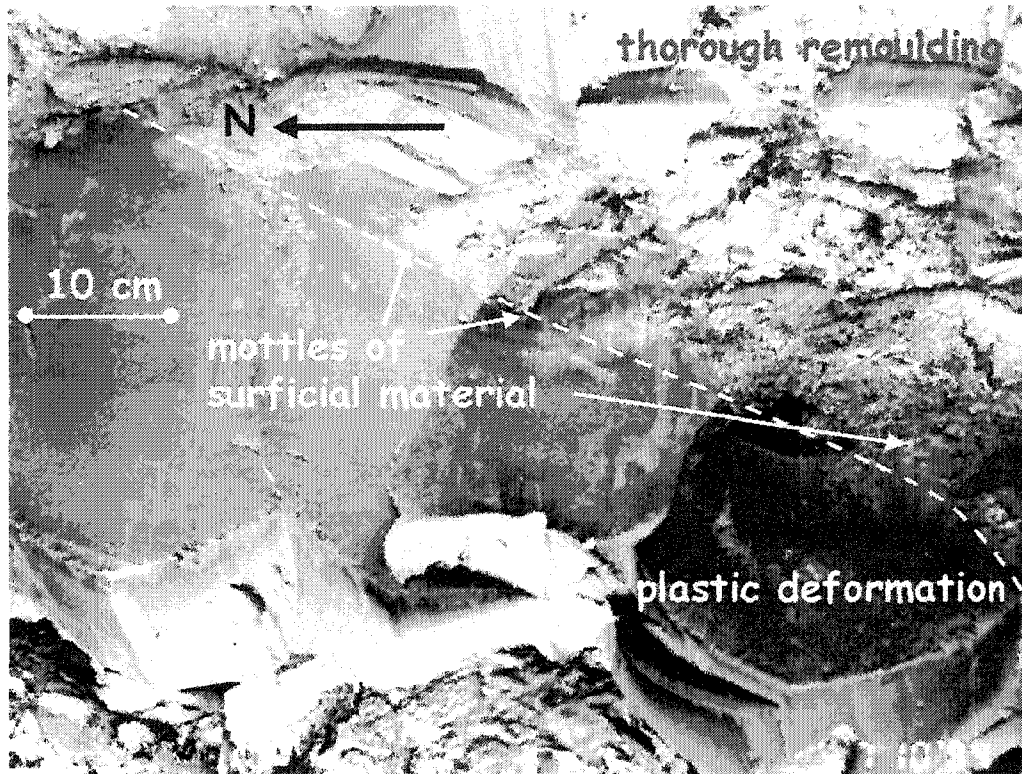


Figure 3.25 Plastic deformation below thorough remoulding with mottles of surficial material in zone 5, south of the Butte.



Figure 3.26 Site 31 – a horizontally stratified ridge in zone 5.



Figure 3.27 Upright trees, are common on grabens in zone 6.



Figure 3.28 A split graben in zone 6, similar to site 18 on the Butte.

3.4.6. Zone 7

Zone 7, the main scarp marginal zone, generally from 10 to 25 m wide, outlines an area transitional between the zone of depletion and material outside of the landslide above the main and lateral scarps. Typically, horizontally stratified ridges are separated from the main scarp by back tilted, horizontal, or forward tilted blocks. The dominant forms in this zone are back-tilted blocks. Less common are horizontally stratified blocks that occur immediately below the main scarp and parallel to it. In two cases, areas with lobate ridge patterns occur, where leading horizontally stratified ridges are separated by forward-tilted blocks. Here the zone is up to 40 m wide. In the Eastern Widening, more of the main scarp is exposed, and ridges are highly disturbed. Stratigraphic observations made in the main scarp are discussed in Chapter 2.

Back-tilted blocks dominate in the western part of zone 1. In several locations a back-tilted block separates the main scarp from a horizontally stratified ridge. Examples occur at sites 16 and 27 (Figure 3.2). At site 6 a horizontally stratified ridge is separated from the main scarp by a series of 30 to 50° back-tilted blocks (Figure 3.29). This ridge is arcuate in plan form in the mirror image of the scarp, thus forming a lobe. Its crest is folded in the down flow direction, and its lee side is covered with a veneer of weathered material. Another such series of blocks is located at site 14, (Figure 3.30). These blocks have undergone complex movement, with slippage in two major directions, perhaps facilitated by pre-existing fissures and the bedding of the material.

In other locations the main scarp is separated from a horizontally stratified ridge by a horizontally stratified graben. Examples include sites 26 and 33 (Figure 3.31). Site 24 is somewhat marginal between these two extremes.

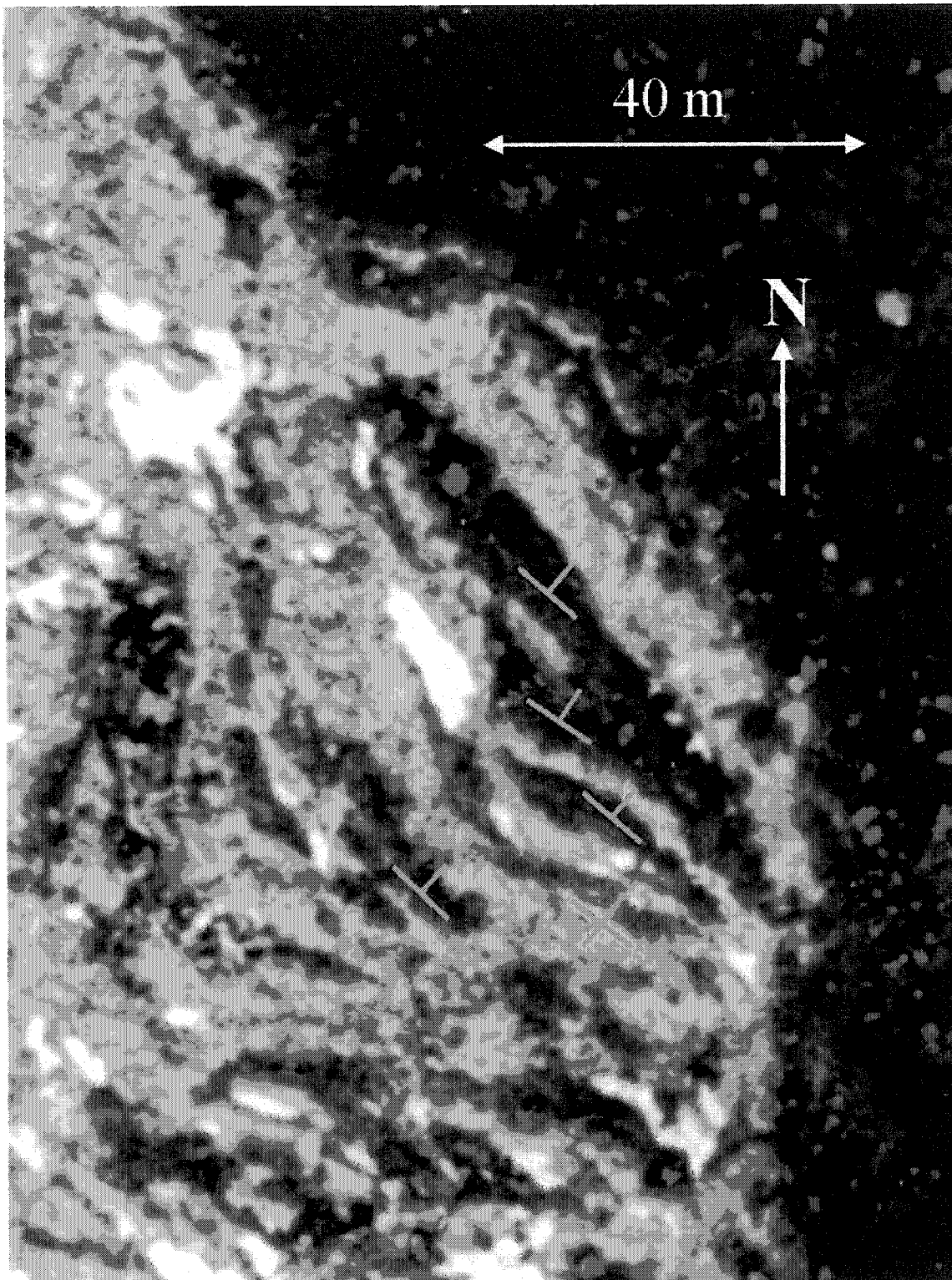


Figure 3.29 Back tilted blocks separate horizontally stratified ridge 6 from the East lateral scarp in the Main Scarp Marginal Zone.

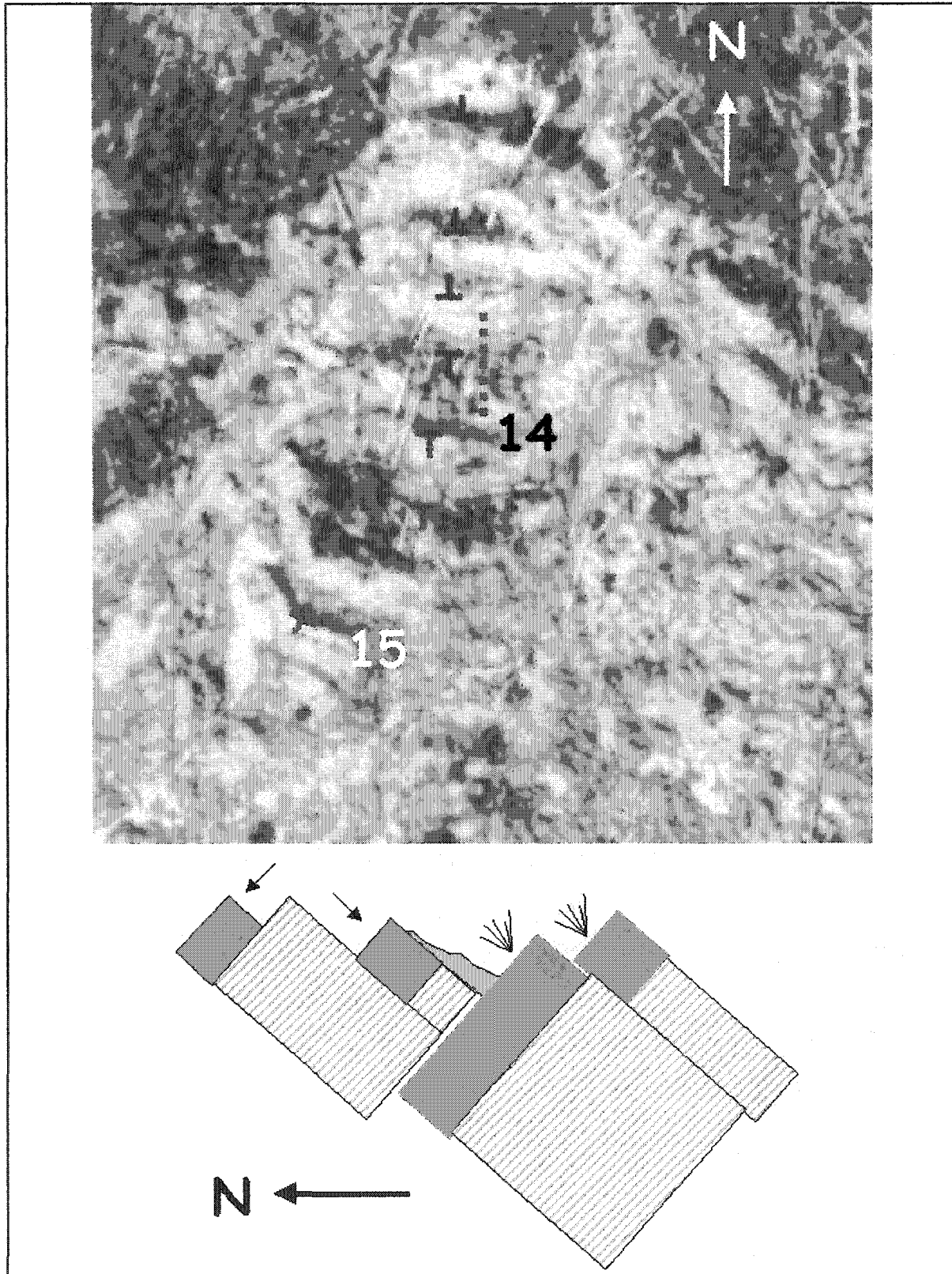


Figure 3.30 Complex movement of blocks in the Main Scarp Marginal Zone. Cartoon depicts a cross-section along the blue dotted line. Note brown surface material overlying grey weathered material in the cartoon.

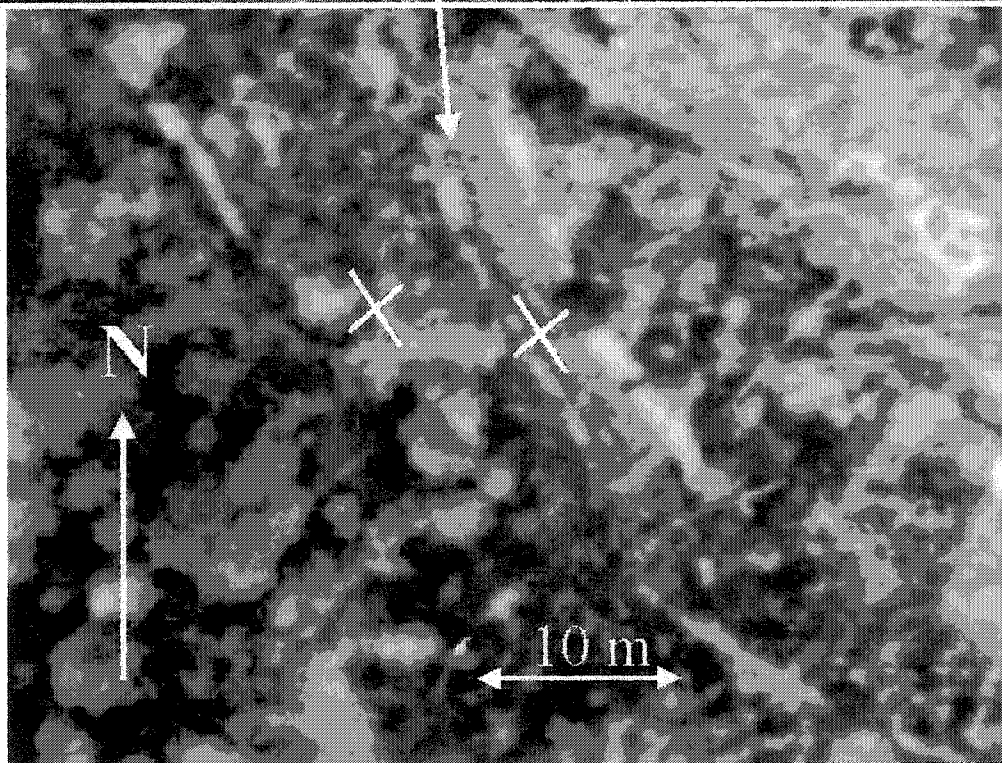


Figure 3.31 A horizontally bedded wedge separates Ridge 33 from the scarp on the western edge of the landslide.

3.5. Discussion/Conclusions

Important features in the zone of depletion, include disturbed and undisturbed ridges, multiple surfaces of rupture, as well as areas of exposed rupture surface. To group common elements, I created seven zones.

Horizontally stratified ridges are common in spreads in glaciomarine sediments in Scandinavia (Odenstad 1951), Alaska (Hansen 1965), Ontario (Eden et al 1971; Evans and Brooks 1994) and Quebec (Carson 1977, 1979). While ridge splitting and fracturing was previously documented (Carson 1979), this is the first reported case of ridge subsidence in these sediments. Many of the relatively intact, upright ridges of near-horizontal muddy strata have been lowered in elevation during translation. This is in contrast to current models of retrogressive spreading in which ridges are created by subsidence of wedges on either side of them (e.g., Odenstad, 1951, Carson, 1977). The evidence for this is horsetail roots in the crests of the ridges which, based on observations around the main scarp, do not penetrate more deeply than about 4.5 m below the ground surface. In the ridge crests they are now found as much as 7 metres below the former ground surface.

At Mink Creek the surfaces of rupture occur at several elevations in the zone of depletion, separated by scarps ranging from 1 m to 8 m in height. Such multiple major rupture surfaces have not been documented in previous historic retrogressive landslides. There are two main surfaces of rupture that appear to be the result of two separate sliding phases, but the general multiplicity of surfaces of rupture may be related to multiple soft or rapid strata.

Exposed rupture surfaces do not occur in spreads but are also uncommon in flows. Flows at Ste-Jean-Vianney (Tavenas et al. 1971), Rissa (Gregersen 1981), and Khyex River (Schwab et al. In press) all have covered rupture surfaces. An exception occurs at the flow on the La Grande River in Ontario (Lefebvre et al. 1991). In this case the rupture surface was perched above the river and sloped up at 6°, a situation similar to (but slightly steeper than) Mink Creek.

Chapter 4

Morphology of the Zone of Accumulation

4.1. Introduction

In this chapter I describe the morphology of the displaced material in the zone of accumulation of the Mink Creek landslide (Figure 4.1). I also describe the small Western landslide, as it lies outside the zone of depletion of the main landslide (Figure 3.1). This chapter is shorter than the previous chapter for two reasons. 1. There were fewer natural exposures in the zone of accumulation. 2. The displaced material in the zone of depletion was easier to interpret with respect to the style and sequence of movement.

I made observations in the zone of accumulation from natural exposures, air photos, topographic maps and hand excavations. No excavators were used here. Furthermore no material from this zone was tested in the laboratory, nor were any vane shear tests made in the field.

4.2. Dimensions of Displaced Material in the Zone of Accumulation

The zone of accumulation covers approximately 20 ha and extends over a horizontal distance of 1200 m in Mink Creek valley, up to a depth of 14 m (Figure 4.1). The surface of the zone of accumulation forms a plain with an average surface slope of 1.5 %, dipping down stream. The total filling of the valley (Figure 4.2) caused the formation of two lakes (Figure 4.3), one extending about 1.2 km upstream, beyond the CNR Terrace-Kitimat railway trestle, and the other was formed by the impoundment of an unnamed tributary of Mink Creek.

4.3. Morphology of the Zone of Accumulation

4.3.1. Material Characteristics

Despite the evidence for widespread subsidence and remoulding in the zone of depletion, in the zone of accumulation much of the visible displaced material shows relatively little deformation. For example, displaced material at the tip of the landslide, forming a steep scarp, had intact to slightly tilted stratified bedding (Figure 4.4). Similar horizontal strata are evident along sections of newly exposed creek banks (Figure 4.5). Such strata are extremely soft (easily remoulded with a finger). Elsewhere strata are folded, contorted or dipping (Figure 4.6).

Figures 4.2 and 4.7 show trees oriented primarily parallel to flow (stumps are difficult to discern from the air), forest floor mats, brown weathered surface soil, and also grey zones representing exposed depth material.

Not all trees moved in the horizontal position. Figure 4.8 gives an example of a raft of trees surrounding a large stump in the upright position. Perhaps its roots gave the mass enough strength to move as a coherent unit. These trees, up to 15 m high, were not as large as mature trees up to 40 m high. Many trees, in the western widening have also been rafted in the upright position. Several standing trees near the margin of the debris are not transported, but rather rooted in place and partially buried by displaced material (Figure 4.7).

Displaced surficial soil in the creek has been eroded into muddy clasts ranging from sand to cobble size (Figure 4.9). These are erosional forms to be contrasted with armoured mud balls that grow upon transport (Bull 1964).

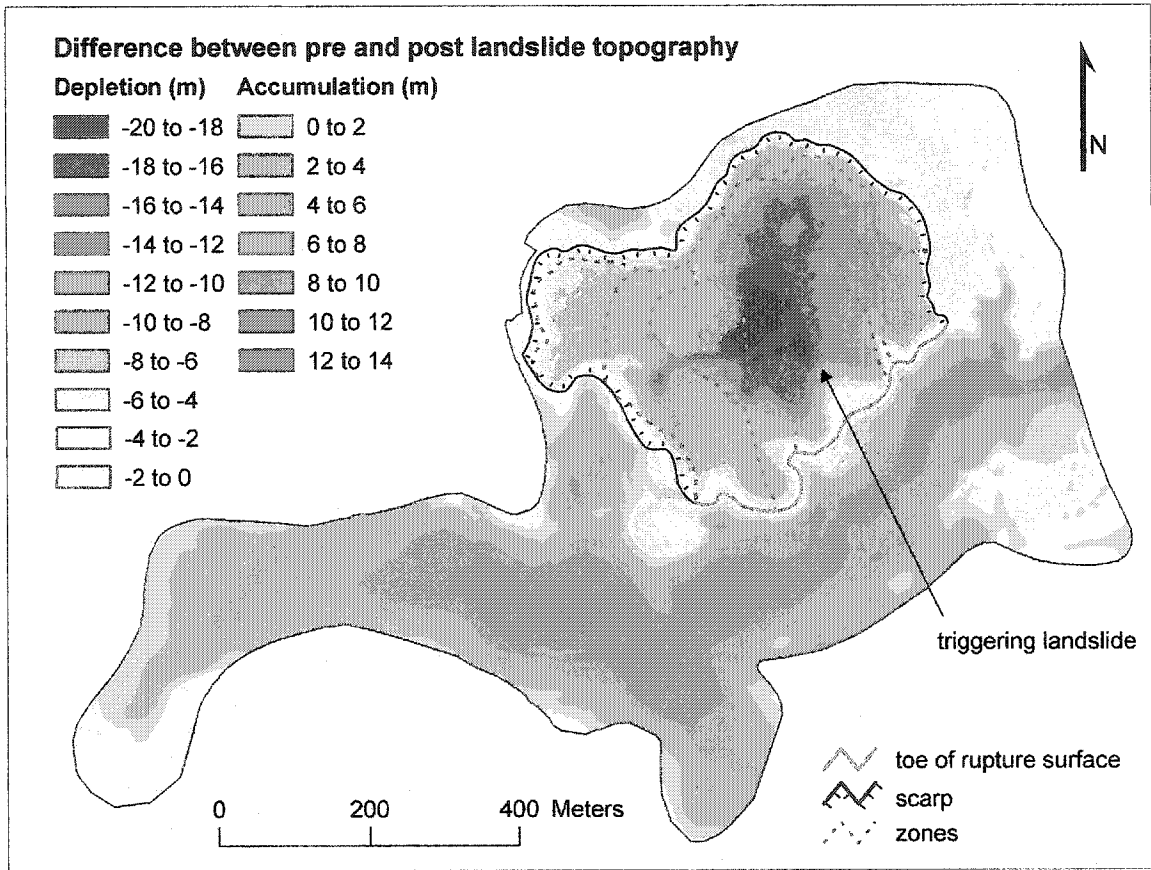


Figure 4.1 This digital elevation model show the difference in elevation between the pre and post landslide surfaces. Up to 14 m of material was deposited in the valley of Mink Creek.



Figure 4.2 Infilled valley of Mink Creek. Note the braided channel patterns and numerous vertically transported trees. Most trees are oriented prone in the direction of flow. The depth of fill is as high as 14 m above the thalweg of the pre-slide creek. The deposit is 90 to 100 m wide.

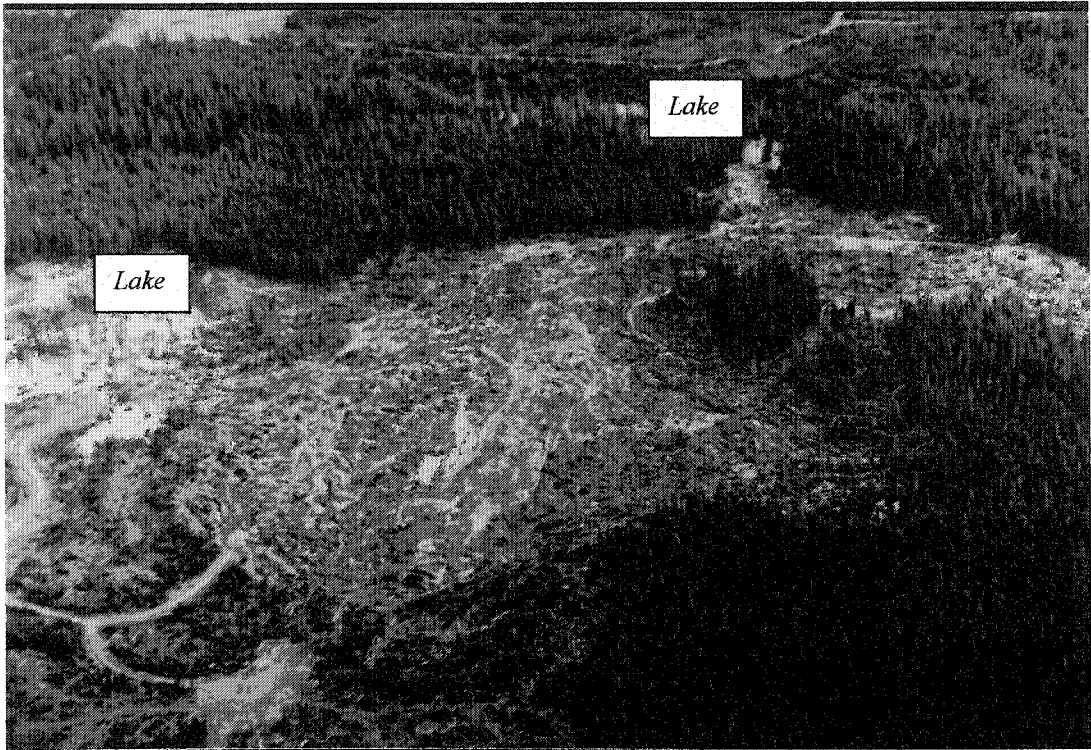


Figure 4.3 The landslide impounded Mink Creek resulting in the damming of two lakes.

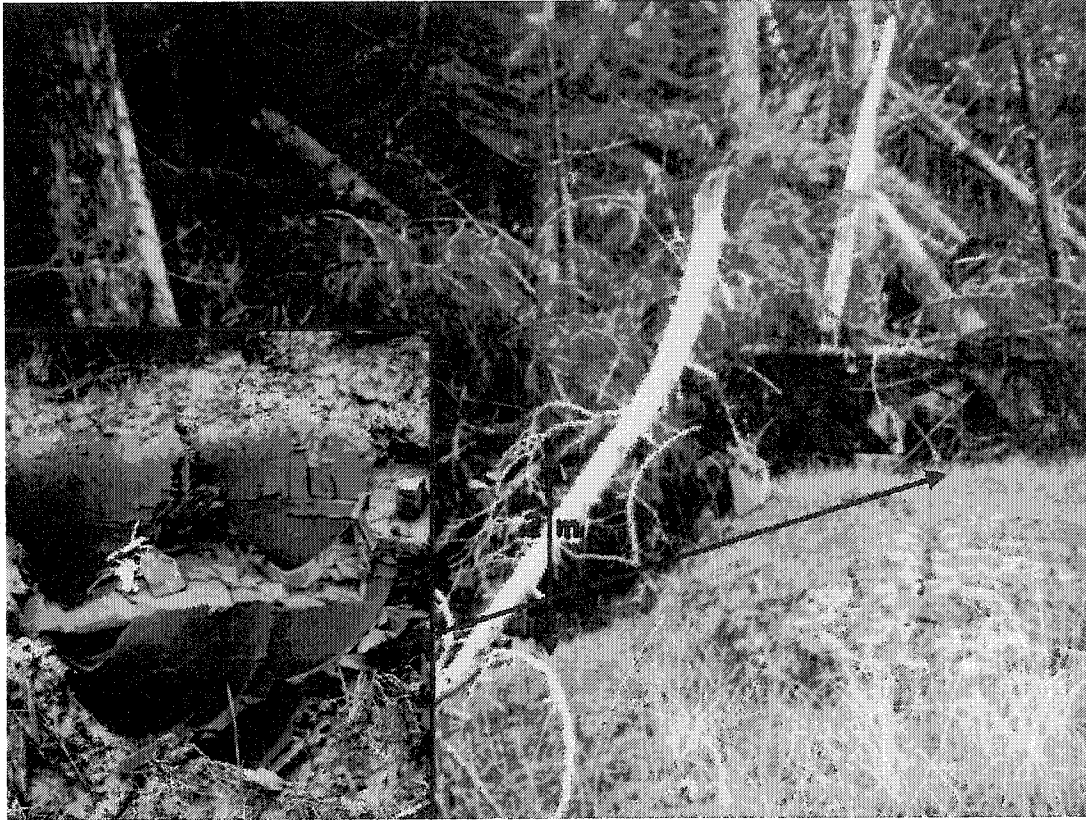


Figure 4.4 Horizontal strata occur at the tip of the landslide in the zone of accumulation.



Figure 4.5 Horizontally bedded strata exposed in the bank of the newly incised creek, in the zone of accumulation south of Zone 1.

3.3.3



Figure 4.6 Plastic deformation of horizontal strata is combined here with injection of brown surficial sediment. Pencil is 15 cm long.

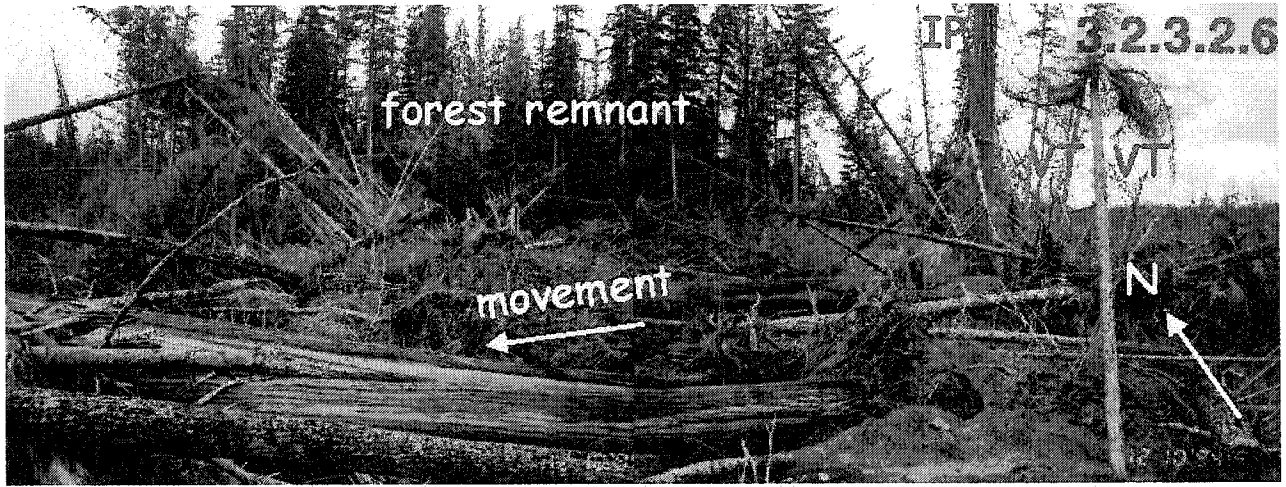


Figure 4.7 Horizontal, leaning, and vertical trees occur in the zone of accumulation below the forest remnant. Some vertical trees are transported (VT), others are in place (IP). Note that prone trees are oriented in the direction of movement.

3.2.3.3.1



Figure 4.8 Trees rafted in the vertical position. This is a common phenomenon in the zone of accumulation as well as in Zones 5 and 6 in the western widening of the zone of depletion.

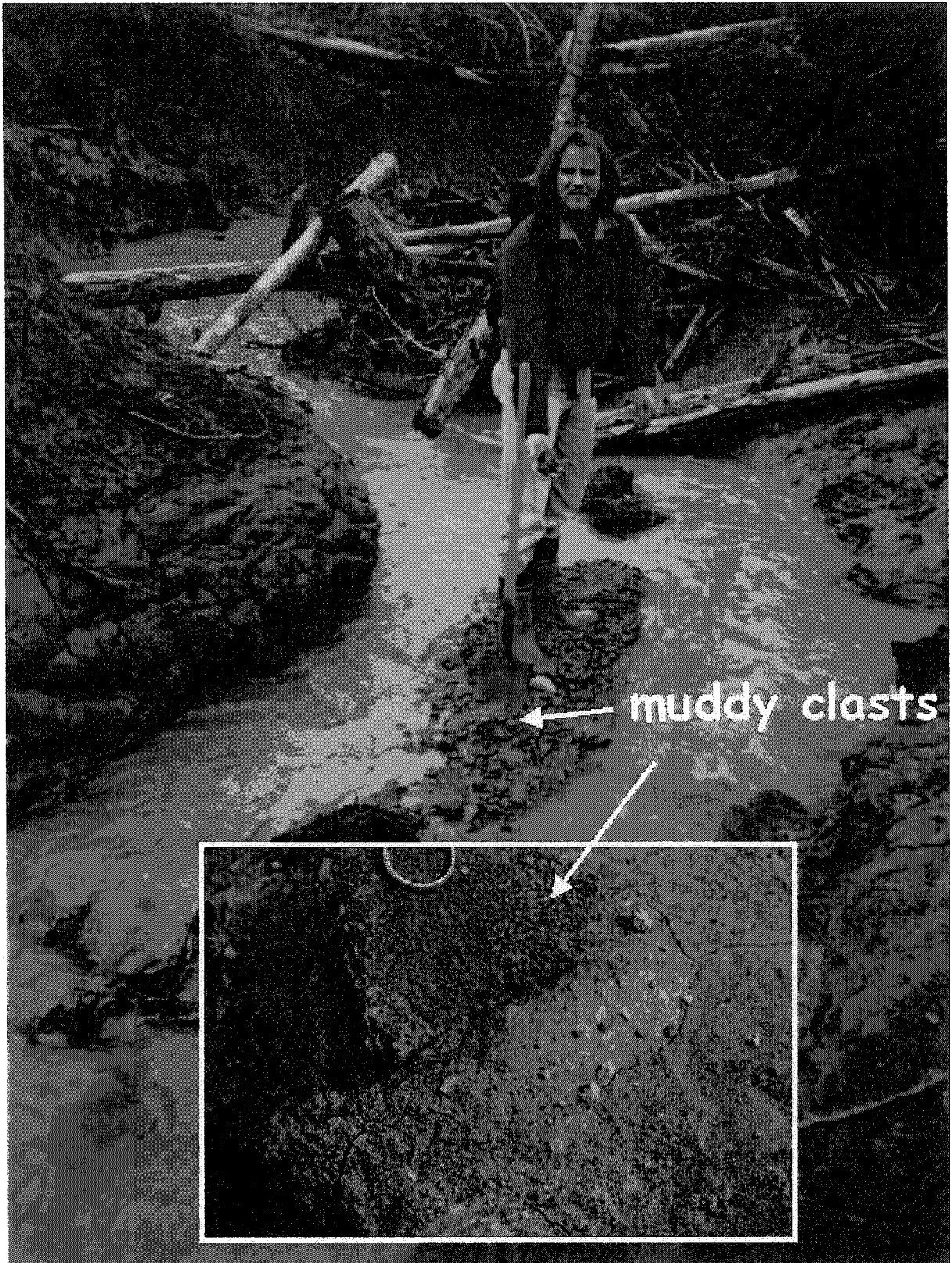


Figure 4.9 Muddy clasts of weathered surficial material range from coarse sand to cobble size in the post-landslide creek.

4.3.2. Landform Features

The zone of accumulation is essentially a flat plain with areas of grey exposed surficial material, and woody debris. The plain of displaced material was partially incised by Mink Creek by April 1994, when the landslide was first discovered by authorities. Features on the plain include three ridges, longitudinal shear zones, and two mud volcanoes.

4.3.2.1. Ridges

While there are many ridges in the zone of depletion (Figure 3.2), there are only three ridges in the zone of accumulation. Most of the zone of accumulation is flat, forming a negative topography where streams have incised it. One ridge is composed of deformed mud, and the other two are composed of a mixture of mud and trees. The ridges are generally flanked by near-horizontal displaced material.

Figure 4.10 shows a ridge (not numbered) of grey depth material directly south of zone 1, against the standing trees on the opposite side of the valley. The 2 m tall ridge is internally deformed. Ridge 35 (Figures 3.2 and 4.11) on the north side of the original valley, also due south of zone 1, rises 4 m above the surrounding surface and is composed of a jumbled mixture of mud and large trees. Ridge 37 (Figure 4.12) is the most dramatic. Here a jumble of large coniferous trees packed with mud forms an 11 m high vertical scarp at the southwestern margin of the forest remnant (Figure 3.2). The up flow slope of the ridge terminating in this scarp is concave upwards (i.e. rising towards the scarp). In front of the scarp there are undisturbed vertical trees and forest floor.

4.3.2.2. Shear Zones

Shear zones are found in the form of long linear grooves (Figures 4.13 and 4.14) rather than ridges common in viscous earth flows (Bovis 1985; Geertsema and Schwab 2004). This probably relates to the fluid nature of these muds. In Figure 4.13 a shear zone separates a zone transporting fallen coniferous trees from a zone transporting stumps. Shears mark the lateral margins and extents of late stage flows.

4.3.2.3. Dewatering Structures

Evidence for dewatering comes from a mud volcano (Figure 4.15). Mud volcanoes are common features on deltas that have undergone liquefaction, and represent the release of pressurized mud through a dike to the ground surface (Clague et al. 1992). At Mink Creek I only found two small (approximately 1 m diameter) mud volcanoes, while the Khyex landslide (Figure 1.3; Schwab et al., In press) had many large dewatering volcanoes up to 4m diameter. Perhaps the difference lies in the paucity of sand layers at Mink Creek (Chapters 2 and 5).

Towards the tip of the zone of depletion the channelized deposit resembles braided or anastomosing channel deposits with concentrated flow around remnant islands (Figure 4.2). Such channelized patterns suggest an increasing down flow water content. Perhaps pore water was expelled from displaced material by loading and remoulding during later stages of the landslide. Alternatively, such patterns might represent the early stages of Mink Creek and its tributary overtopping the landslide valley fill prior to stream incision of the accumulated mass.

4.4. Trees Controlling Movement

The strength that large trees impart to the displaced mass is clear in the case of ridge 37 (Figure 4.12), where an 11m high wall of mud built up against woody debris. Here it is not difficult to comprehend that large numbers of jumbled trees can impart considerable strength to the displaced mass (Figure 4.12 inset). Perhaps sufficient numbers of trees can add sufficient strength to the displaced material, to hinder flowage from a temporary main scarp, possibly resulting in aborted retrogression (Carson and Lajoie 1981).

Other examples of trees controlling movement of material are provided by trees acting as small dams, where the accumulation surface on the down flow side of the tree is up to 30 cm lower than on the up flow side. There were also examples of this in the zone of depletion.

Mud lines on trees (Figure 4.16) are evident due south of zone 2 (Figure 3.1), and localized stripping of bark was observed (Figure 4.12). Without knowing the viscosity of the flow, there must have been enough velocity to cause piling up of displaced material, against trees, and enough to strip bark. Flows at Rissa, Norway were measured at 30-40 kilometres per hour (KPH) (Gregersen 1981), and 26 KPH at St.-Jean-Vianney in Quebec (Tavenas et al. 1971). The 10 m drop from the rupture surface to the creek would have also added velocity and remoulding energy to the

landslide. Thus, despite some control by trees, the landslide was perhaps extremely rapid as per the definition of greater than 3 m/s (10.8 KPH) in Cruden and Varnes (1996).

4.5. The Western Landslide

The western landslide is small in comparison to the main landslide at Mink Creek, its maximum dimensions 200 by 100 metres. Two narrow linear depressions, up to 20 m wide (Figures 4.1 and 4.16), occur on either side of this slide, with a seemingly undisturbed centre between them, below the crown. This central area is however heavily loaded with fallen coniferous trees from the disturbed areas to either side. The western side of the landslide infilled a preslide gully.

It is uncertain whether the western landslide (Figures 3.2 and 4.16.) was part of the main landslide event, or simply a separate landslide. Because of its downstream position relative to the main landslide, it might seem reasonable that the small slide occurred first, dammed the creek, flooding the toe of the main landslide, causing movement. There are several lines of evidence against this.

Subsidence in the vicinity of ridge 28, and to the north (Figure 3.2) seems clearly evident on the air photos. However at its head, vertical trees on slopes suggest very limited if any subsidence. Nonetheless from the airphoto, depressed grabens and fractures seem to occur between the western zone and the western slide. If these features are preserved in the zone of depletion of the main landslide, they would have occurred later.

There is also no evidence for substantial damming of Mink Creek by this landslide. The eastern portion of the landslide terminates in standing water with vertical drowned trees. Perhaps displaced material gently flowed around standing trees here without toppling them. Trees and mud in the western portion did not move far enough to reach the creek. There are vertical trees and undisturbed forest floor between the western tip of this landslide and displaced material from the main Mink Creek landslide.

A further argument against the western landslide triggering the main event involves the high rupture surface of the Mink Creek landslide. It is unlikely that such a small landslide would create a sufficient dam to trigger retrogressive failure 10 m above the Creek (Figure 4.1).

Alternatively, the elevation of the water table caused by the accumulation of the deposits of the main landslide in the creek may have triggered the western landslide. It might, thus, be a successive landslide (Cruden and Varnes 1996).



Figure 4.10 A transported ridge in the zone of accumulation.

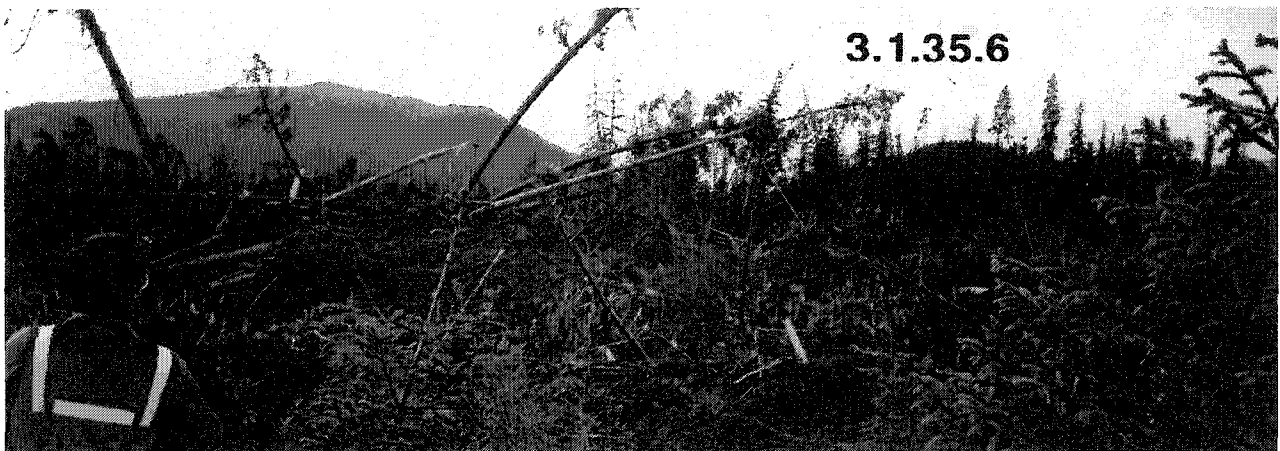


Figure 4.11 Trees and mud are jumbled together in a 4 m tall ridge at site 35 in the zone of accumulation (Figure 3.2).



Figure 4.12 Mud has built up against a resisting network of trees to form ridge 37 (Figure 3.2), east of the forest remnant. The resultant wall is 11 m high. Note the dense interlocking network of trees and stripping of bark (inset).

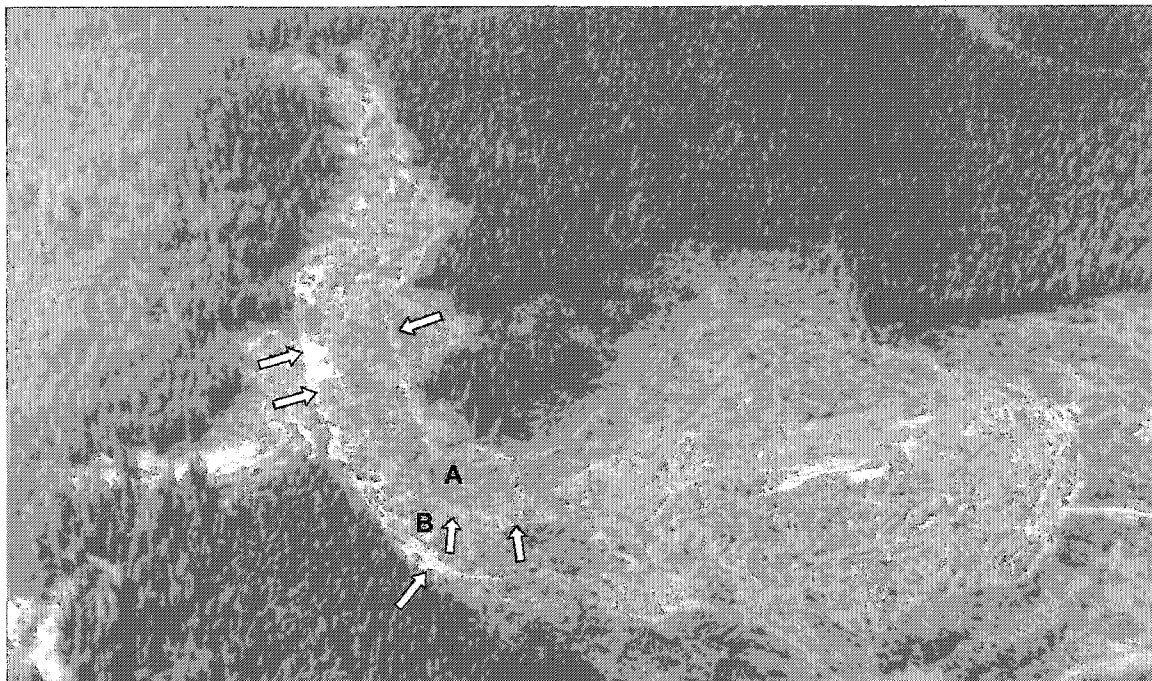


Figure 4.13 Shear zones (arrows) in the zone of accumulation are prominent and continuations of shear zones in the zone of depletion. Note the distinction between transport zones of (A) forested and (B) clearcut materials. View to the west.

3.2.2.1.2

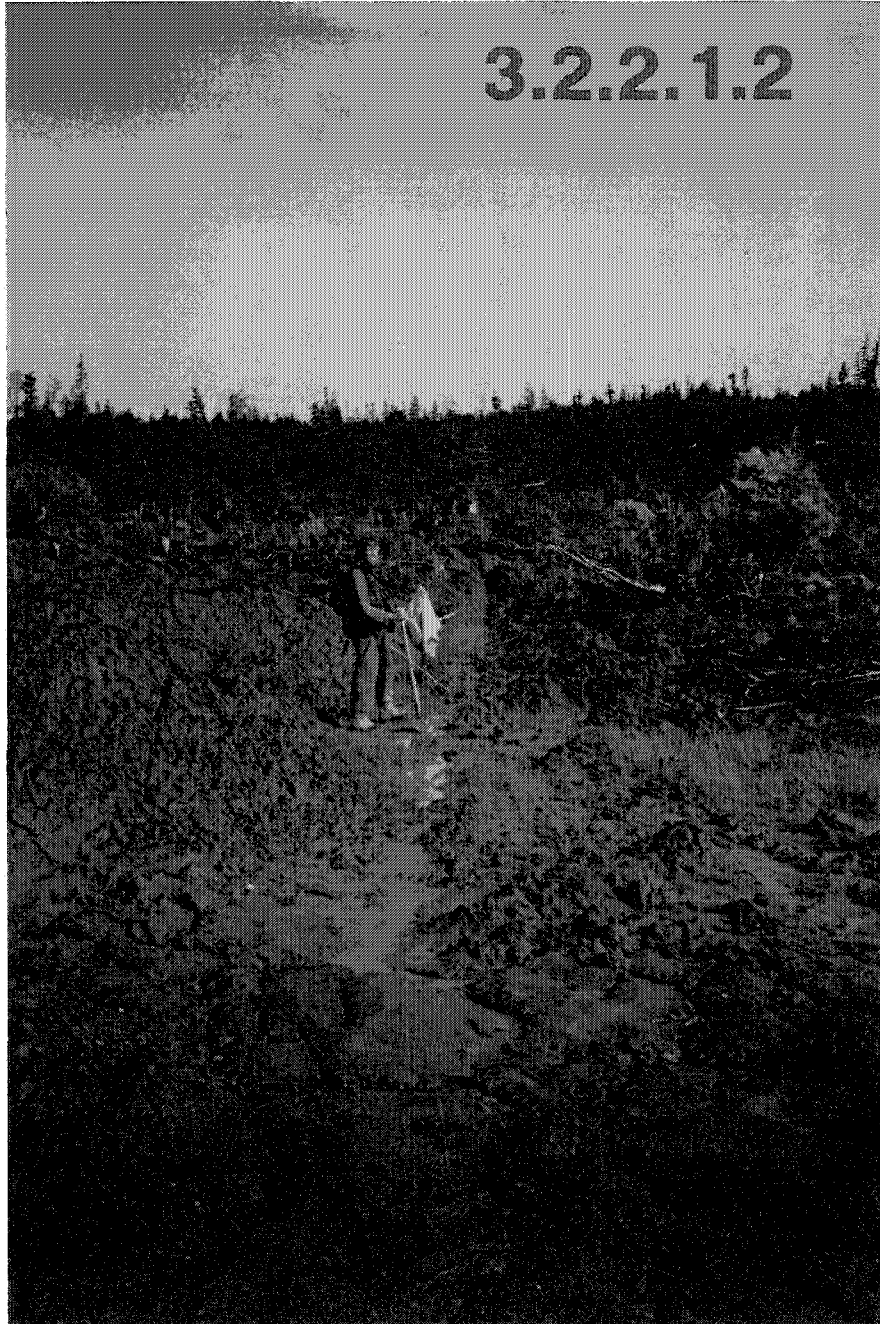


Figure 4.14 A linear shear zone in the zone of accumulation. The absence of a lateral shear ridge attests to the fluid nature of the displaced material. Location is southeast of the forest remnant.

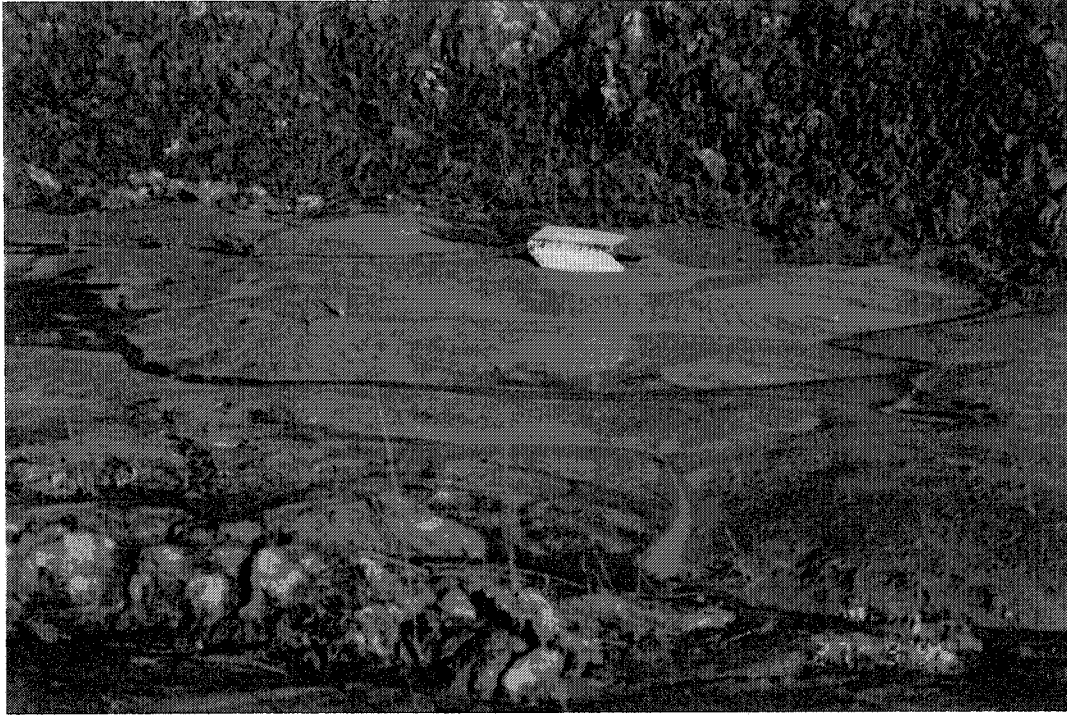


Figure 4.15 A mud volcano in the zone of accumulation indicating liquefaction. The field book is 20 cm long. Location is south of Zone 1.

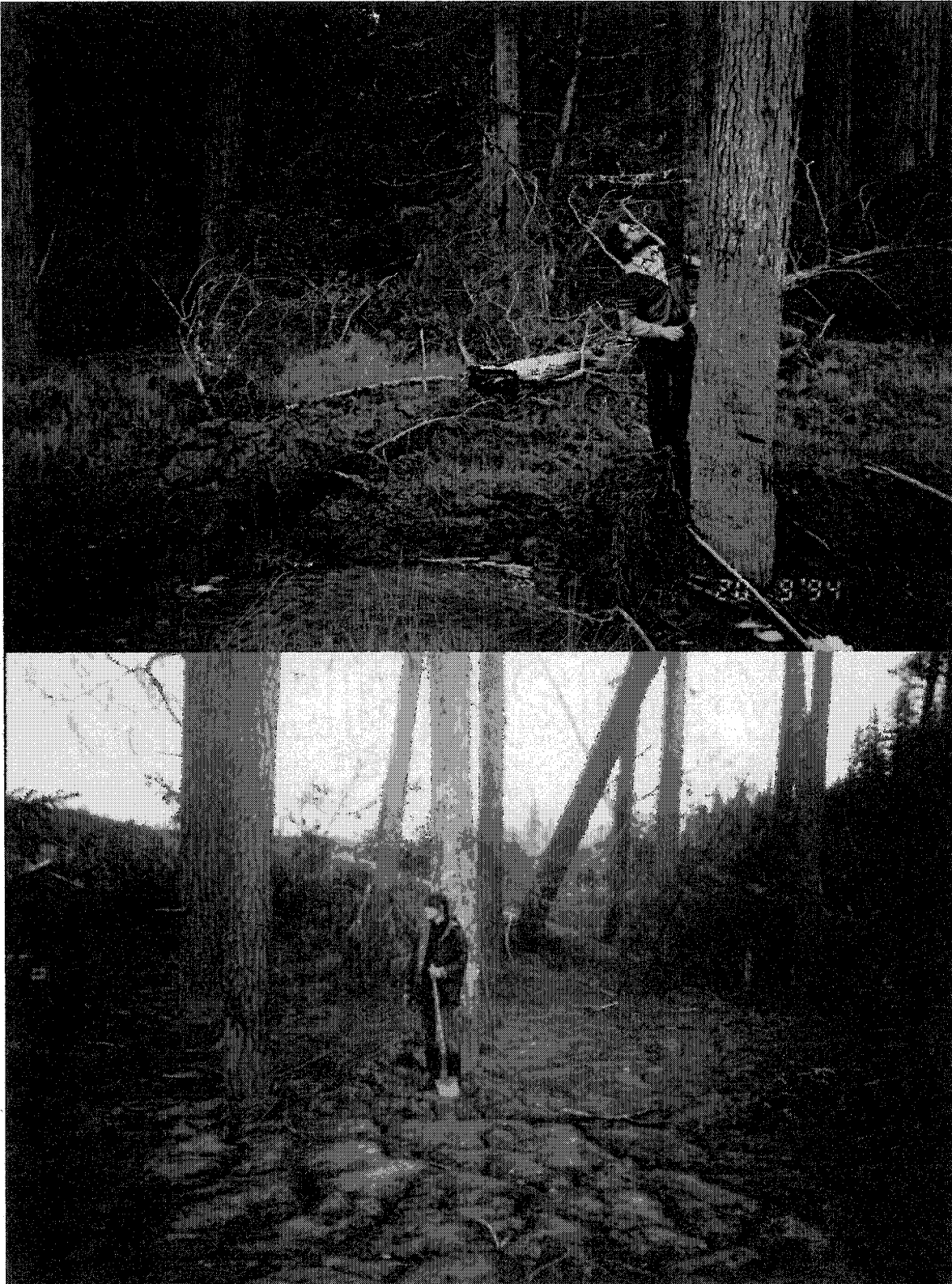


Figure 4.16 Mud lines on trees with the highest mark in the up flow direction. *Bottom:* Note the steep gradient from the leading to the down flow side of the tree. Directly south of Zones 1 and 5, respectively.

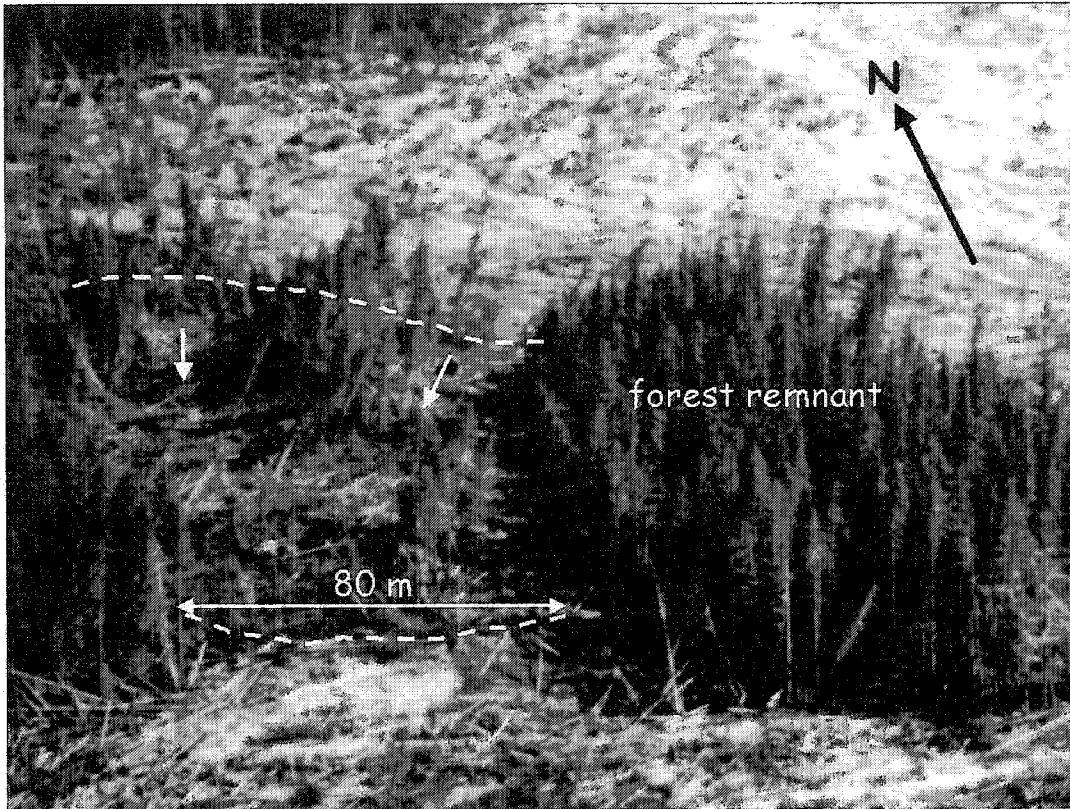


Figure 4.17 The western landslide was a separate event. Arrows indicate movement direction and narrow linear depressions.

4.6. Conclusions

The zone of accumulation is a 20 ha plain (1.5 % gradient) which filled the preslide valley of Mink Creek to a maximum depth of 14 m. Flooding from the landslide dam extended upstream 1.2 kilometres beyond the upstream margin of the displaced material.

Features on the plain included three ridges of mud and mud and trees, two small mud volcanoes, and prominent narrow lateral shear zones. The flat nature of the shear zones indicates the flow was very fluid. Despite the evidence for widespread remoulding in the zone of depletion, much of the material in the zone of accumulation had intact to only slightly disturbed bedding.

Many trees were rafted along in the upright position, or tilting to varying degrees - others were prone and mostly oriented in the direction of flow. There is evidence however, that trees strengthen and limit the mobility of the displaced material. At one location, an 11 m high wall of mud was backed up against a network of displaced trees against rooted standing trees. In some cases this could influence the extent of retrogression.

Observations of stripped trees, mud lines on trees, and flat shear zones suggests the movement may have been extremely rapid.

A small landslide occurred in a gully to the west and south of the main landslide. There is no evidence to suggest this landslide preceded the larger one. Perhaps it occurred in succession to the main event.

Chapter 5

Geotechnical Properties, Mineralogy, and Salinity of Sediment Associated with the Mink Creek Landslide

5.1. Introduction

In this chapter I describe the physical properties of the sediment associated with the Mink Creek landslide. I obtained a core above the main scarp at site B, hand-excavated clay samples at sites C and D and below A in the main scarp, and vane shear data at sites A to E (Figure 5.1). The data provided here are used for back analysis of the landslide in Chapter 6.

Laboratory work included grain size analysis, natural water contents and derived Atterberg limits and indices, as well as shear strength and density measurements. I also report on pH, porewater salinity and clay mineralogy of sediment from the borehole – analyses I commissioned from the laboratories acknowledged.

5.2. Geotechnical Properties

Physical properties of samples from a borehole at site B (Figure 5.1) are summarized in Table 5.1. The borehole was 29.3 m deep and Shelby tubes and vane shear samples were obtained alternatively. Shear strength data were obtained with a Nilcon vane borer at sites A, C, D, and E.

5.2.1. Particle Size Analysis

Visual inspection of sediment in borehole samples showed that bands of clayey silt were separated by thin, generally less than 1 mm thick, silt partings and occasional sand seams. Gravel seams and seams containing drop stones are relatively rare. Particle size analysis was determined according to the procedure ASTM D 422-63 "Standard test method for particle-size analysis of soils". Particle size data are presented in Table 5.1. Silt content generally ranges from 50 to 70%, typically about 55%, with clay ranging from 30 to 70%, typically 45%. Sand is only occasionally present. The soil thus is a clayey silt, but according to the Atterberg tests, is a silty clay. Results are dependant on the

degree of disaggregation of clay – and it is possible that disaggregation was not always complete.

5.2.2. Atterberg Limits

Atterberg limits of borehole subsamples were determined according to the standard procedure ASTM D4318-83 “Standard test methods for liquid limit, plastic limit, and plasticity index of soils”. Atterberg limit data are presented in Table 5.1.

The natural moisture contents, W , were relatively low compared with sensitive glaciomarine sediments in eastern Canada (Mitchell and Markell 1974). Moisture contents were 40% in the crust; 35 % in the sensitive area below the crust; 25% where small amounts of sand were encountered; and 6-10% in gravelly seams. Moisture contents were greater than the liquid limit below 8 m.

The samples are inorganic clays of low plasticity, in the CL range. Liquid limits, W_L , decreased as follows: 38 to 56 %, in the first 9 m; 32 to 37 %, from 9 to 15 m; and 30 to 21 %, to a depth of 30 m. Plastic limits, W_P , were around 20 % for most samples, with a maximum of 24 % in the crust, and 17 to 18 % below 20 m. Liquid and plastic limits for silty clay determined on Lakelse landslide samples were similar, 30 to 35 %, and 20 %, respectively for silty clay (unpublished data, 1962, on file at British Columbia Ministry of Transportation and Highways, Terrace, B.C.).

Liquidity index, I_L , values at Mink Creek (Table 5.1) compare with sensitive sediments in eastern Canada (Mitchell and Markell 1974). Values of 2 to 4 are not uncommon for marine sediments dominated by primary, non-clay minerals (Quigley 1980). The low contents of primary minerals in the clay-size fractions and the high silt contents at Mink Creek may account for liquidity indices ranging from 0.5-1.9. Values from the nearby landslide at Khyex River (Schwab et al., in press) and the 1962 Lakelse landslides (Figure 1.3) also fall within this range.

The sediment qualifies as low activity material (activity is the plasticity index divided by the percent clay), a requisite for quick and sensitive soils (Torrance 1987). Activity, I_a , of the soil was less than or equal to 0.3 for approximately half of the samples and the highest activity observed was 0.6 in the weathered crust.

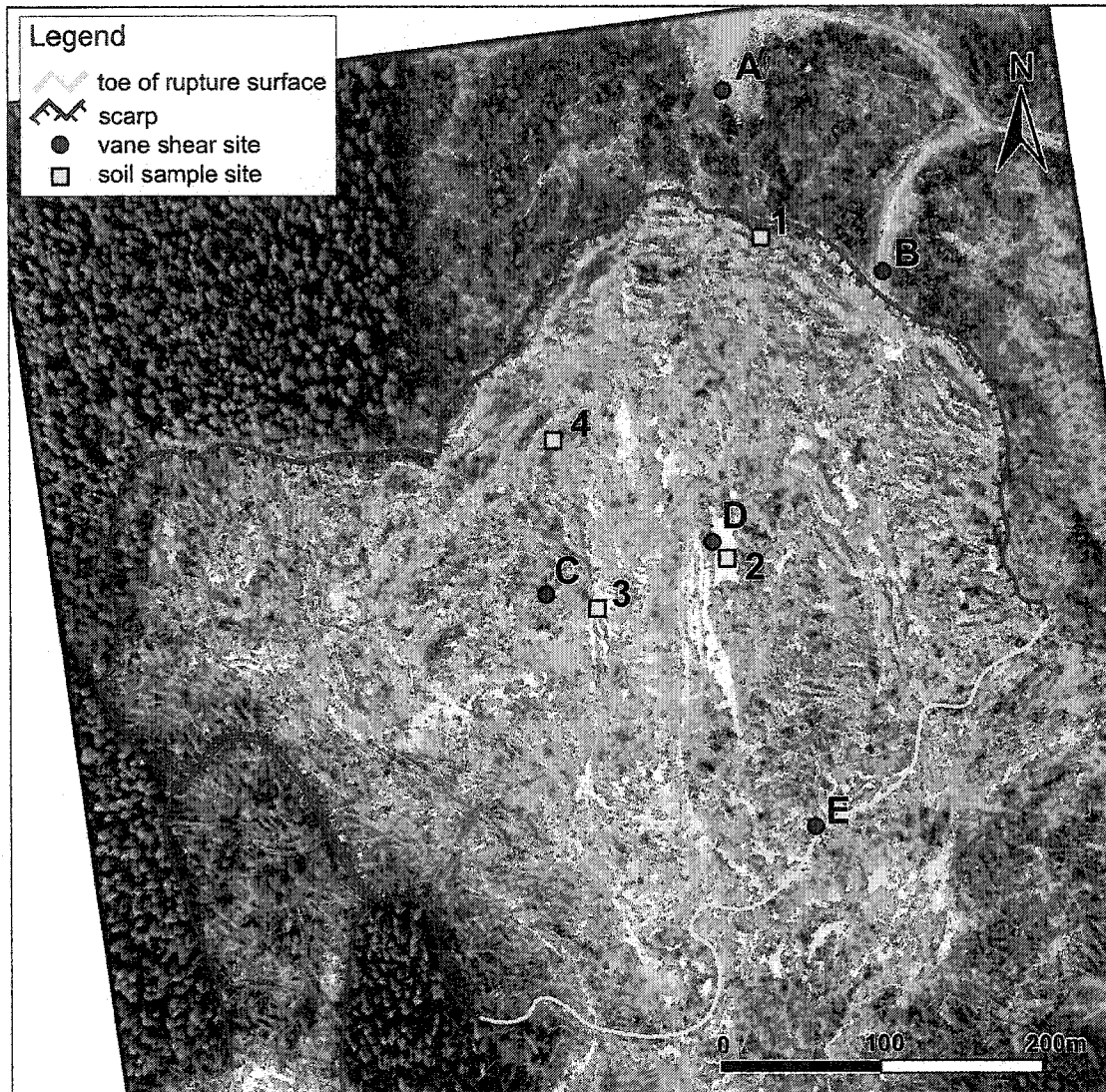


Figure 5.1 Orthophoto of the Mink Creek landslide showing vane shear and soil sample sites (including a borehole at site B).

Table 5.1 Material properties of the samples from borehole B¹

Depth (m)	W (%)	W _L (%)	W _P (%)	I _P	I _L	Activity	Sand (%)	Silt (%)	Clay (%)
1.28-1.30	38.9	55.8	24.4	31.4	0.46				
1.31-1.34	33.4	51.5	23.4	28.1	0.35	0.61	0.3	54	46
2.82-2.90	38.0	46.0	23.6	22.4	0.65	0.55	0.6	58	41
2.90-2.94	39.0								
3.05-3.16		49.5	21.6	27.9	0.67				
3.16-3.19	40.5								
3.28-3.33	34.5	45.3	22.6	22.7	0.52	0.52	0.2	56	44
5.54-5.62	37.5	41.6	24.4	17.1	0.76	0.39	0.4	56	44
5.64-5.72	40.4	44.4	21.9	22.5	0.82				
5.74-5.78	38.1	45.7	21.1	24.6	0.69				
5.87-5.94	37.9	44.8	23.5	21.2	0.68	0.46	0.4	54	46
5.97-6.01	38.4								
7.37-7.45	33.1	42.7	20.9	21.8	0.56	0.46	0.8	52	47
7.45-7.47	37.5								
7.47-7.49								48.7	51.3
7.56-7.59		38.4	22.1	16.3	0.99				
7.62-7.64								52.0	48.0
7.66-7.67		44.5	22.1	22.4	0.75				
7.70-7.75	38.9								
7.75-7.77		44.3	23.1	21.2	0.75				
7.79-7.83	35.7	40.3	19.0	21.4	0.78	0.45	0.1	52	48
8.88-8.89	36.8								
8.95-9.02	30.9	40.3	21.0	19.3	0.51	0.39	0.2	51	49
9.06-9.07	38.5								
9.06-9.14								50.2	49.8
9.21-9.24	39.0	35.4	21.7	13.7	1.26				
9.24-9.29		36.9	20.6	16.3	1.14				
10.37-10.40	35.9	33.3	20.8	12.5	1.21				
10.48-10.55	31.0	34.3	21.7	12.6	0.74	0.29	0.4	56	44
10.59-10.63	35.4	34.7	20.7	14.0	1.05				
10.71-10.76							2.1	56.8	41.1
10.79-10.86	32.3	33.2	19.0	14.3	0.93	0.34	0.8	57	42
10.89-10.91							0.4	60.7	38.9
10.91-10.95	33.8	31.9	20.5	11.4	1.17				
11.95-11.97	33.5								
12.02-12.09	30.9	32.4	18.0	14.3	0.90	0.35	1.1	58	41
12.14-12.15	35.0								
12.19-12.22	34.2								
12.24-12.29	36.8								
12.29-12.32		35.2	21.5	13.7	1.12				
12.32-12.34		35.0	21.2	13.8	1.13				
12.34-12.42	31.6	32.3	19.6	12.7	0.94	0.29	0.5	56	44
12.42-12.48		32.1	20.1	12.0	1.39				
13.49-13.57	33.1	35.4	17.3	18.0	0.87	0.39	0.4	54	46
13.65-13.69	38.0	35.3	20.8	14.5	1.19				
13.76-13.77							3.6	54.0	42.4
13.77-13.80							0.6	55.2	44.2
13.80-13.82							0.4	50.8	48.8
13.82-13.85							0.5	58.7	40.8
13.90-13.96	32.3	32.6	16.5	16.2	0.98	0.37	1.0	55	44
13.96-13.99	31.9								
15.00-15.07	33.8	32.6	19.5	13.1	1.10	0.32	0.5	59	41
15.14-15.17	33.4								
15.14-15.19		30.8	19.0	11.8	1.22				
15.19-15.22								56.7	43.3
15.23-15.26	34.8	33.8	19.4	14.4	1.07				
15.26-15.29	26.8							66.6	33.4
15.32-15.34								54.4	45.6
15.35-15.37	25.7						6.9	71.3	21.8
15.37-15.39		26.4	17.4	9.0	0.92				

Depth (m)	W (%)	W _L (%)	W _p (%)	I _p	I _L	Activity	Sand (%)	Silt (%)	Clay (%)
15.39-15.45	27.4	23.4	19.3	4.1	1.94	0.12	2.6	64	33
18.03-18.06	30.1								
18.08-18.16	33.7								
18.30-18.34		30.9	19.3	11.6	1.16				
18.34-18.38		31.4	19.9	11.5	1.04				
18.35-18.38								58.3	41.7
18.38-18.41	31.9								
18.41-18.48	30.6	32.1	19.7	12.4	0.88	0.30	1.0	58	41
19.54-19.56	25.8						0.2	70.6	29.2
19.56-19.64	25.6	38.0	20.2	9.8	0.54	0.26	2.1	61	37
19.64-19.66	28.7								
19.66-19.74		28.4	19.1	9.3	1.03				
19.76-19.79		27.4	18.4	9.0	0.84				
19.79-19.81	26.0						1.1	68.4	30.5
19.81-19.89	23.1	29.5	16.6	12.9	0.50	0.42	14.0	55	31
19.91-19.99		28.9	18.4	10.5	0.72				
22.90-22.96	32.3	30.6	22.0	10.6	1.16	0.30	0.5	65	35
22.96-22.99	27.8								
22.99-23.01		23.5	16.1	7.4	1.57				
24.1-24.7	29.8	32.1	19.0	13.1	0.82				
24.1-24.7	26.5	30.3	20.5	9.8	0.62	0.26	1.7	61	37
25.6-26.2	27.3	24.4	17.4	7.0	1.41				
25.6-26.2						7.0	58	35	
27.1-27.7	10					60 grav	25 snd	15 fin	
28.7-29.3	6					35 grav	55 snd	10 fin	
28.7-29.3	20.2	20.9	16.8	4.1	0.83	1 gravel	2 sand	97 fin	
Site 2	33.2	35.4	21.1	14.3	0.80	0.32	0.3	56	44
Site 3	36.9	39.9	22.1	17.8	0.83	0.41	0.1	57	43
Site 3	38.5	34.5	21.4	13.1	1.30	0.30	0.5	57	43

1. Borehole sample analysis done by M. Geertsema, at Ministry of Transportation and Highways Geotechnical Laboratory, Terrace, British Columbia; shaded data provided on contract by J.K. Torrance at Carleton University, Ottawa; all depths relative to site B (8 m below site A (Figure 5.1)).

5.2.3. Shear Strength

Field vane shear strength profiles (Table 5.2) were obtained at two locations above the main scarp (Sites A and B, Figure 5.1) and at three locations in the zone of depletion (Sites C to E, Figure 5.1). At site B, I used a truck-mounted shear vane, and did separate lab vane tests on Shelby samples. Site A, in undisturbed terrain, is approximately 60 m behind the main scarp of the landslide, and about 6 m west of the main scarp of the 5000 year old landslide to the east. Site B is located 10m behind the 1994 main scarp but within the prehistoric landslide just noted. Site C is in the zone of depletion on top of the Butte at an elevation of 83.5 m asl. Site D is 90 m east of Site C on the main surface of rupture of the landslide at an elevation of 78 m asl. Site E is also located on a portion of the main, gently southward dipping, rupture surface, 180 m south of Site D at a surface elevation of 73 m, a few metres above the toe of the surface of rupture (Figure 3.8).

Above the main scarp, a characteristic pattern of relatively-strong undrained shear strength in the dry crust followed by a soft, weak intermediate zone and a strong deep zone is evident. The most sensitive material ($S_t = 17-33$) measured by the Nilcon vane borer occurred between 15 and 18 m depth, where the remoulded strength ranged from 0.7-1.5 kPa (Table 5.2).

Within the zone of depletion, the lowest undrained shear strength (Table 5.2) measured by the Nilcon vane borer (field vane) was 15.5 kPa at 18.5 m depth relative to site A (Figure 5.1), and the lowest remoulded strength was 0.5 kPa at 19 m. Sensitivities in the low-remoulded-strength zone (from these field vane results) ranged from 17 to 39. Below this most sensitive zone, the undrained shear strength gradually increased from 30 to 95 kPa and the remoulded strengths increased from 2 to 32 kPa; the field-vane-determined sensitivity decreased from 15 to 1.4 through this same depth range.

The truck-mounted field vane was not capable of accurately measuring low remoulded strengths, thus I measured remoulded strengths in the laboratory using the laboratory-vane method (ASTM D4648). Because the Shelby tube samples from site B were transported in the back of a pickup truck over a very rough logging road, I could not determine undisturbed field strengths in the laboratory. Therefore I combined the field-vane undisturbed strength and the laboratory-vane remoulded strengths to determine

sensitivity of the borehole sediment. Here I determined sensitivities of 72 ($S_r = 0.65$ kPa) and 118 ($S_r = 0.22$ kPa) at 18.5 and 19 m, respectively. Thus there is a zone, at least 2 m thick, which meets quick clay criteria (Torrance 1983). Similar shear strengths and sensitivities were obtained for the Lakelse landslides (Figure 1.3) and for the site of a nearby CN railway bridge (unpublished data, 1962, on file at British Columbia Ministry of Transportation and Highways, Terrace, B.C.).

Despite these general observations of shear strength, I observed that blue layers appeared to remould and flow out of excavations more readily than layers of other colours. At various locations bluish layers exposed in excavations flowed out of exposed faces. A trench in zone 4b showed the rupture surface in a blue stratum (Figure 5.2). Vane shear tests on similar blue strata showed no striking differences in S_u , S_r or S with other strata of different colour. Perhaps the difference lay in the higher rapidity of some of these blue layers. Rapidity is a term introduced by Söderblom (1974) and expanded on by Söderblom (1983) and Tavenas et al. (1983) referring to the energy required to transfer from the undisturbed state to the remoulded state, independent of the respective strengths of these two states. An exposed highly rapid layer would be more likely to transport material, than a layer of equal sensitivity, but lower rapidity.

5.2.4. Density and Stability Numbers

I measured the oven-dry density of fifteen samples collected from sites 1, 3 and 4 in the zone of depletion. The material in site 1 was remoulded, while the material at sites 3 and 4 was undisturbed (Figure 5.1). The oven dry density, in grams per cubic centimetre, for sites 1, 3 and 4 was 1.57, 1.41 and 1.44 respectively. Density is a component of the bulk unit weight calculation of the stability number (N_s) used by Mitchell (1978) in the prediction of landslide retrogression.

$$N_s = \gamma \cdot H / S_u, \quad (1)$$

where γ is bulk specific weight and H is height above the surface of rupture.

Given that the majority of the preslide material was undisturbed (the prehistoric landslide deposit involved only a small percentage of the sediment), I use the undisturbed oven dry densities from sites 3 and 4 to calculate the bulk specific weight (γ). By adding the unit weight of water, using an average water content of about 35% from Table 5.1, the

total bulk specific weight becomes 1.75 g/cm^3 or 17.5 kN/m^3 , values in line with Champlain Sea landslide sediments (Mitchell and Markell 1974; Mitchell 1978).

Profiles of N_s (based on local H prior to the slide) are shown in Figure 5.3. The values are very high (averaging about 12, at all depths below the weathered crust), and are at the upper limit of N_s values reported by Mitchell and Markell (1974) and Mitchell (1978) for flowslides.

Table 5.2 Vane shear data¹.

Depth (m)	A ²			B			C			D			E		
	Su	Sr	St	Su	Sr	St	Su	Sr	St	Su	Sr	St	Su	Sr	St
3	>68														
3.5	56.4	14.7	3.8												
4	35.3	7.8	4.5												
5	22.1	4.9	4.5												
6	21.1	4.9	4.3												
6.5	21.3	4.2	5.1												
7	21.6	4.2	5.1												
7.5															
8	19.9	3.9	5.1												
9	22.1	4.9	4.5												
9.5				59.8	31.5	1.9									
10	23.5	4.2	5.6												
11	24.5	4.9	5.0												
11.5				36.5	7.2	5.1									
12	23.5	5.4	4.4												
13	25.8	3.7	7.0	27	6.7	4.0									
13.5															
14	24.3	2.2	11.0												
15	23.3	0.7	33.3												
15.5	25.5	1.5	17.0	34	4.7	7.2									
16	25.0	1.2	20.8												
16.5				37	2.4	15.4									
17	27.5	1.0	27.5												
18	> 29			46	0.65	72	17.0	1.0	16.5						
18.5	14.7	0.7	21.0				15.5	0.8	20.0						
19	16.4	2.0	8.2	26	0.22	118	19.8	0.5	38.5						
20							22.1	1.3	17.2						
21							23.2	1.0	22.5						
21.5				47	1.1	43									
22.5							26.8	1.0	26.0						
23							23.2	1.5	15.0	24.7	1.0	24.0			
23.5				65	1.7	38									
24							25.2	2.1	12.3	30.6	2.1	14.9			
25							27.3	2.6	10.6	31.9	2.8	11.3			
26							30.4	2.6	11.8	38.1	3.1	12.3			
26.5				76	2.9	26									
27							33.0	3.9	8.5	35.5	2.8	12.5			
27.5				76	2.6	29									
28							35.5	4.6	7.7	39.9	4.1	9.7	25.6	6.0	4.3
29							37.6	3.6	10.4	40.4	4.6	8.7	25.3	4.1	6.2
30							35.0	4.1	8.5	43	10.0	4.3	12.8	6.5	2.0
31							47.4	7.2	6.6	29.1	6.4	4.5	32.1	3.8	8.4
32											12.9		31.9	6.3	5.1
32.5							44.3	10.3	4.3						
33							43.3	9.8	4.4				38.1	8.4	4.5
34							54.6	13.4	4.1				39.7	7.9	5.0
35							59.2	15.5	3.8				40.6	11.7	3.5
35.5										39.1	27.8	1.4			
36							56.7	19.6	2.9	38.6	27.8	1.4	40.6	13.9	2.9
37							62.8	22.7	2.8	25.2	13.6	1.8	67.0	32.7	2.1
37.5							56.7	16.5	3.4						
38										63.3	13.4	4.7	57.2	20.1	2.8
39										52.5	25.2	2.1	52.3	15.8	3.3
40										49.4	30.9	1.6	52.8	17.4	3.0
40.5										50.5	24.7	2.0			
41													95.3	18.5	5.1

1. A,C,D and E measured with Nilcon Vane Borer. B – Su measured with truck mounted field vane, Sr from adjacent sample with lab vane. Grey bars represent preslide material removed during the landslide. Su and Sr units are KPa.

2. All depths are relative to site A. See Figure 5.1 for site locations.

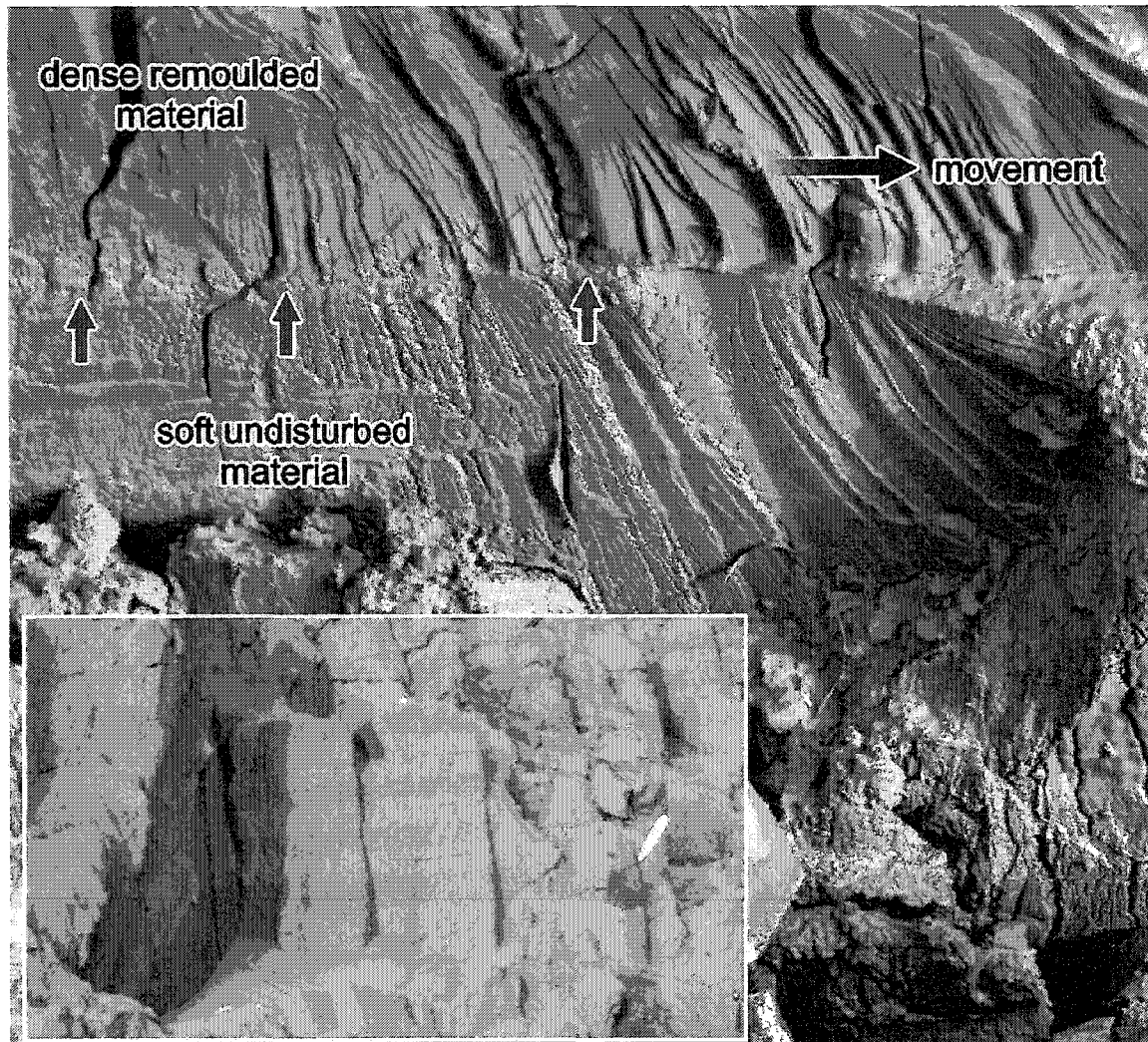


Figure 5.2 A rupture surface is exposed in a blue layer (10 cm thick) in a trench in Zone 4b (Figure 3.16). Perhaps this was a layer of high rapidity. The displaced material is dense and remoulded while the lower material is soft and undisturbed. The inset photo shows the colour banded nature of the sediment at depth. Photos courtesy of Nichole Boulton.

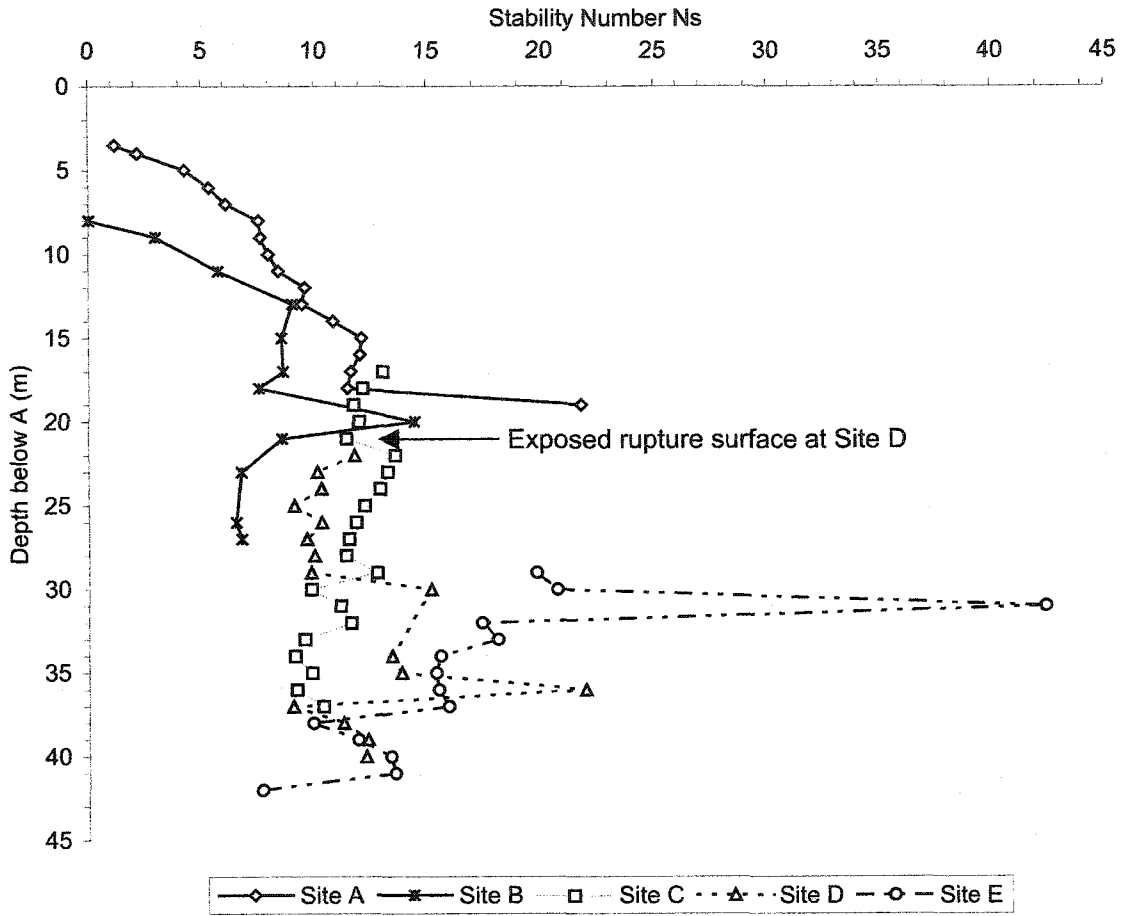


Figure 5.3 Profiles of the stability number (N_s) –see Figure 3.1 for locations). Depths are relative to site A.

5.3. Mineralogy

Mineralogy of the clay-size fraction from sediment exposed in the walls of the Butte was determined by X-ray diffraction in laboratories at Carleton University (J.K. Torrance), the University of British Columbia (L. Lavkulich), and the University of California, Riverside (R.C. Graham and K.R. Tice). The results below are listed in order of abundance. Samples sent to Carleton University yielded chlorite, illite, feldspar and quartz, with the possibility of kaolinite. Samples sent to the University of British Columbia yielded kaolinite, chlorite, illite, vermiculite, quartz and feldspar. Samples sent to the University of California, Riverside, yielded chlorite, illite, kaolinite, quartz and feldspar. These small differences may reflect varying interpretations of peaks or actual mineralogical variability in the sediment.

Mineralogy of glaciomarine sediment in the Terrace area has been reported by Clague (1984) and is also available as unpublished data with the British Columbia Ministry of Transportation and Highways. Clague (1984) listed clay mineralogy as 41% chlorite, 37% illite, and 22% kaolinite for a site located approximately 2 kilometres from the Mink Creek landslide and kaolinite 44%; illite 31%; and chlorite 25% for the sediment from a landslide at Lakelse Lake. Mineralogy of the nearby Lakelse landslides is also recorded as: illite 40%; chlorite 35%; quartz 20%; and feldspar 5% (unpublished data, 1962, on file at British Columbia Ministry of Transportation and Highways, Terrace B.C.).

Although there are some differences in the reported clay-size fraction mineralogies, the samples consisted of predominantly low activity, non-swelling clay minerals and rock flour-derived quartz and feldspar. Figure 5.4 provides a scanning electron micrograph of the sediment showing its flocculated structure.

5.4. Salinity and pH

Pore water salinity was determined on samples from the borehole by J.K. Torrance (Carleton University). The salinity increases with depth, but the maximum value of <2 ‰ indicates that these originally high-salinity sediments (15-20 ‰ (Clague 1984)) have been heavily leached (Table 5.3). The profiles of increasing salinity and increasing Na with depth, indicate that the water flow which accomplished leaching at this site has

been downward. These low salinities in an originally glaciomarine sediment are consistent with the development of high sensitivities (Torrance 1983).

The pH increased from neutral at 2.8 m to 8.1 at 10.5 m. Below 10.5 m pH remained relatively constant (Table 5.3). This may relate to depletion of CaCO_3 with surface weathering.

Table 5.3: Salinity and pH from a borehole at the Mink Creek landslide.

Depth ¹	Salinity	pH
(m)	(‰)	
9.4	0.08	
10.8	0.28	7.05
11.3	0.36	7.32
13.5	0.57	7.40
13.9	0.65	7.64
15.4	0.69	7.41
15.8	0.98	7.35
17.0	0.87	7.78
18.5	1.12	8.10
18.8	1.12	8.16
20.1	1.12	8.24
20.4	1.12	8.38
21.5	1.25	8.16
21.8	1.19	8.12
23.0	1.13	8.05
23.4	1.17	7.90
26.1	1.23	8.04
26.5	1.19	7.95
27.6	1.15	8.24
27.9	1.17	8.18
31.4	1.10	8.08
33.0	1.99	
34.6	1.36	
B _{high} ²	0.78	7.66
B _{low} ²	0.92	7.73

¹ Relative to Site A – thus 8 m lower.

² From the Butte area, above the main rupture surface (site 3 – Figure 5.1)

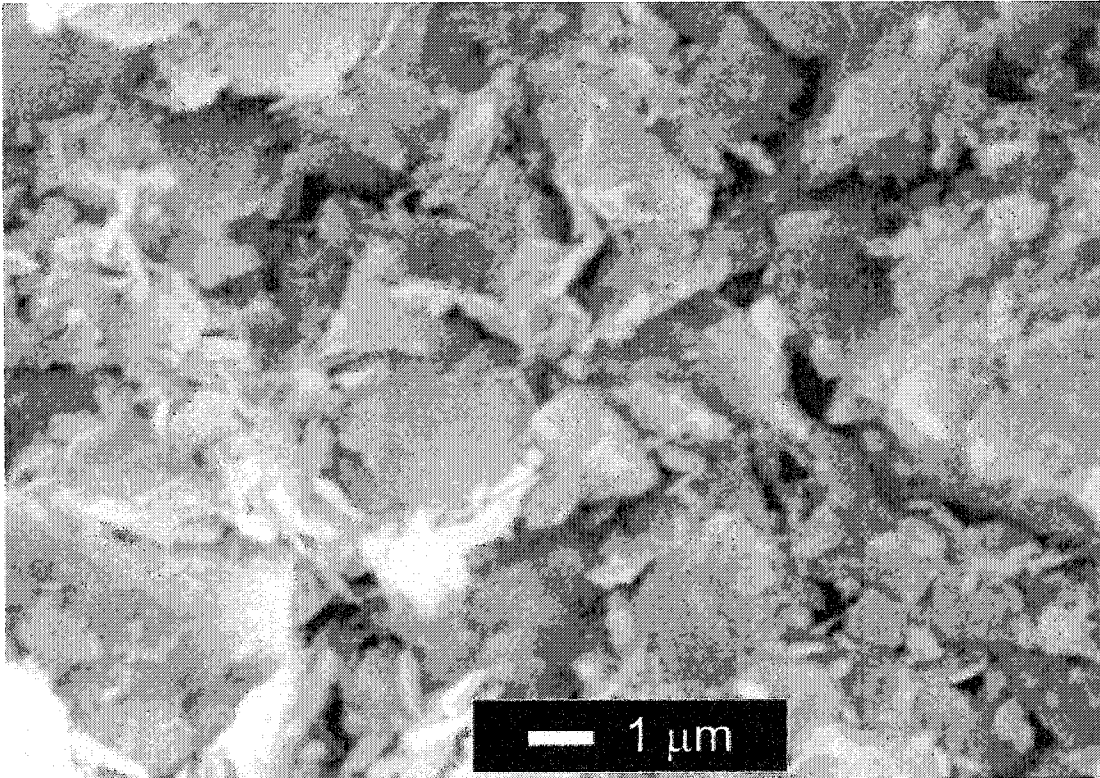


Figure 5.4 Scanning electron micrograph of flocculated glaciomarine sediment from the Mink Creek landslide. Image provided by J.K. Torrance.

5.5. Conclusions

The glaciomarine sediment associated with the Mink Creek landslide is essentially a mud, about 55 % silt and 45 % clay, but based on the Atterberg tests, a silty clay. The flocculated material has been leached of salt and as a result of this has developed into a sensitive, and some cases, a quick clay. In one location, sensitivity was greater than 100. The soil has a characteristic undrained shear strength profile with stronger material in the weathered crust and at depth, and weaker material in an intermediate zone.

Despite high sensitivities and low remoulded strengths, liquidity indices were generally low, although near the depth of the rupture surface they were consistent with values reported by Mitchell and Markell (1974). This may be attributed to the low primary mineral content of the sediment (Quigley 1980). The mineralogy of the clay-size fraction is predominantly chlorite and illite, with lesser amounts of quartz and feldspar. The profile of decreasing salinity with depth indicates the salt has been leached from the sediment by downward movement of ground water.

The sediment at Mink Creek has Atterberg properties, strength, and mineralogy similar to eastern Canadian (Mitchell and Markell 1974; Quigley 1980) and Scandinavian Rosenqvist 1953; Söderblom 1974; Torrance 1987) marine clays. The general model for quick clay development (Torrance 1983) proposes that certain depositional and post-depositional requirements should be met for a sediment to develop into a quick clay. The required depositional factors are: development of a flocculated structure at the time of deposition; and the domination of the sediment by minerals of low activity, and the absence of swelling clay minerals (high activity). The post-depositional requirement is that salt-removal occur (whether by leaching or diffusion) which results in a decrease of the liquid limit while the water content remains constant. The Mink Creek material meets the requirements of the general model and takes its place with the glaciomarine sediments of eastern Canada and Scandinavia (Torrance 1983).

Chapter 6

Movement History of the Mink Creek Landslide

6.1. Introduction

In this chapter I show how detailed morphologic analyses of displaced material, together with pre and post landslide surface topographic profiles, and shear strength data can be used to reconstruct movement style and sequences of the Mink Creek landslide (Figure 2.1). I propose a sequence of macro scale movements that I infer from geomorphological observations.

I also show how the available geotechnical data (Chapter 5) support the conclusions inferred from the morphologic analyses. I caution, however, that geotechnical data collected after a landslide occurs should be treated with some skepticism. The properties of the displaced material may have changed, and the properties of materials not displaced by the landslide do not necessarily reflect the properties of the materials that were involved in the landslide.

Finally, I compare the Mink Creek landslide to other landslides in similar sediments.

6.2. Triggers

Nearly a decade of warming and increasing precipitation preceded the Mink Creek landslide. A wet fall and early winter before the landslide resulted in elevated water levels in wells and streams. These hydroclimatic conditions may have been important preconditions for the landslide. I expand on this in Chapter 7.

Although large landslides in glaciomarine sediment have been attributed to earthquakes (e.g. Aylsworth et al. 2000), a seismic trigger can be ruled out for the landslide at Mink Creek. No earthquakes were recorded or were felt in the Terrace area before or at the time of landslide (Personal communication, Geological Survey of Canada, National Earthquake Database, Sidney B.C., 2002).

Portions of the forests around the Mink Creek landslide were harvested in 1981 and 1985, respectively (Figure 1.3). The possibility that forest harvesting contributed to the landslide cannot be ruled out.

6.3. Inferred Movement History and Supporting Evidence

The detailed morphological descriptions of features in the zone of depletion provide clues as to how and when movements may have occurred relative to each other. Comparison of detailed pre and post landslide topographic maps, observations of main scarp stratigraphy, and strength characteristics provide additional important data for the reconstruction of movements. Figure 6.1 shows the zones described in Chapter 3, with major and minor movements indicated.

6.3.1. Initial landslide

Large landslides in sensitive glaciomarine sediments are often observed or interpreted to enlarge retrogressively, starting with a small earth slide and enlarging into spreads or flows (e.g. Carson 1977, Gregersen 1981). A broad depression indicated on Figure 6.2, has the rough outline of an old landslide scar. This may have been the location of an initial landslide that began a series of complex and much larger movements. Beside the landslide-shaped profile of this slope, two other features support this location as the beginning of the initial landslide. 1. The 1988 airphotos show ponded water on the road above the bend to the west and above this slope (Figure 1.3). 2. The ridges in zone 2a and broad bands in zone 2b (Figures 3.13 and 6.1) are roughly equidistant from this potential triggering landslide. The orientation of those ridges and bands (interpreted as collapsed ridges) suggest westward and eastward movement, respectively into a central cavity.

There are other steep locations on the north slope of the valley that could have experienced landslides, but an enlarging zone of depletion above the triggering landslide indicated in Figure 6.1 is the only location that corresponds well with the interpreted eastward and westward movements described above.



Figure 6.1 1994 orthophoto of the Mink Creek flowslide. Note the numbered zones distinguished on the basis of morphology and style and direction of movement (Chapter 3). The landslide to the southwest is separate from the main landslide. Red and blue arrows indicate direction of primary and secondary movements, respectively.

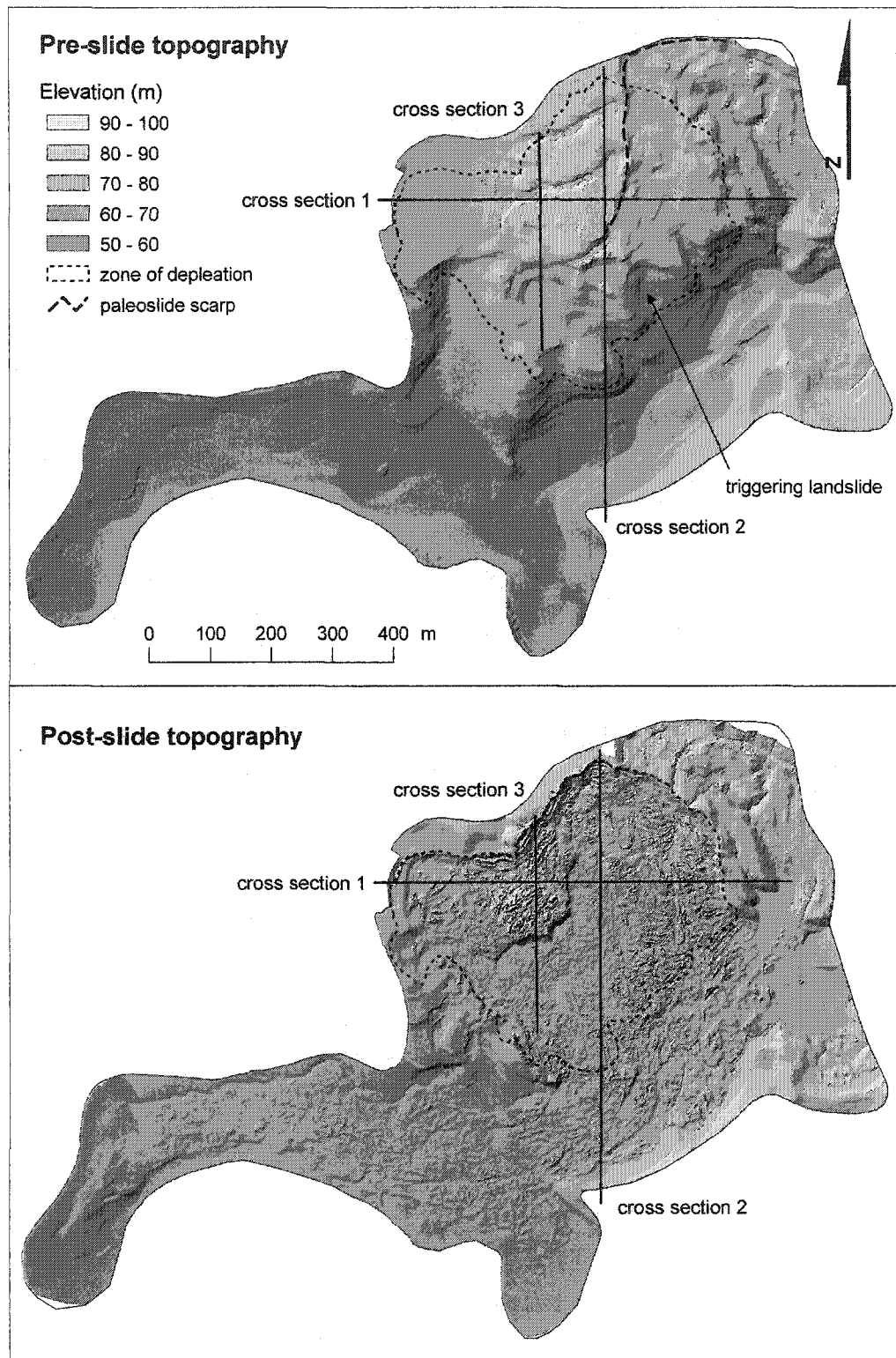


Figure 6.2 Hillshade image of pre and post landslide topography. Note the locations of the cross-sections, the gully to the east of the landslide, and the scarp of a 5000 year old landslide.

6.3.2. The First Flow

I assume that a very sensitive layer was exposed in the main scarp of the initial landslide in the depression indicated on Figure 6.2. Such a sensitive stratum would have liquefied, resulting in retrogressive enlargement of a central translational landslide. The elevation of this rupture surface was about 73 m at the edge of the zone of depletion, increasing up slope along the stratigraphic dip (2 to 3°). This is the map-measured elevation of site E (Figure 6.1), where the exposed convex rupture surface (Figure 3.8) marks the edge of the zone of depletion and is perched about 10 m above the creek (Figure 6.2). I suggest this second landslide was a flow that displaced material moved out of a relatively long narrow zone. Evidence for the presence of a long, narrow central zone of depletion is provided in the following section.

6.3.3. Spreading into a Central Zone of Depletion

The argument for lateral movement into a central zone of depletion is based on the presence and orientation of the ridges in zone 2a and the broad bands in zone 2b (Figure 3.9 ; Figure 6.1). Let us assume that the broad bands were once transverse ridges mirroring the transverse ridges in zone 2a. The northern, up-flow end of these ridges bend toward each other. The presence of brown weathered material on ridge faces (Figure 3.9) is generally interpreted to represent the leading, down-flow side of transverse ridges (Carson 1979, Geertsema and Schwab 1996). Accordingly, the brown weathered material draping the west slopes of ridges in zone 2a suggests movement to the west. In a similar fashion, the broad bands in zone 2b suggest movement to the east. Both movements are interpreted to have been spreads in the direction of a central zone of depletion, normal to the southward stratigraphic dip.

6.3.4. Further Spreading in Response to Lateral Movement

Westward movement of ridges in zone 2a would have created a longitudinal temporary scarp trending roughly N-S (Figure 6.1). Following this westward movement, transverse ridges in zone 3 moved southward. The orientation of several sets of ridges, with inter-ridge weathered and surface material, suggest that the movement occurred by retrogressive spreading. The narrowness of zone 3 probably relates to the presence of a pre-slide gully immediately to the east of the landslide.

Gullies often constrain retrogression, as landslides are often flanked by large pre-existing gullies. Examples include the 1971 South Nation landslide (Eden et al. 1971; Mitchell 1978) and the 1993

Lemieux landslide (Evans and Brooks 1994). Gullies can limit retrogression by: 1. providing a negative topography, eliminating lateral earth pressure; 2. lowering the water table locally; and 3. development of stronger sediment in the gully walls (Carson and Geertsema 2002).

Eastward movement of ridges (later collapsed to broad bands – see Chapter 3) in zone 2b also triggered more spreading (evidence is presented in section 6.3.5). In this case, the surface of rupture may still have been perched 5 m above the rupture surface in the central zone of depletion. The two arcuate widenings on the Butte (zones 4a and c, and zone 4b), with east moving ridges, followed the eastward movement of the broad bands in zone 2b.

The westward and southward extent of these widenings is constrained by the preslide topography. Figure 6.3 illustrates why it was possible to have a perched rupture surface at the elevation of the upper Butte (zone 4a) surface, and why it was impossible to have movements continue at this elevation, where preslide slopes decreased below a certain N_s -dependent threshold. These figures do not explain why movement occurred at this surface, rather than at a perhaps equally suitable lower surface. It is possible that movement simply occurs in particularly sensitive layers, or perhaps in blue layers of high rapidity (Figure 3.2) as discussed in section 3. Projecting the Butte surface southward, using a 4° southward bedding dip, Figure 6.4 shows that the slope height (H) is rapidly reduced along the south facing preslide slope. Given that the stability number (N_s) should generally be greater than or equal to 6 for retrogression to occur (Mitchell and Markell 1974), H places constraints on S_u . Similarly, a range of undisturbed shear strength (S_u) values can give a range of constraints on the slope limits to retrogressive enlargement. Figure 3.3 shows how N_s varies with depth at Mink Creek.

I use the lowest S_u value of 15.5 kPa from the Mink Creek landslide (Table 5.2) and a γ of 17.5 kN/m³ to calculate a limit on H . Using Mitchell's (1978) minimum N_s of 5 – his requirement for retrogression in “flowslides” and “earthflows”, any H less than 4.4 m would halt enlargement by retrogression.

CROSS SECTION 1

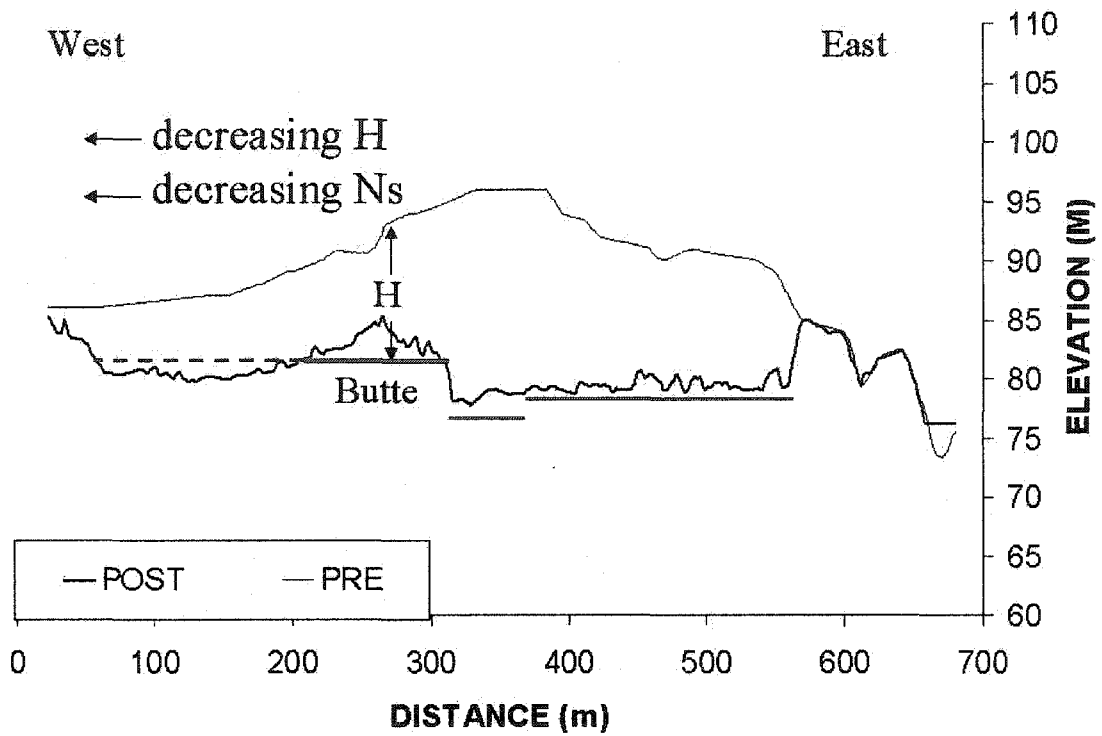


Figure 6.3 Cross-section 1 trends E_W through the zone of depletion (see Figure 6.2 for location). The red lines represent various surfaces of rupture. The dashed line extends the perched rupture surface of the Butte (zone 4a) to illustrate how H and Ns would become too small at that elevation for westward retrogression to continue (see Figure 6.1 for movement directions). Note the preslide gully to the east of the landslide.

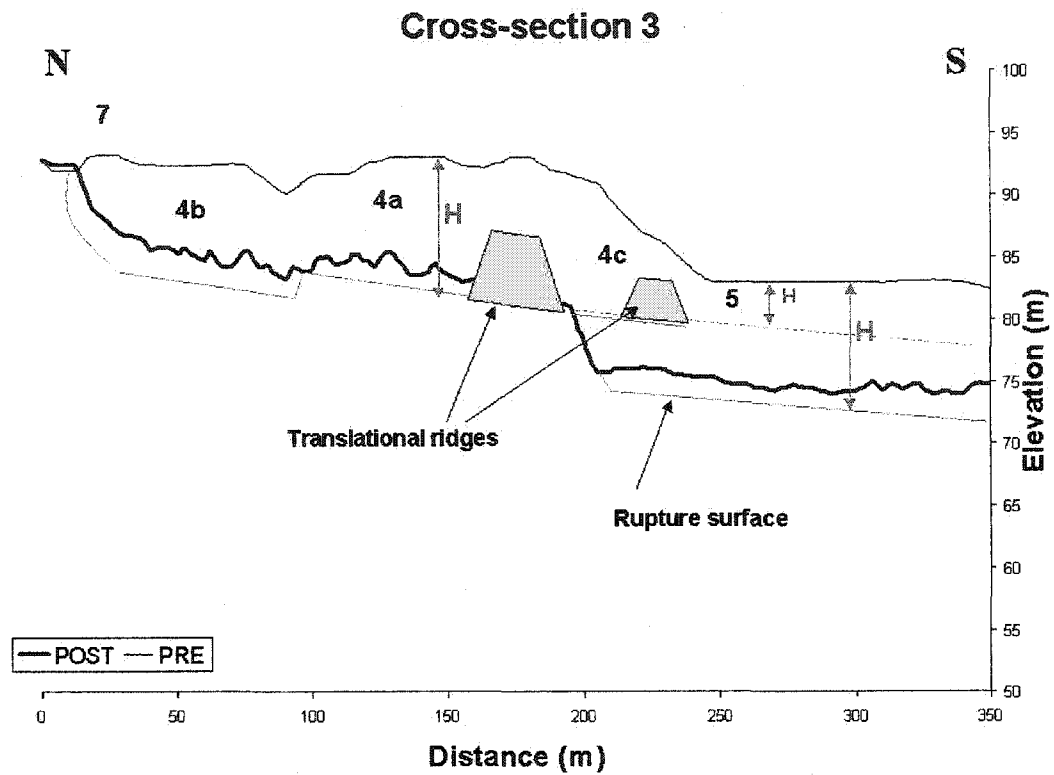


Figure 6.4 Cross-section 3 (see figure 6.2 for location). Spreading occurred in zones 4 a to c (Figure 6.1). In zone 4c the initial spread occurred on the upper rupture surface, followed by subsidence to the lower surface. The grey blocks represent translational ridges from the initial spread (Figure 6.5). The preslide slope between zones 4c and 5 illustrates why the spread was constrained to the south. Flow occurred in zone 5 and rotational sliding in zone 7.

6.3.5. Subsidence Associated with Spreading

The next major event in the eastern widening involved widespread subsidence (Figure 6.5). Subsidence south and east of the Butte likely occurred first, with squeezed out material flowing south, along the general dip slope into the zone of accumulation. This subsidence was probably shortly followed by subsidence in zone 4b with flow to the east and southeast. Evidence for subsidence comes in several ways and is presented in the following paragraphs.

1. Transverse ridges on the southern edge of the upper Butte surface (zone 4a) have steep cross-sectional faces accordant with the Butte wall. One such face occurs in the south wall (Figure 6.8) and another in the wall separating zones 4a and b.
2. The pattern of broad grey and brown bands, representing ridges and wedges (grabens), respectively in zone 4c, conforms to the ridge pattern in zone 4a and has a similar mid-ridge spacing (Figure 6.5). Together these bands and ridges form arcuate planform crescents. Using form analogy, the broad bands in zone 2b can also be interpreted as ridges that have subsided along materials beneath a perched rupture surface. These ridges then mirror the orientation of ridges in zone 2a.
3. The orientation of the walls of the Butte is straight rather than arcuate like the main scarp (Figure 6.5). This geometry suggests vertical subsidence occurred south and west of the Butte.
4. Zone 4b has a low horizontally stratified ridge (site 18, Figure 3.2) protruding from a split graben (Figure 3.21). This ridge crest is separated from the mid point of collapsed grey material (a broad grey band) by about 30 m, a distance similar to the ridge spacing on the upper Butte (zone 4a) and of the broad bands (Figure 6.5). Particularly noteworthy is the presence of *Equisetum arvense* (horsetail) root channels in the ridge crest at elevation 84 m, while the preslide elevation was about 95 m here. Measured depth of these roots in excavations in the main scarp ranged from 4 to 4.6 m. Thus the presence of horsetail roots places this crest about 4 m below the preslide surface. This indicates that the ridge subsided 7 m. The middle rupture surface is about 2.5 m lower than the upper rupture surface, indicating that amount of subsidence between the two surfaces. Thus the original height of the ridge was 4.5 to 5 m, which corresponds to ridge heights of 4.5 m on the upper surface in zone 4a.

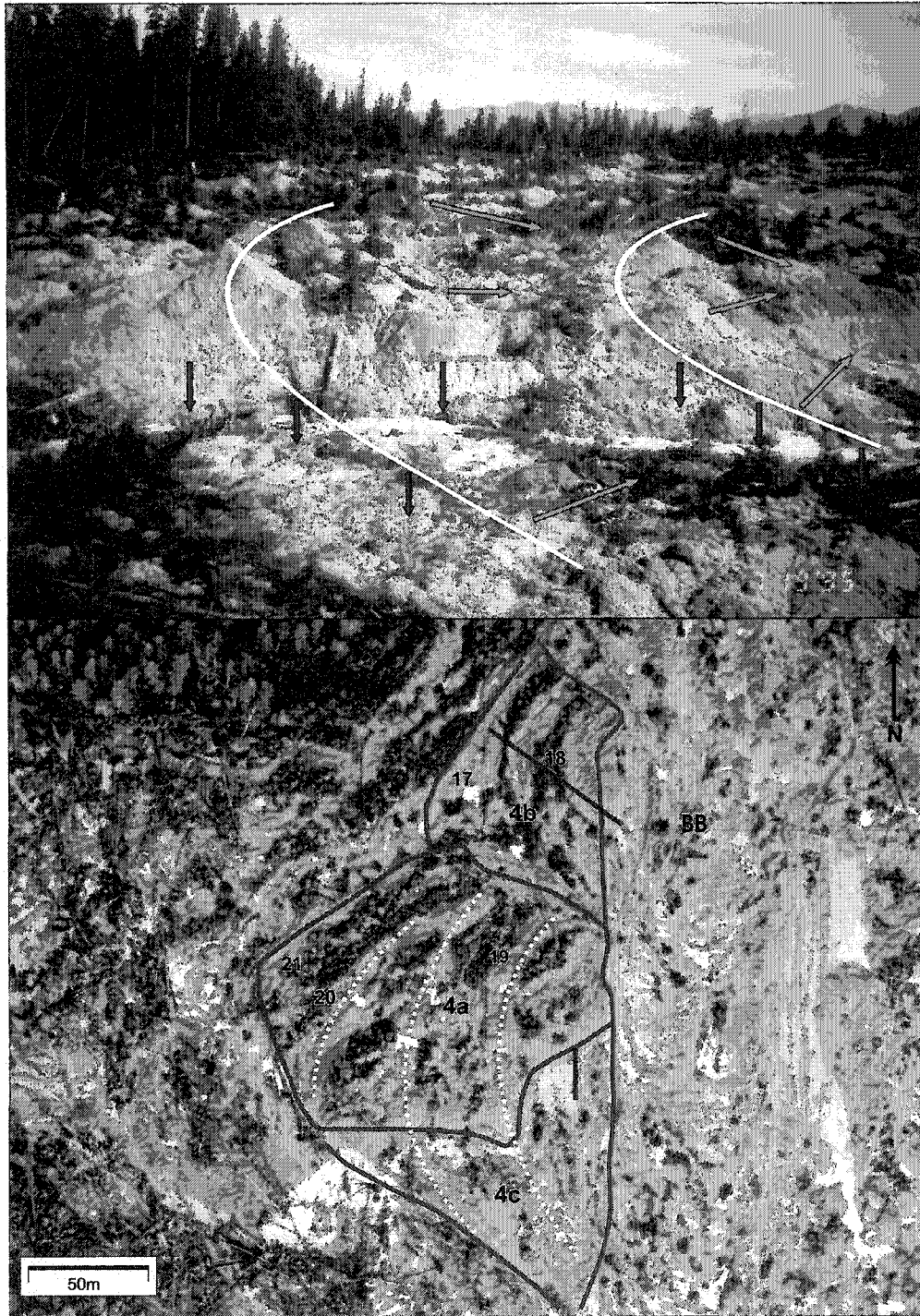


Figure 6.5 Top. The upper and lower surfaces of the Butte (zone 4). Dashed blue line represents the perched rupture surface. The white lines represent the pattern of arcuate ridges shown below. The blue arrows indicate the direction of first movement (spreading). The red arrows indicate subsequent collapse. Bottom. Vertical airphoto (1994) showing the zones on the Butte and the arcuate planform of the ridges. Note the similarity of the collapsed ridges in zone 4c and the broad bands (BB) to the east in zone 2a. Note the transverse faulting of the grey ridge at A.

6.3.6. Spreading and Flow in the Western Widening

The preslide ground surface sloped westward and southward in the western widening (Figures 6.3 and 6.4), yet the direction of movement of displaced material is primarily to the east and southeast. The preslide topography would suggest the gully east of the forest remnant, would have been a more likely movement route. It is likely that westward enlargement from the initial landslide in zone 1 (Figure 6.1), combined first with eastward spreading and then southward flow from zone 2b, and Butte collapse (Zone 4c) opened a channel for southeastward movement out of the western widening.

Once material began moving southeast through zone 5, radial retrogressive enlargement of zone 6 began, and material on the western side of the Butte and west of the divide east of zone 4b (Figure 6.1) moved southwest into the midwest zone. Evidence for westward movement is clearly provided by the eastward displacement of the forest-clearcut boundary (Figure 6.1), and by transverse faulting of a ridge on the Butte (Figure 6.5). Later stage evidence for westward movement into the western widening is provided by tracing the displaced half of a split cedar stump back to its other half on the main scarp just east of zone 6b.

6.3.7. Late Stage Movements

Final movements in the zone of depletion included rotational sliding in zone 7. It is likely that the extent of retrogression was controlled by the upslope inclination of the rupture surface along the stratigraphic dip (Figure 3.5). While the removal of material would be facilitated by the dipping rupture surface, the inclination of this surface reduces H and N_s in the upslope direction. As we have shown earlier, a threshold N_s is required for retrogressive movement.

Additional secondary (minor) movements occurred throughout the landslide. The movements included: 1. flow down the stratigraphic dip between N-S trending ridges; 2. stretching of disturbed ridges; 3. splitting and lowering of "undisturbed" ridges; and 4. block gliding in zone 1 (Figure 3.5).

6.3.8. Movement Classification

In summary, using the nomenclature of Cruden and Varnes (1996), indicators of velocity from evidence in Chapter 4, and moisture contents in Chapter 5, the first major movement was a retrogressive, rapid, very wet earth flow. This was followed by a retrogressive, rapid, very wet earth spread. Hence the landslide can be classified as a composite earth flow – spread, or simply

the Mink Creek composite earth flow, which indicates that a lot of the ridges are still there, but some flow has occurred.

6.4. Comparison to Other Landslides in Marine Sediments

The Mink Creek landslide is among the large retrogressive landslides common in marine sediments around the world. In Chapter 5 I compare the material properties of this landslide to other landslides. Here I show how the Mink Creek landslide is morphologically different from other similar landslides, with emphasis on flowing and spreading movements.

6.4.1. Other Landslides

The presence of multiple rupture surfaces as at the Mink Creek landslide has not been reported for other historic marine clay landslides though Potvin et al. (2002) have identified four sliding surfaces in a prehistoric landslide at the site of the 1971 Saint-Jean-Vianney landslide. Both the Mink Creek and Saint-Jean-Vianney landslides had main surfaces of rupture below rupture surfaces of prehistoric landslides.

The eastern widening of the Mink Creek landslide had a small amount of remaining displaced material in the zone of depletion, most of the sediment accumulating in the valley in front of, and downstream of the toe of the surface of rupture. As such, the Mink Creek landslide is different from most of the marine "flowslides" in eastern Canada. There, the typical zone of depletion contains a thick depleted mass above the surface of rupture. The thickness of the depleted mass is usually in the range 45% to 65% of the depth to the slide surface from the original ground surface (Carson and Lajoie 1981). Exceptions include the 1898 Saint-Thuribe and 1971 Saint-Jean-Vianney slides which both had little material remaining in the zone of depletion (Carson and Lajoie 1981). Preliminary evidence (Figure 6.6) suggests that this distinction between flows with little material remaining in the zone of depletion and the more common spreads with thick ribbed masses of displaced material may be related to the undrained strength of the sediment. Zones of depletion with little remaining depleted mass seem to require soft sediment relative to the weight (and thus thickness) of overlying sediment.

The relatively empty zone of depletion at Mink Creek shows a strength profile fully consistent with the pattern shown in Figure 6.1. The profile is largely in the sector grouped as flows, although the uppermost 15 metres (that affected by the slide) is essentially transitional to spreads. It should be

noted that the shear strength data were obtained from the eastern widening where flow was more common than in the western widening, dominated by spreading.

Reconstruction of the mode of failure from landslide morphology is relatively simple in cases where there has been little remoulding of sediment such as in the spreads at Skottorp, Sweden (Odenstad 1951) and Lemieux, Canada (Evans and Brooks 1994). Reconstruction difficult in flows where almost all the displaced material remoulds and flows out of the zone of depletion, e.g. Saint-Jean-Vianney, 1971 (Tavenas et al, 1971).

The Mink Creek landslide belongs somewhere between these two extremes (Figure 6.6). Reconstruction is possible in part only. For this reason, it is useful here to summarize the key processes documented by video in the flow at Rissa, Norway in 1981 (Norwegian Geotechnical Institute 1982), because some of the morphological evidence at Mink Creek is indicative of the same mode of movement.

6.4.2. Rissa Landslide, Norway

The Rissa landslide was a complex flow, involving the coalescing of several movements. Most of the movements were dominated by vertical subsidence with little evidence of rotational sliding. There was also little displaced material left in the zone of depletion.

Although the eastern widening (Figure 3.1) of the Mink Creek landslide shows many features of the Rissa landslide (Gregersen 1981), there are some important differences. One major difference was the narrowness of the valley at Mink Creek available to accommodate the displaced material in comparison with the open lake at Rissa. Another was the impediment to flow down the Mink Creek valley resulting from the interlocking of large trees (Figure 4.12), in contrast to Rissa where the displaced ground was farmland. Thus, for two reasons, impediments to retrogression, through congestion of the displaced material, were much greater at Mink Creek. Thirdly, although most of the central area of the Mink Creek landslide had, like Rissa, little remaining displaced material, there are large areas in which a ribbed topography developed, more like the spreads in Eastern Canada. This composite morphology of the Mink Creek landslide is consistent with its plotting on Figure 6.6 in both flows and spreads. Finally, inspection of displaced material in the valley of Mink Creek provides little field evidence of mud that actually liquefied: deformed, but still recognizable, depth material occurs. Possibly, only mud in particular soft and rapid layers actually fully remoulded.

There are, nonetheless, numerous similarities between the two landslides. In particular, there is clear evidence at Mink Creek that subsidence occurred in the zone of depletion. What is not clear is whether temporary ridges developed between these subsiding wedges at Rissa as they did in many parts of the Mink Creek landslide. Even in the exposed rupture surface in zone 1 (that part of the Mink Creek landslide most similar to Rissa) there is evidence of ridges: two pyramidal blocks (ridge fragments) clearly slid a long distance, thereby, in fact, creating the exposed rupture surface (Figure 3.5).

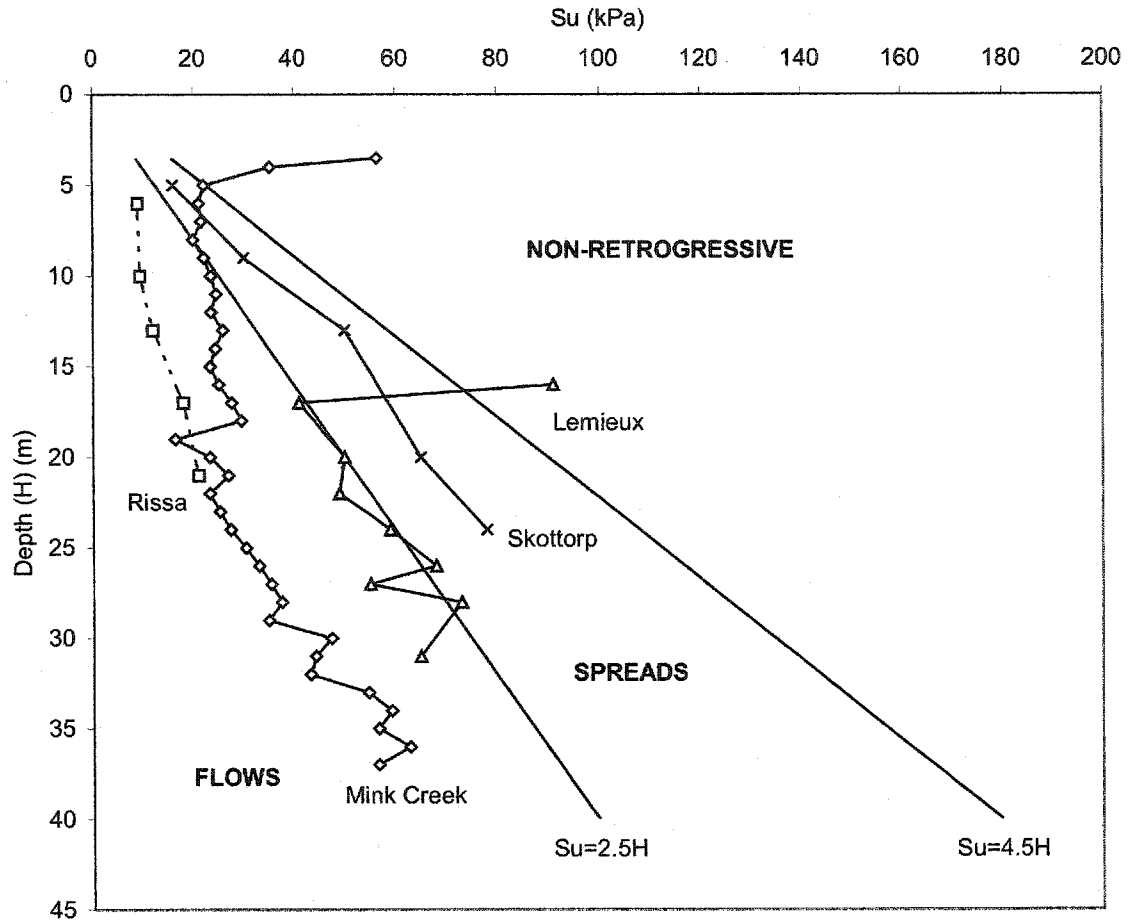


Figure 6.6 Plot of Undisturbed shear strength vs. depth for various types of flowslides. While most of the Mink Creek data plot under flows, the vane shear data were obtained from near the area in the slide that flowed rather than spread.

6.5. Conclusions

In this chapter I have used morphologic features (described in Chapter 2) to interpret the style of movement. Transverse ridges of undisturbed material indicate spreading. Remoulded lobes indicate flow. Collapsed grey and brown planform bands indicate subsidence.

Although there is no known trigger, there is evidence that an initial earth slide, exposing sensitive clay occurred as indicated in Figure 4.2. The evidence includes the orientation of ridges in zone 2.

The first southward flow in zone 1, in the direction of stratigraphic dip, triggered westward and eastward spreading towards zone 1 (Figure 6.1). In this case movement was normal to the stratigraphic dip. Spreading in zone 2 triggered further spreading in zones 3 and 4. In zone 4 spreading occurred along a rupture surface perched 5 m above the main rupture surface in zones 1 to 3.

Spreading in zone 4 included, and was followed by, widespread subsidence – both of ridges and the entire subzone 4c. Given that there is strong evidence for elevated spreading in 4c, using form analogy the same interpretation can be made for the collapsed broad bands in subzone 2b.

Subsidence and flow in the eastern widening opened a channel for the evacuation of sediment from zones 5 and 6 in the western widening. These movements included both flowing and spreading.

Late stage movements included rotational sliding along the main scarp, as well as minor movements such as secondary slippage and stretching and splitting of ridges in the zone of depletion.

Using pre and post landslide topographic profiles, I have shown how the height of the original slope above the rupture surface (H) diminishes to the north and to the west. As H diminishes for a given undisturbed shear strength (S_u), so does the stability number (N_s). In this way both strength and topographic data can be used to place limits on the extent of retrogression.

Given the sequence of movements described, the landslide can be classified as a retrogressive, rapid, very wet, composite earth flow – earth spread according to the nomenclature of Cruden and Varnes (1996).

The Mink Creek landslide has elements of both spreads and flows that frequently occur in marine sediments. The landslide is unique in that it is the only reported case where both modes of movement were significant. Particularly in the eastern widening there are substantial areas with remoulded lobes which indicate flow (similar to the St-Jean Vianney and Rissa landslides). The western widening, in contrast, is dominated by transverse ridges, which indicate spreading (similar to the South Nation and Lemieux landslides). But both elements occur throughout the zone of depletion making the landslide composite.

The Mink Creek landslide is also unique with respect to its multiple horizontal rupture surfaces. The presence of multiple surfaces of rupture has not been documented in other retrogressive landslides in marine sediments.

Chapter 7

Potential for Future Large Retrogressive Landslides

7.1. Introduction

An important goal of landslide research is the prediction of landslide hazard. Is there potential for future landslides? What are the conditions that result in landslides? Are these conditions changing for better or worse?

I start by considering the spatial and temporal distribution of landslides in the area between Terrace and Kitimat. I also consider landscape evolution and prehistoric and historic climatic conditions associated with landslides. Finally I consider the impact of projected climate change on landslides.

7.2. Prehistoric Landslides in the Terrace-Kitimat Area

7.2.1. Prehistoric Landslide Depressions

Certain portions of the low-lying landscape between Terrace and Kitimat show many landslide depressions (Figure 7.1). The landslides occurred in glaciomarine muds, although in some instances the muds are blanketed with post-glacial alluvium, and with glaciofluvial gravels. Clague's (1984) surficial geology map depicts historic landslides at Lakelse Lake and also the prehistoric scarps at Nalbeelah Creek (Figure 7.1).

Using aerial photographs, I determined whether or not features were landslide depressions on the basis of their macro-morphology. I supplemented the aerial photo interpretation with ground truthing. I used two criteria to distinguish landslides. 1. Only those depressions that had identifiable earth flow characteristics were mapped, so as not to include, for example, channel erosion features. Typically the zones of depletion are gently sloping and broad with steep, but usually low scarps. 2. Only scarps and depressions clearly recognizable as individual landslides were delineated. Hence, I did not try to reconstruct events in complex terrain that may have been influenced by multiple sequences of landslides and incised by subsequent gully erosion.

The largest landslides mapped in Figure 7.1 are recent, and include the two Lakelse landslides of 1962 (Clague 1978; Evans 1982) and the more recent Mink Creek

landslide. This does not necessarily imply that such large landslides have not occurred in the past. It does suggest that old large landslides may not remain distinct due to subsequent landsliding and gully erosion. Large, hanging landslide depressions, presumably old are however, particularly well-preserved in muds blanketed with glaciofluvial gravels. A smaller example of a well-preserved landslide is shown in Figure 7.2.

Ribbed morphology, common in eastern Canada, was not observed in the landslides, despite the fact that a portion of the Mink Creek landslide did have a ribbed surface expression. Although translational ridges, that give earth spreads their ribbed appearance, degrade rapidly and substantially (Geertsema and Schwab 1996), it is likely that some subdued surface expression would remain. Therefore we suspect that the absence of residual ribbed morphology may tell us something about the dominant mode of movement in the Terrace-Kitimat area.

Carson and Lajoie (1981) distinguished between ribbed earth flows and the cleaner *coulées d'argile* - spreads and flows using the nomenclature of Cruden and Varnes (1996). Lack of ribbed morphology in the Terrace-Kitimat area may indicate the ease of the removal of displaced material from the zones of depletion, and suggests that most of the landslides were flows.

7.2.2. Landslide Distribution

The spatial distribution of landslides is interesting. One area with a particularly high abundance of landslides is the area around Mink Creek (Figure 7.1). Other areas include the foreslope of the Onion Lake delta (Figures 7.1 and 7.3) and the Nalbeelah wetland complex (Figure 7.1 and 7.4).

As on the foreslope of a delta in front of the Ste. Narcisse moraine in Quebec (Lebuis et al. 1983), the abundance of landslides on the distal side of the Onion Lake delta may be related to the presence of a confined aquifer where delta foreslope deposits are buried by marine muds. Even without this excess pore pressure, the faster movement of water through the aquifer leads to removal of salts from the porefluid of overlying muds, increasing their sensitivity (LaRochelle et al. 1970; Carson 1983). Bank erosion by the Kitimat River is, likely, yet another factor contributing to the high incidence of landslides in this location.

In contrast, the foreslope of the large delta northwest of Lakelse Lake (Figure 7.1) does not have many associated landslides. Lack of a major eroding stream in this area may partly explain the difference in slide incidence between the two foreslopes.

Absence of scarps at the north and southeast ends of Lakelse Lake does not necessarily imply that no landslides occurred there. Local accounts of trees buried in clay being exposed during excavations suggest they may be earth flow deposits (C. Sowa, personal communication 1997). The scarps could have become obliterated over time, particularly by alluvium and organic deposits in these low-lying, flood-prone areas.

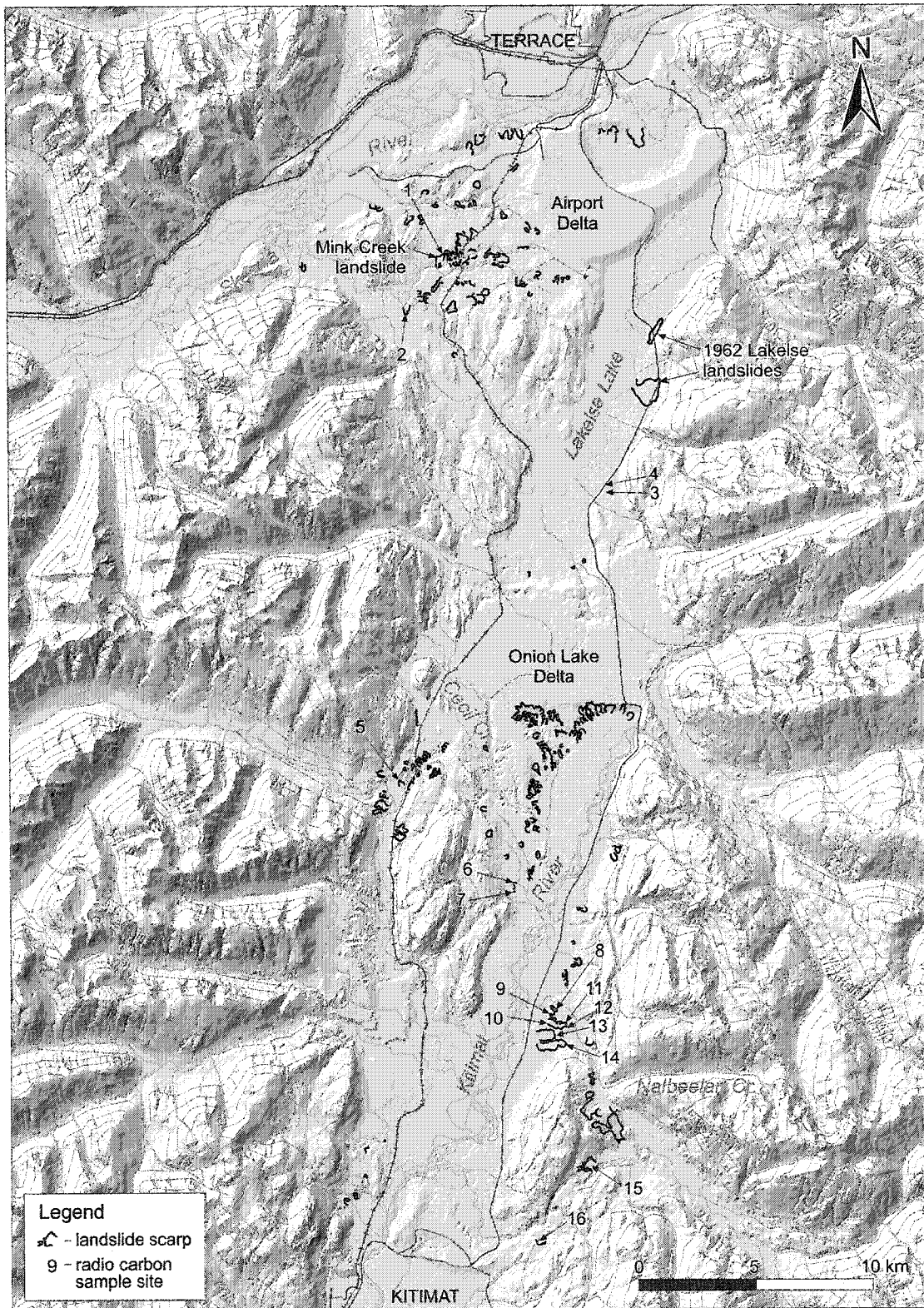


Figure 7.1 Distribution of landslide scarps in glaciomarine sediment in the Terrace-Kitimat area.

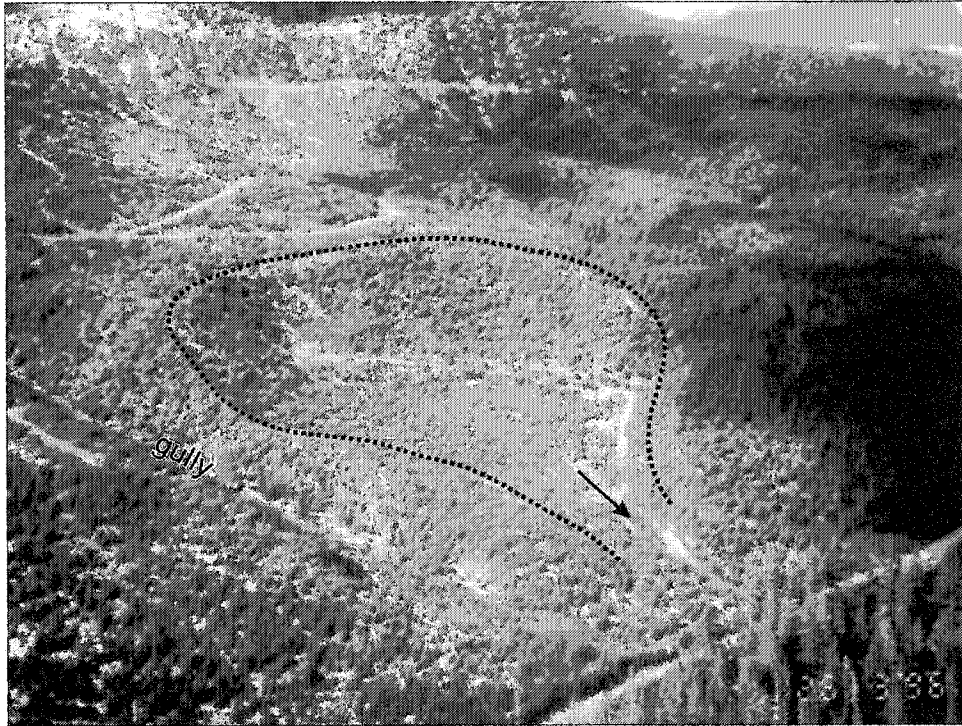


Figure 7.2 A prehistoric earth flow with a "bottleneck" shape, south of Nalbeelah Creek. Stipple pattern outlines its scarp. Outlet is about 70 m wide. Note the presence of the major gully immediately to the left of the landslide. Deep gullies often control the dimensions of landslides.

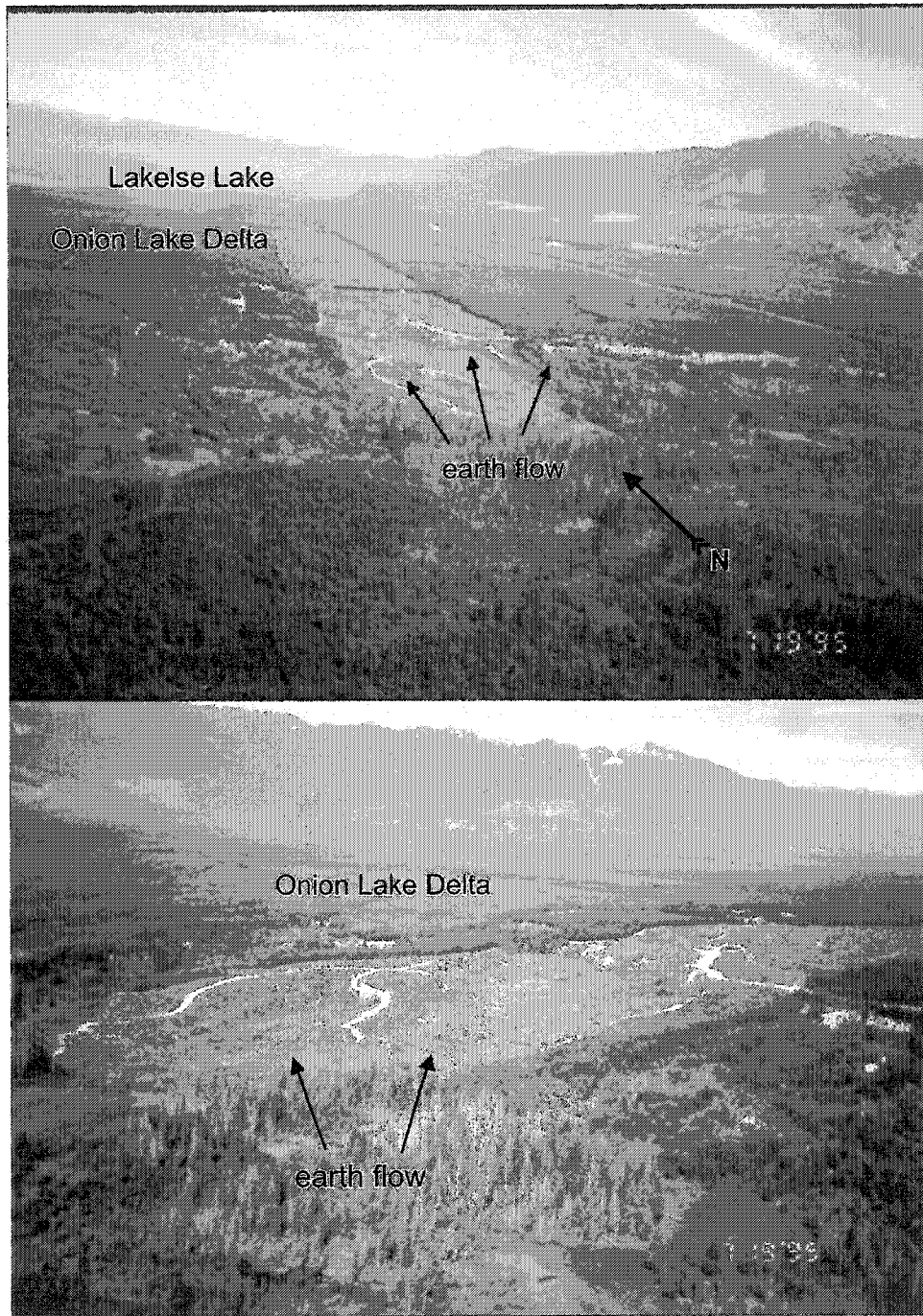


Figure 7.3 The foreslope of the Onion Lake delta with prehistoric earth flows.



Figure 7.4 An earth flow filled with peat at Nalbeelah Creek.

7.2.3. Landslide Ages

Numerous old landslides contain wetlands in their zones of depletion (Figure 7.4). By radiocarbon dating peat (obtained with a Hiller peat sampler) at the mineral/organic contact (Figure 7.5) I established minimum ages of occurrence for the landslides (Table 1). The ages obtained do not necessarily give accurate dates for the landslides but they do establish dates after which the movement could not have occurred. A further caution with using these numbers is that wetlands do not necessarily develop uniformly (e.g. Foster and Wright Jr. 1990). The centre can be older than the edge, or several pockets could have started earlier than other areas. In addition, the rate of peat accumulation can be extremely variable (Goudie et al. 1990).

The most significant cluster of these wetland-filled landslide depressions is the Nalbeelah wetland complex (Figures 7.1 and 7.4) east of Kitimat River. Peat depth varied between 2 and 4 metres in these wetlands. In other areas, peat was much thicker (6.9 m at a site along Hirsch Creek) or thinner (0.65 m near Lonewolf Creek). The Nalbeelah cluster is above the trendline in the scatter graph in Figure 7.6 indicating a more rapid accumulation of peat than in other locations. The clustering of dates suggests that the faster accumulation is related to local favourable site conditions. The slope of the trendline yields a thickness of 0.86 m per 1000 radiocarbon years (Figure 7.6).

The landslide at Hirsch Creek occurred in clays blanketed with glaciofluvial gravels, and from its minimum date of about 9000 ^{14}C BP, occurred shortly after deglaciation. While it appears to be an anomaly in Table 7.1 and Figure 7.6, other nearby landslides exposed in thick glaciofluvial gravels, such as north of Hirsch Creek (Figure 7.1) may also be old, possibly having occurred shortly after deglaciation. Over time the gravels could have consolidated the underlying mud, increasing its strength, and thus reducing the likelihood of retrogressive failure.

While the landslides with wetlands represent a small number of the total mapped, more than one third of the dated landslides occurred between 3300 and 1990 ^{14}C BP. Most of these dates when calibrated to years before present fall between 3300 and 1900 yr BP, a cool wet period identified by Clague and Mathewes (1996) near Berendon Glacier, about 200 km northwest of the study area. Thus there may have been greater landslide

activity during Neoglacial time (the last 5000 years) than during the warmer and drier Hypsithermal (8000 to 5000 years ago – Pielou 1991), suggesting the possibility of climatic controls on the overall incidence of landslide activity. Other factors to consider in this regard are paleo-stream activities, extent of salt removal from the sediments, and the possibility of wetlands forming in previously drier slide craters in response to a wetter and cooler climate.



Figure 7.5 A Hiller peat corer showing the marine clay – peat interface. I sampled peat at these contacts to obtain minimum ages for the landslides.

Table 7.1. Thickness of peat occupying historic landslides and the ages of the landslides¹

Site (ID)	Laboratory Number	¹⁴ C age ² (years BP)	Material	Peat Thickness (m)
1 (Mink 1)	Beta-120749	5160 +/- 50	soil organic matter	not in peat
1 (Mink 2)	Beta-12750	5190 +/- 90	soil organic matter	not in peat
2 (White 1A)	Beta-89110	3300 +/- 70	peat over clay	1.4
2 (White 1B)	Beta-89111	2030 +/- 80		
3 (Lake 1)	Beta-89107	3140 +/- 130	peat over sand	1.85
4 (Lake 2)	Beta-89108	150 +/- 90	soil o.m. over clay	0.50
5 (Lonewolf)	Beta-89105	1380 +/- 70	peat over clay	0.65
6 (240-1)	Beta-89102	2750 +/- 90	peat over clay	2.0
7 (240-2)	Beta-89104	4500 +/- 100	peat over sand	3.9
8 (Nab 13A)	Beta-89124	1610 +/- 70	peat over clay	2.3, 2.3
8 (Nab 13 B)	Beta-89125	1760 +/- 90		
9 (Nab 9)	Beta-89118	2280 +/- 70	peat over clay	2.7, 2.7
9 (Nab 10)	Beta-89119	2650 +/- 70		
10 (Nab 7)	Beta-89116	2470 +/- 70	peat over clay	4.0, 4.0
10 (Nab 8)	Beta-89117	2360 +/- 90		
11 (Nab 3)	Beta-89114	2270 +/- 90	peat over clay	2.7, 2.7
11(Nab 5)	Beta-89115	2310 +/- 70		
12 (Nab 2)	Beta-89112	1990 +/- 90	peat over clay	2.6
13 (Nab 11)	Beta-89120	1500 +/- 110	peat over clay	2.25
14 (Nab 12A)	Beta-89122	1490 +/- 80	peat over clay	2.3, 2.3
14 (Nab 12B)	Beta-89123	1530 +/- 40		
15 (Hirsch 1)	Beta-89098	9140 +/- 130	peat over clay	6.9
16 (Hirsch 2)	Beta-89100	3530 +/- 90	peat over sand	1.6

1. Analysis done by Beta Analytic Inc., Miami, Florida –minimum age for peats – maximum age for site 1.
2. ¹⁴C years before A.D. 1950, with 1 sigma error

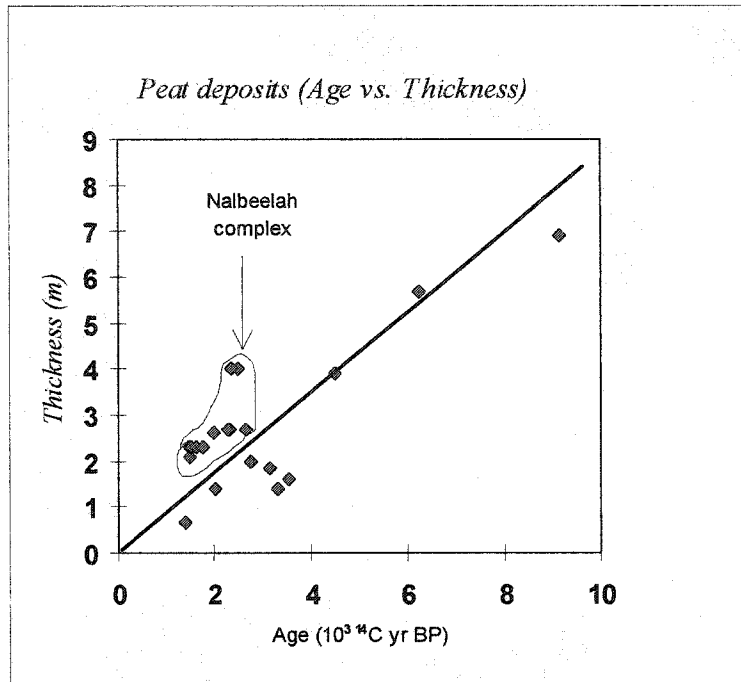


Figure 7.6 Scatter graph showing distribution of minimum landslide ages (from peat) plotted against peat thickness.

7.3. Influence of Valley Formation

Stream erosion is the most common trigger of retrogressive landslides in marine sediments (Bjerrum et al. 1969; Lebuis et al. 1983; Viberg 1983). Both Bjerrum et al. (1969) in Norway, and Lefebvre (1986) in Quebec, used a landscape evolution approach to map zones of earth flow potential in sensitive clay areas. They were interested in stream incision.

Bjerrum et al. (1969), working on the premise that stream bank erosion was the main trigger of quick clay slides, determined equilibrium gradients for streams from which it was possible to predict future erosion. They defined three zones of erosion for streams. 1. A lower zone, no longer actively downcutting, is characterized by old slide scars, and localized cutbank failures in stream bends. This is a mature zone and the danger of quick clay landslides is small. 2. An intermediate zone exists where streams are flowing almost exclusively on displaced landslide deposits, and in general, the streams are eroding back to their old levels. As long as streams are cutting through old landslide deposits, Bjerrum et al. (1969) argued that earth flows will be restricted to that material, and the risk of quick clay landslides triggered by erosion is low. However, in eastern Canada, the Saint-Jean-Vianney slide (Tavenas et al. 1971; Potvin et al. 2002) and in British Columbia the Mink Creek landslide (at least partly) involved the remobilization of old landslide deposits. 3. An upper zone is identified as the original horizontal plateau where streams are cutting into undisturbed clay. It is at the boundary between these latter two zones that the risk of retrogression was found to be the greatest. They called this boundary the front of aggression. Each time an earth flow occurred, depositing displaced material into the valley, the intermediate zone would be extended, moving the front of aggression upstream.

Lefebvre (1986) described three phases of valley formation with associated groundwater flow regimes (Lafleur and Lefebvre 1980). An early phase involved relatively shallow stream incision into deep mud deposits where groundwater flow was not influenced by lower pervious till. An intermediate phase of valley formation was characterized by strong artesian pressures and thus favoured large, retrogressive landslides. A late phase occurred when streams have incised through the lower pervious till (if it exists) resulting in downward flows. Only small landslides were expected during the early and late phases of valley formation.

Few streams in the Terrace-Kitimat valley are incised into bedrock (Clague 1984). They are still incising deep glaciomarine sediments (Geertsema 1998) and appear to be in the early and intermediate stages of valley formation, thus large landslides are still occurring and more are expected.

While the zones proposed by Bjerrum et al. (1969) do not relate directly to Lefebvre's (1986, 1996) phases of valley formation, in both approaches the intermediate zones present the greatest hazards for retrogressive flowsliding. It appears that Lefebvre's valley formation approach is more applicable to the Terrace-Kitimat area than the front of aggression approach of Bjerrum et al. (1969) because prehistoric landslides are already well distributed throughout the area (Figure 7.1), and large landslides are occurring in areas with previous retrogressive failures.

7.4. Climatic Conditions Leading up to the Landslide

Figures 7.7 to 7.9 show climatic conditions at Terrace Airport leading up to the time of the landslide. Figure 7.7 is a precipitation graph showing percent cumulative deviation from the mean. The plot shows a period of increasing precipitation from 1986 to 1994. Figure 7.8 is a temperature graph showing a period of warming from 1985 to 1995. Figure 7.9 shows temperature and precipitation for the period September 1993 to end January 1994. This was a period of above average temperatures when most precipitation occurred as rain. Water levels in wells were higher than normal (F. Maximchuk, personal communication August 1994) and the water level in Mink Creek was about two feet (60 cm) higher November 26 1993 than in mid September of 1993 (C. Clomeau, personal communication Oct. 1994). Higher temperatures may also have delayed ground freezing, promoting infiltration.

The combination of climate data and water level observations indicate that the time of the landslide coincided with the culmination of eight years of increasing precipitation, nine years of increased warming, and a warmer than average fall and early winter. These hydroclimatic conditions likely contributed to high ground water and stream levels, setting up the preconditions for the Mink Creek landslide. Such preconditions have been shown to be important contributors to activity in large landslides (Patton 1984).

7.5. Climate Change Scenarios

In British Columbia, studies of landslide–climate relationships have largely been restricted to shallow debris slides and flows in steep mountainous terrain (Schwab 1983; Church and Miles 1987; Evans 1989; Hogan and Schwab 1991). However Bovis and Jones (1992) have shown that large, deep-seated, earth flow activity in Southern British Columbia corresponded to wet climatic periods in the Holocene.

Figure 7.10 depicts climate change plots scenarios for Terrace for 2020, 2050 and 2080 from 58 global circulation models (Canadian Institute for Climate Studies: <http://www.cics.uvic.ca>). Almost invariably all the models predict warmer and wetter conditions. Figures 7.7 to 7.9 show that almost a decade of increasing precipitation and temperature, plus a mild wet fall and early winter led up to the landslide at Mink Creek. Thus we can expect similar conditions that led up to the landslide in the decades ahead.

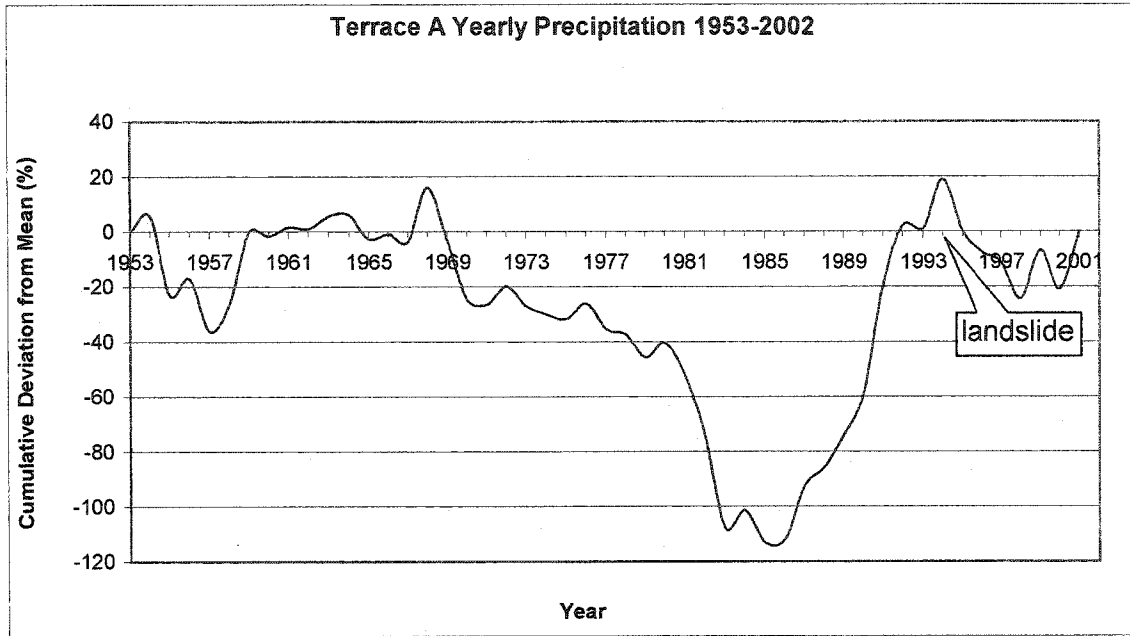


Figure 7.7 Percent cumulative deviation from mean precipitation at Terrace Airport for the period 1953 to 2002. The graph shows a period of increasing precipitation from 1986 to 1994. Environment Canada data.

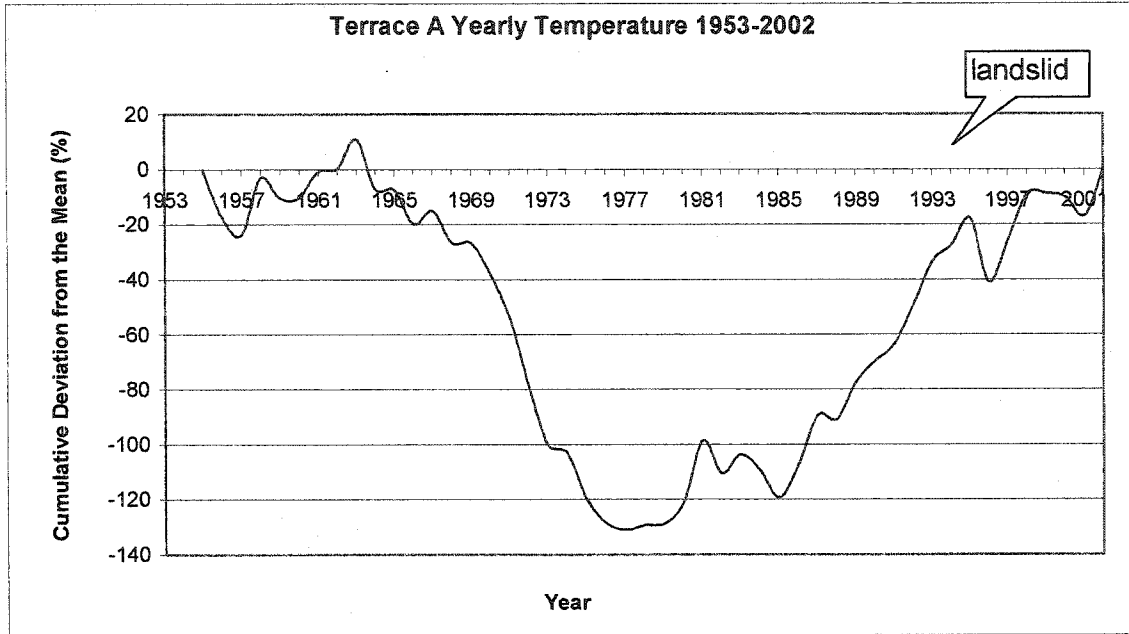


Figure 7.8 Percent cumulative deviation from mean temperature at Terrace Airport for the period 1953 to 2002. The graph shows a period of increasing temperature from 1985 to 1995. Environment Canada data.

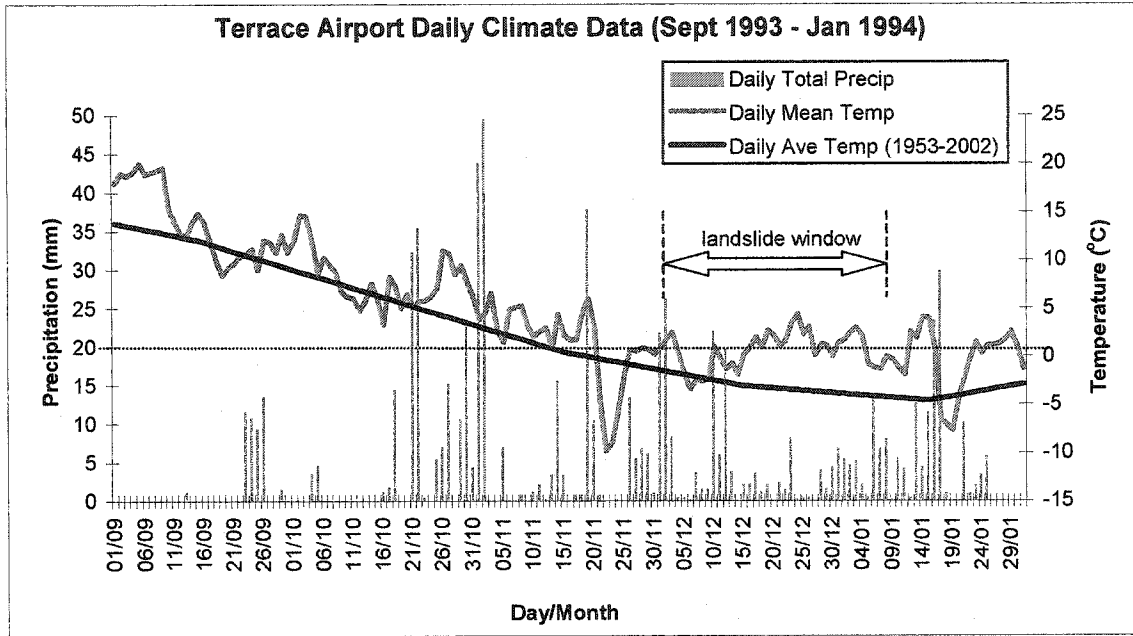


Figure 7.9 Terrace airport daily precipitation and temperature data for the period September 1993 to January 1994. Note that this period experienced warmer than average temperatures. Most of the precipitation was rain. Environment Canada data.

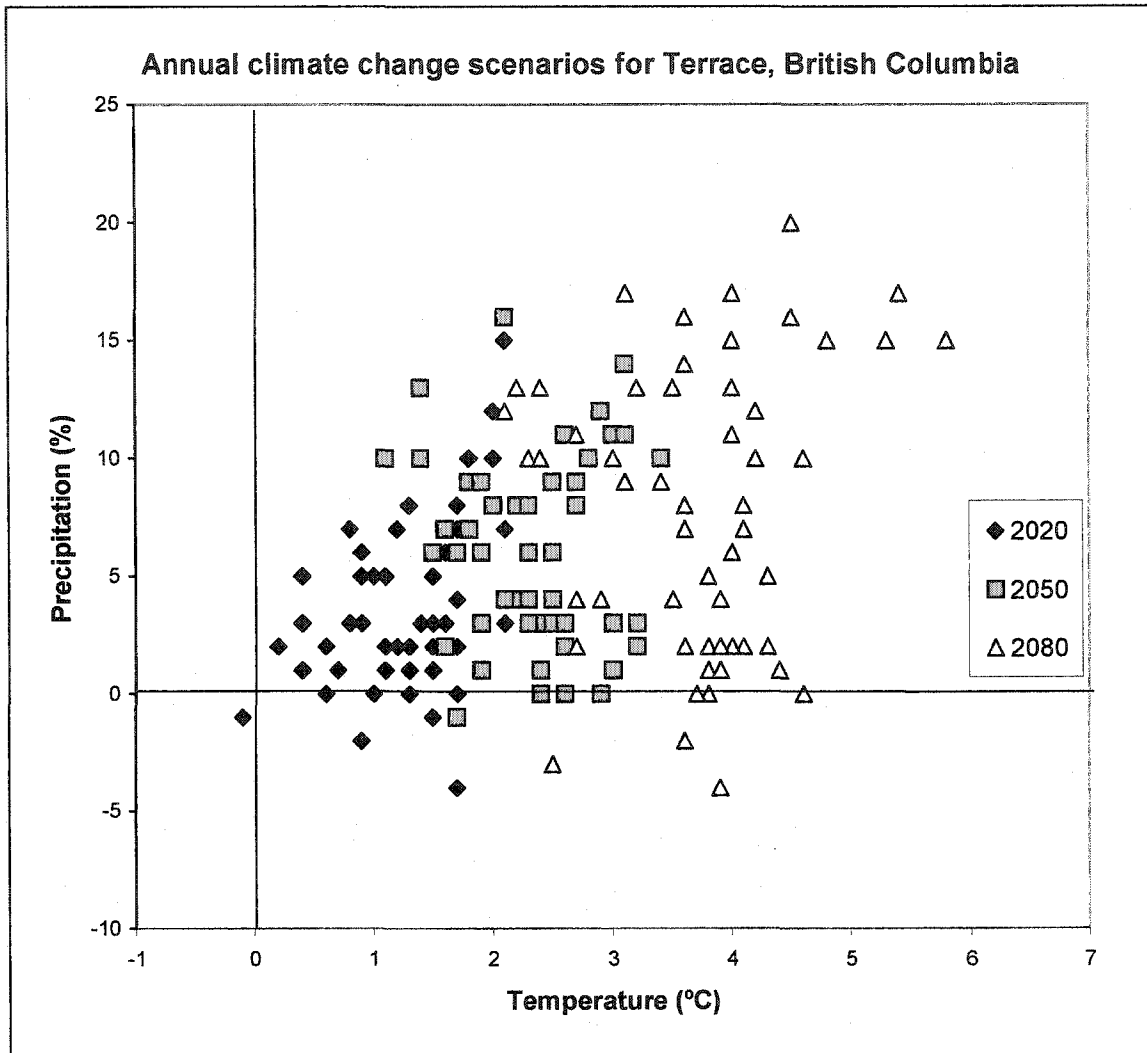


Figure 7.10 Annual climate change scenarios for 2020, 2050, and 2080 for Terrace, British Columbia, with respect to a 1961-1990 global climate model baseline. The points represent the results of 58 different global circulation models, generally predicting a progressively warmer and wetter climate for Terrace. The data was obtained from the Canadian Institute for Climate Studies website (<http://www.cics.uvic.ca>).

7.6. Conclusions

There are abundant prehistoric landslides in the Terrace-Kitimat area. They are especially abundant near Mink Creek, on the foreslope of the Onion Lake delta, and in the Nalbeelah Creek area. As the most common trigger for large earth flows is bank erosion, these movements may have occurred during a period when rivers eroded slopes below these landslides. Streams in the Terrace area are still in the early to intermediate phases of valley formation – a condition that favours large landslides.

There are three interesting points to be made about climate. 1. About one third of the dated prehistoric landslides occurred during a wet climatic period. 2. Almost a decade of increasing precipitation and temperature and a wet and warm fall and early winter preceded the landslide. 3. Climate change scenarios predict a wetter and warmer future climate for Terrace.

Given the phases of valley formation, the history of previous landsliding, and the link between climate and landslides, the climate change scenarios for Terrace should alert us to the increased likelihood of future large landslides.

Chapter 8

Conclusions

A large composite landslide occurred in glaciomarine sediments at Mink Creek near Terrace, British Columbia between 1 December 1993 and 9 January 1994. Detailed mapping of morphologic features and the deposits of the landslide at Mink Creek allow:

1. tentative reconstruction of the style and sequence of the movement, illustrating complex behaviour; and
2. identification of interesting features not previously well-documented in most retrogressive landslides.

The material properties associated with the Mink Creek landslide are similar to those of other sensitive marine clays. Essentially the sediment is a medium to low plasticity, flocculated silty clay, composed of low activity clay minerals and rock flour. The sediment has been sufficiently leached of salt to meet the requirements for quick clay.

Many of the relatively intact, upright ridges of near-horizontal muddy strata have been lowered in elevation during translation. The evidence for this is horsetail roots in the crests of the ridges which, based on observations around the main scarp, do not penetrate more deeply than about 4.5 m below the ground surface. In the ridge crests they are now found as much as 7 metres below the former ground surface.

Some of this lowering is due simply to sliding of the blocks (ridges) down an inclined basal rupture surface. Much of it, though, appears to be attributable to remoulding of the base of the ridges during that translational movement. In addition, there is evidence that some ridges have subsided in place. This is in contrast to current models of retrogressive spreading in which ridges are created by subsidence of wedges on either side of them (e.g., Odenstad, 1951, Carson, 1977). The Mink Creek landslide shows that, where there is a significant thickness of quick clay at depth (rather than a thin seam), several metres subsidence of ridges can accompany the spreading.

Material between ridges ranged in consistency from thoroughly remoulded to barely disturbed with the original stratification intact. Even at the most distal part of the zone of accumulation well-preserved horizontal bedding was found.

At Mink Creek the surfaces of rupture occur at several elevations in the zone of depletion, separated by scarps ranging from 1 m to 8 m in height. Such multiple major rupture surfaces have not been documented in previous historic retrogressive landslides. There are two main surfaces of rupture that appear to be the result of two separate sliding phases, but the general multiplicity of surfaces of rupture may be related to multiple soft or rapid strata.

Inspection of the displaced material in the zone of accumulation indicated significant resistance to further downvalley movement by tangled masses of large trees in the narrow valley. Almost half of the land in the landslide, however, had been clearcut. This raises the question as to whether downvalley movement of displaced material would have been greater, and the zone of depletion larger, if the entire area had been clearcut. The question is obviously one of more general significance in British Columbia than simply in the context of the Mink Creek landslide.

In summary, the landslide morphology shows both the lobes of flows and the ridges of spreads. The dominant mode of movement was spreading, however, the landslide probably began in sediment which liquefied readily and flowed. This allowed a zone of depletion to retrogress into less easily liquefiable sediments which then spread. The movement ended with rotational sliding close to the present main scarp. Previous examples of landslides in glaciomarine sediments that involve both flowing and spreading do not appear to have been documented. From this composite mode of movement, and material properties, it follows that the landslide should be referred to as *a retrogressive, rapid, very wet, composite earth flow – earth spread* in accordance with Cruden and Varnes (1996), or simply a *composite earth flow - spread*.

Many earth flows have occurred in the Terrace-Kitimat area since deglaciation, particularly during a cool wet phase 2000-3000 years ago. In addition, most global circulation models predict a warmer and wetter future for the area. The Mink Creek landslide was preceded by a decade of increasing precipitation. In addition, the area is in an intermediate phase of valley formation – a phase that promotes large landslides. Considering the association of retrogressive landslides with prehistoric wetter climates, and historic wetter climate, plus the intermediate phase of valley formation, the potential for new large landslides may be significant.

References

- Aylsworth, J.M.; Lawrence, D.E.; and Guertin, J. 2000. Did two massive earthquakes in the Holocene induce widespread landsliding and near-surface deformation in part of the Ottawa Valley, Canada? *Geology* 28: 903-906.
- Bjerrum, L. 1954. Geotechnical properties of Norwegian marine clays. *Geotechnique*, 4: 49-69.
- Bjerrum, L., Løken, T., Heiberg, S., and Foster, R. 1969. A field study of factors responsible for quick clay slides. *Proc. 7th ICSMFE, Mexico*, 2 pp. 531-540.
- Bovis, M.J. 1985. Earthflows in the Interior Plateau, southwest British Columbia. *Canadian Geotechnical Journal* 22: 313-334.
- Bovis, M.J. and Jones, P. 1992. Holocene history of earthflow mass movements in south-central British Columbia: The influence of hydroclimatic changes. *Canadian Journal of Earth Sciences* 29: 1746-1755.
- Brawner, C.O. 1962. Report on Lakelse slide, Terrace-Kitimat Highway. British Columbia Ministry of Highways, Unpublished Document.
- British Columbia Ministry of Forests. 1997. Climate data summaries for the biogeoclimatic zones of British Columbia. Version 4. Unpublished Excel file. B.C. Min. For., Victoria, B.C.
- Bull, W.B. 1964. Alluvial fans – near-surface subsidence in Western Fresno County California. *Geological Survey Professional Paper*, 437-A.
- Carson, M.A. 1977. On the retrogression of landslides in sensitive muddy sediments. *Canadian Geotechnical Journal* 14: 582-602.
- Carson, M.A. 1979. Le glissement de Rigaud (Quebec) du 3 Mai 1978: une interpretation du mode de rupture d'apres la morphologie de la cicatrice. *Géographie physique et Quaternaire* XXXIII: 63-92.
- Carson, M.A. 1983. Influence of porefluid salinity on instability of sensitive marine clays; a new approach to an old problem. *Earth Surface Processes and Landforms* 6: 499-515.

- Carson, M.A. and Geertsema, M. 2002. Mapping in the interpretation and risk assessment of flowslides in sensitive Quaternary muddy sediments. *Geoenvironmental Mapping, Methods, Theory and Practice*. Edited by P.T. Bobrowsky. A.A. Balkema Publishers, The Netherlands. 667-698.
- Carson, M.A. and Lajoie, G. 1981. Some constraints on the severity of landslide penetration in sensitive deposits. *Géographie physique et Quaternaire* 35: 301-316.
- Church, M. and Miles, M.J. 1987. Meteorological antecedents to debris flows in southwestern British Columbia; some case studies, in J.E. Costa and G.F. Wieczorek, *Geological Society of America, Reviews in Engineering Geology, Volume VII:63-79*.
- Clague, J.J. 1978. Terrain hazards in the Skeena and Kitimat River Basins, British Columbia; Current Research, Part A, Geological Survey of Canada, Paper 78-1A, 183-188.
- Clague, J.J. 1984. Quaternary geology and geomorphology, Smithers-Terrace-Prince Rupert area, British Columbia. Geological Survey of Canada, Memoir 413.
- Clague, J.J. and Mathewes, R.W. 1996. Neoglaciation, glacier-dammed lakes, and vegetation change in northwestern British Columbia, Canada. *Arctic and Alpine Research* 28: 10-24.
- Clague, J.J., Naesgaard, E. and Sy, A. 1992. Liquefaction features on the Fraser delta: evidence for prehistoric earthquakes? *Canadian Journal of Earth Sciences* 29: 1734-1745.
- Cody, W.J. and Wagner, V. 1981. The biology of Canadian weeds 49 *Equisetum arvense* L. *Canadian Journal of Plant Science* 61: 123-133.
- Cruden D.M., and Varnes, D.J. 1996. Landslide types and processes. *In* Special Report 247: Landslides investigation and mitigation. A.K. Turner and R.L. Shuster (editors). TRB, National Research Council, Washington D.C., pp. 36-75.
- Duffel, S. and Souther, J.G. 1964. Geology of the Terrace map-area, British Columbia (103 I E 1/2). Geological Survey of Canada, Memoir 329.
- Eden, W.J., Fletcher, E.B. and Mitchell, R.J. 1971. South Nation River landslide, 16 May 1971. *Canadian Geotechnical Journal* 8: 446-451.

- Evans, S.G. 1982. Landslides and surficial deposits in urban areas of British Columbia: A review. *Canadian Geotechnical Journal* 19: 269-288.
- Evans, S.G. 1989. Rain-induced landslides in the Canadian Cordillera, July 1988. *Geoscience Canada* 16: 193-200.
- Evans, S.G. and Brooks, G.R. 1994. An earthflow in sensitive Champlain Sea sediments at Lemieux, Ontario, June 20, 1993, and its impact on the South Nation River. *Canadian Geotechnical Journal* 31: 384-394.
- Fair, A.E. 1978. A soil analysis of the marine clay in the Terrace-Kitimat area and how they relate to slope stability problems in the area. B.Sc. Thesis. The University of British Columbia, Vancouver, 93 pp.
- Foster, D.R. and Wright Jr., H.E. 1990. Role of ecosystem development and climate change in bog formation in central Sweden. *Ecology* 71: 450-463.
- Geertsema, M. 1998. Flowslides in waterlain muds of northwestern British Columbia, Canada. In D.P Moore & O.Hungr (eds.), *Proc. 8th IAEG Congress, Vancouver, B.C.* Vol III: 1913-1921.
- Geertsema, M. and Schwab, J.W. 1996. A photographic overview and record of the Mink Creek earthflow, Terrace, British Columbia. B.C. Min. For., Victoria, B.C. Res. Rep. 08 .
- Geertsema, M. and Schwab, J.W. 1997. Retrogressive flowslides in the Terrace-Kitimat, British Columbia area: from early post-deglaciation to present - and implications for future slides. *In Proceedings of the 11th Vancouver Geotechnical Society Symposium*: 115-133.
- Geertsema, M. and Schwab, J.W. 2004. Challenges with terrain stability mapping in northern British Columbia – the special case of large, complex landslides. *In Proceedings of the 57th Canadian Geotechnical Conference*.
- Goudie, A., Anderson, M., Burt, T., Lewin, J., Richards, K., Whalley, B., and Worsley, P. 1990. *Geomorphological Techniques*. 2nd ed. Unwin Hyman, London.
- Gregersen, O. 1981. The quick clay slide in Rissa, Norway. *In Proc. 10th ICSMFE, Stockholm*, Vol 3, pp. 421-426.

Hansen, W.R. 1965. Effects of the earthquake of March 27, 1964 at Anchorage, Alaska. *US Geological Survey Professional Paper 542-A*.

Hogan, D.L. and Schwab, J.W. 1991. Meteorological conditions associated with hillslope failures on the Queen Charlotte Islands. Land Management Report 73, BC Ministry of forests. 36 pp.

Holland, S. S. 1976. Landforms of British Columbia. A Physiographic Outline. British Columbia Department of Mines and Petroleum Resources. Bulletin No. 48 Victoria, B.C., 138 p.

Lafleur, J. and Lefebvre, G. 1980. Groundwater regime associated with slope stability in Champlain clay deposits. *Canadian Geotechnical Journal* 17: 44-53.

La Rochelle, P., Y.J. Chagnon, and G. Lefebvre. 1970. Regional geology and landslides in the marine clay deposits of eastern Canada. *Canadian Geotechnical Journal* 7: 145-156.

Lebuis, J., J.-M. Robert, and P. Rissmann. 1983. Regional mapping of landslide hazard in Quebec. *In Symposium on slopes on soft clays*. Bergren, B. and Lindgren, J. (editors) Swedish Geotechnical Institute. Report No. 17 pp. 205-262.

Lefebvre, G. 1986. Slope instability and valley formation in Canadian soft clay deposits. *Canadian Geotechnical Journal* 23: 261-270.

Lefebvre, G. 1996. Soft sensitive clays. *In Special Report 247: Landslides investigation and mitigation*. A.K. Turner and R.L. Shuster (editors). TRB, National Research Council, Washington D.C., pp. 607-619.

Lefebvre, G., Rosenberg, P., Paquette, J., and Lavallee, J.G. 1991. The September 5, 1987, landslide on the La Grande River, James Bay, Quebec, Canada. *Canadian Geotechnical Journal*, 28, 263-275.

Mitchell, R.J. 1978. Earthflow terrain evaluation in Ontario. Ontario Ministry of Transportation and Communications. 30 pp.

Mitchell, R.J. and Markell, A.R. 1974. Flowsliding in sensitive soils. *Canadian Geotechnical Journal*, 11, 11-31.

NGI 1982. The Rissa landslide video. Norwegian Geotechnical Institute. Oslo Norway (video).

Odenstad, S. 1951. The landslide at Sköttorp on the Lidan River. *In Proceedings of the Royal Swedish Geotechnical Institute* 4, pp. 1-38.

Patton, F.D. 1984. Climate, groundwater pressures and stability analyses of landslides. *In Proceedings 4th International Symposium on landslides Toronto, Canada* 3: 43-59.

Pielou, E.C. 1991. *After the Ice Age - The return of life to glaciated North America*. University of Chicago Press. 366 pp.

Potvin, E.C., Pellerin, F., Demers, D., Robitaille, D., La Rochelle, P., Chagnon, J-Y. 2002. Revue et investigation complémentaire du site du glissement de Saint-Jean-Vianney. *In Proceedings – 2001 An Earth Odyssey, Canadian Geotechnical Society*, 792-800.

Quigley, R.M. 1980. Geology, mineralogy, and geochemistry of Canadian soft soils: a geotechnical perspective. *Canadian Geotechnical Journal* 17: 261-285.

Rosenqvist, I.Th. 1953. Considerations on the sensitivity of Norwegian quick-clays. *Géotechnique* 3: 195-200.

Schwab, J.W. 1983. Mass wasting: October-November 1978 storm, Rennell Sound, Queen Charlotte Islands, British Columbia. *Research Note 91. BC Ministry of Forests*, 23 pp.

Schwab, J.W., Geertsema, M., and Blais-Stevens, A. *In press*. The Khyex River landslide of November 28, 2003, Prince Rupert British Columbia Canada. *Landslides*.

Söderblom, R. 1974. A new approach to the classification of quick clays. *Swedish Geotechnical Institute reprints and preliminary reports no. 55*, pp. 1-17.

Söderblom, R. 1983. Studies of the rapidity number: can this number be used to determine the slide tendency of a clay? *In Bergren, B. and Lindgren, J. (ed.s) Symposium on slopes on soft clays. Swedish Geotechnical Institute. Report No. 17* pp. 381-395.

Tavenas, F, Chagnon, J.Y., and La Rochelle, P. 1971. The Saint-Jean-Vianney landslide: observations and eyewitnesses accounts. *Canadian Geotechnical Journal* 8: 463-478.

Tavenas, F., Flon, P., Leroueil, S., and Leblais, J. 1983. Remolding energy and risk of slide retrogression in sensitive clays. *In Bergren, B. and Lindgren, J. (ed.s) Symposium on slopes on soft clays. Swedish Geotechnical Institute. Report No. 17* pp. 423-454.

Torrance, J.K. 1983. Towards a general model of quick clay development. *Sedimentology* 30: 547-555.

Torrance, J.K. 1987. Quick clays. *In*. Slope Stability, M.G. Anderson and K.S. Richards (ed.s). John Wiley and Sons Ltd, pp. 447-473.

Viberg, L. 1983. Experiences of mapping and classification of stability conditions. Swedish Geotechnical Institute, Report No. 17, Linköping. Pp. 455-461.